January 2016

REGULATION OF T CELLS AND TISSUE INFLAMMATION BY SHORT CHAIN FATTY ACIDS

Jeong Ho Park
Purdue University

Graduate School Form
30 Updated 12/26/2015

PURDUE UNIVERSITY
GRADUATE SCHOOL
Thesis/Dissertation Acceptance

This is to certify that the thesis/dissertation prepared

By Jeongho Park

Entitled
REGULATION OF T CELLS AND TISSUE INFLAMMATION BY SHORT CHAIN FATTY ACIDS

For the degree of Doctor of Philosophy

Is approved by the final examining committee:

Chang H. Kim
Chair

Harm HogenEsch

Yava L. Jones

John A. Patterson

To the best of my knowledge and as understood by the student in the Thesis/Dissertation Agreement, Publication Delay, and Certification Disclaimer (Graduate School Form 32), this thesis/dissertation adheres to the provisions of Purdue University's "Policy of Integrity in Research" and the use of copyright material.

Approved by Major Professor(s): Chang H, Kim

Approved by: Chang H. Kim 10/7/2016
Head of the Departmental Graduate Program Date

REGULATION OF T CELLS AND TISSUE INFLAMMATION BY SHORT CHAIN FATTY ACIDS

A Dissertation

Submitted to the Faculty

of

Purdue University

by

Jeongho Park

In Partial Fulfillment of the

Requirements for the Degree

of

Doctor of Philosophy

December 2016

Purdue University

West Lafayette, Indiana

To my Lord

TABLE OF CONTENTS

Page

LIST OF FIGURES

Figure Page

Figure Page

ABSTRACT

Jeongho Park. Ph.D., Purdue University, December 2016. The Impact of Gut Metabolites on Tissue Inflammation and Immunity. Major Professor: Chang H. Kim.

Intestinal microbiota has an essential role and act like a functional organ in the body. Compared to other organs, the largest number of bacteria reside and produce various metabolites in the intestines. Gut microbiota produce short chain fatty acids (SCFAs) via dietary fiber fermentation. SCFAs contribute to immune homeostasis by regulating gut barrier function, intestinal cell proliferation, differentiation, and metabolism. Importantly, SCFAs control immune cell-mediated inflammation and balance immune system homeostasis. When the normal microbial composition is disturbed, the production of SCFAs is inhibited. Consequently, our body is prone to inflammation and autoimmune diseases.

Moreover, the breakdown of gut microbial symbiosis results not only in inflamed intestines, but also in other inflamed organs, such as the lungs, skin, or kidneys tissues. Recently, many studies recommend the use of gut metabolites on diseases in non-intestinal tissues. Accordingly, understanding SCFAs effect on the immune system will provide therapeutic application for various immune disorders. Our studies investigated the roles of SCFAs in T cell differentiation and peripheral tissue inflammation.

In Part I, we examined the role of SCFAs in T cell differentiation and T cell-dependent intestinal inflammation and immunity. Major SCFAs-acetate, propionate, and butyrate-enhanced Th1/Th17 effector T cell differentiation. SCFAs also promoted IL-10^{+} T cell generation in effector T cell-inducing conditions. SCFA-treated T cells showed suppressive and anti-inflammatory activity via IL-10 expression in colitis models. Moreover, SCFAs enhanced Th17 cell during bacterial infection and efficiently cleared invading pathogens. GPR41 and GPR43 are major SCFA receptors, but expression in T cells was not detected. SCFAs promoted T cell differentiation in a GPR41 and GPR43 independent manner. Instead, we suggested that SCFAs utilize other mechanisms and regulate T cell differentiation. First, SCFAs stimulated mTOR activity in T cell differentiation. Next, we found that SCFAs inhibited histone deacetylase (HDAC) activity and upregulated acetylation of p70 S6 kinase, a kinase of mTOR, in T cells.

In Part II, we investigated the role of SCFAs in the renal system. We exposed mice to a high concentration of SCFAs in drinking water for up to six weeks. The treatment caused a profound effect on ureteral obstruction, which developed into hydronephrosis. T cell or gut microbiota is required in SCFAs-mediated renal inflammation. In affected tissues, Th1 or Th17 cells were increased and the neutralization of IL-17 or IFNγ inhibited disease progression. We found that SCFAs activated mTOR signaling in renal T cells and developed T cell-dependent inflammation. Moreover, rapamycin administration protected the host from SCFA-induced renal disease.

We studied the roles of SCFAs in T cell differentiation and T cell-dependent inflammatory diseases. We speculate that SCFAs have binary roles in immune regulation. Depending on environmental stimulation, SCFAs direct T cells to either suppress

inflammation or fight against invading pathogens. In the renal system, SCFAs developed unexpected ureteral obstruction and kidney inflammation. This suggests that excessive SCFAs can result in unexpected inflammatory diseases of peripheral organs. Although SCFAs are produced in the colon, they regulate inflammation in remote organs; therefore, SCFAs have the potential to control autoimmune diseases in various peripheral organs.

CHAPTER 1. LITERATURE REVIEW

1.1 Regulation of short chain fatty acids on T cell differentiation and intestinal inflammation.

1.1.1 Short chain fatty acids production in the intestines by commensal bacteria

In the gastrointestinal tract, microbial metabolites play a critical role in the maintenance of intestinal homeostasis. Microbial products are used by the host as nutrients and are regulating factors for the host immune system (1). Short chain fatty acids (SCFAs) are a major group of gut metabolites produced by colonic microbiota from fermenting non-digestible fiber. Acetate (C2), propionate (C3), and butyrate (C4) are the most abundant SCFAs and have 2~4 carbons (2). In the large intestine, the molar ratio of is these SCFAs are 50:20:20 respectively, and the total concentration is ~130mM (3-5).

While starch or starch-like polysaccharides are absorbed in the upper gastrointestinal (GI) tract, nonstarch polysaccharides (NPS) remain undigested. Accordingly, anaerobicbacteria in the proximal colon produce each SCFA by different mechanisms. Acetogens, such as Firmicutes produce C2 via Wood–Ljungdahl pathway, which converts CO_2 and H_2 into acetate. Bifidobacteria also produce C2 by Catabolizing fructose (6-8).Gut

bacteria produce C3 through three mechanisms: succinate, arylate or propanediol pathways (9). C4 is produced by bacteria that expresses the genes that encode butyryl CoA / acetyl CoA transferases (10).

Bacterial composition impacts SCFA production. There are ~1,000 different species of gut microbiota. The gut microbiota composition is altered by environmental factors like diet, which changes the production of SCFAs. For example, when mice are fed a high-fiber diet, Bacteroidetes or Actinobacteria are abundant in cecal contents, while Firmicutes and Proteobacteria populations are scarce (11). Taking this into consideration, sustaining the normal population of beneficial microbiota is required for beneficial metabolite production.

SCFAs regulate energy metabolism, cell differentiation, proliferation, and gene expression in the host. Several different pathways mediate SCFA function. SCFAs are absorbed into colonocytes through anionic diffusion (Na^+ or K^+ & H^+ exchange) or monocarboxylate transporters (MCTs) such as H^+-coulpled MCT1 (12-14). Furthermore, SCFAs activate a number G protein coupled receptors (GPCRs) (15). Among various GPCRs, SCFAs activate GPR43 and GPR41, which are highly expressed in human adipose and intestinal tissues (16). While, shorter SCFAs, such as acetate and propionate, have a higher GPR43 affinity, propionate and butyrate show preferred binding to GPR41(17). GPR109A is a niacin (vitamin B3 or nicotinate) receptor and is highly expressed in intestinal epithelial cells. This receptor also has an affinity for butyrate (18, 19).

1.1.2 T cell development and differentiation

T cells are mainly produced in the thymus. Initially, T cell expresses neither CD4 nor CD8. When lymphoid progenitors are introduced to the thymus, CD4 and CD8 double negative thymocytes develop into αβ-TCR expressing cells, which are double positive for CD4 and CD8. Subsequently, they become mature single-positive cells ($CD4^+$ or $CD8^+$) (20, 21). $CD4^+$ T cells are maintained in a naïve form in secondary lymphoid tissues, such as the spleen or lymph nodes. Upon antigenic signaling or cytokines stimulation, naïve T cells differentiate into Th1/Th17 effector T cells and regulatory T cells in peripheral organs (22). The IL-12 family signals differentiation in Th1 cells, which express inflammatory cytokines, such as IFNγ, and fight against intracellular pathogens. In the last decade, Th17 cells caught the attention of immunologists due to its inflammatory impact in autoimmune diseases. IL-6, IL-23, and TGFβ1 signals stimulate naïve $CD4^+$ T cells to differentiate into Th17 cells, which produce IL-17. During Th17 cell differentiation, RoRγt, a major transcription factor, is activated (23, 24). Regulatory T cells, such as IL-10 producing T cells are generated by IL-27 signals and have anti-inflammatory functions. The combination of TGFβ1 and IL-2 induces fox-head box P3 (FoxP3) expressing cells, which is characterized by immune suppressive functions(25, 26).Moreover, chemokines or gut metabolites are involved in T cell differentiation. For example, CCL2 suppresses IL-12 mediated Th1 differentiation, but supports Th2 generation (27). Retinoic acid (RA), a small intestine metabolite, supports $FoxP3^+$ T cell generation, but blocks IL-6 induced Th17 cell differentiation (28).

1.1.3 Role of SCFAs in T cell differentiation and underlying mechanisms

Recent studies reported the role of SCFAs in T cell differentiation and investigated the related molecular or intracellular mechanisms. Furusawa et al. showed that C4 treatment elevated FoxP3$^+$ T cell expression both in vitro and in vivo. In colonic lamina propria, FoxP3$^+$ cells were expanded by C4 feeding. C4 also increased the generation of FoxP3$^+$ T cells not only in Tregs but also in Th1/Th17 polarizing culture conditions; the level of transcription factors, T-bet or RoRγt were unchanged. As an intracellular mechanism, the authors suggested that C4 enhanced H3 acetylation in the *Foxp3* promoter region or the conserved non-coding sequence (CNS) regions. However, C4 did not affect the acetylation of other transcription factors, *tbx21*, *Gata3*,or *Rorc* (29). A complementary study examined the effect of C3 and C4 in regulatory T cell induction. C4 feeding increased the population of colonic FoxP3$^+$ T cells in a CNS1 dependent manner. However, antibiotics feeding decreased fecal C3 and C4 concentrations, and subsequently suppressed FoxP3$^+$ T cell expansion in the colon. This suppression was reversed by oral SCFA administration (30).

A number of studies disputed the role of SCFA receptors in T cell differentiation. A study reported that GPR43, a major SCFA receptor, played an essential role in regulatory T cell generation. C2, C3, and C4 treatment augmented populations of colonic FoxP3$^+$ and IL-10$^+$ T cells. C3, especially, enhanced HDAC6 inhibition and H3 acetylation in a GPR43 dependent manner (31). Another article suggested the role of GPR109a, a receptor for both niacin and C4, in regulatory T cell expansion. GPR109a-deficient mice showed decreased colonic FoxP3$^+$ and IL-10$^+$ T cell populations; this strain was more susceptible to DSS-induced colitis than WT mice(19).While these studies emphasize the requirement of SCFA

receptors, our group showed that GPR41 and GPR43 are not necessary in SCFA-promoted T cell differentiation. The expressions of GPR41 and GPR43 in splenic or colonic $CD4^+$ T cells were are low. Accordingly, SCFA-enhanced IL-10^+ T cell and Th1/Th17 cell differentiation occurred independently of GPR41 and GPR43. Instead, we suggest that C2, C3, and C4 regulate HDAC and mTOR activity for both effector and regulatory T cell differentiation. A recent study showed similar data, that C4 increased Th1/Th17 cell differentiation and $FoxP3^+$ T cell induction (32). These studies agreed on the common effects of SCFAs on regulatory T cell generation, while effector T cell induction is regulated in defined conditions. Yet, the effect of SCFA receptors in T cell regulation must be investigated further.

1.1.4 Beneficial effect of SCFAs on intestinal inflammation

So far, we have discussed the production of SCFAs and the mechanisms of SCFA enhanced T cell differentiation. Next, we will discuss the effect of SCFAs on intestinal inflammation. Gut microbiota produces SCFAs, which are absorbed into intestinal tissue through epithelial cells. Absorbed SCFAs provide energy to colonocytes and contribute to general colonic health (33). In human studies, SCFAs administration ameliorates colitis. For example, dietary changes expanded SCFA-producing bacteria, which suppressed intestinal inflammation(33, 34).

SCFAs regulate immune system by indirect or direct mechanisms and control intestinal inflammation. First, SCFAs activate major G-protein-coupled receptors (GPCR), such as GPR41, GPR43, and GPR109a. These receptors are highly expressed in gut epithelial cells and in neutrophils. When SCFAs activate GPCRs, intestinal integrity is enhanced and hosts are more resistant to inflammation (18, 35). Among these receptors,

the role of GPR43 in intestinal inflammation was demonstrated by several studies. In GPR43-deficient mice, SCFA signals vanished, which exacerbated DSS-induce colitis as compared to WT mice. Oral SCFA administration ameliorated neutrophil infiltration and inflammation dependent on GPR43. This study further confirmed the role of GPR43 in hematopoietic cells using bone marrow chimeras. When WT mice were reconstituted with GPR43-deficient bone marrow cells, these mice showed severe colitis as GPR43 deficient mice(36). However, a contrasting role of GPR43 was also suggested. In GPR43-deficienct mice, a chronic DSS-induced inflammation was less severe and intestinal neutrophils were less infiltrated than in WT mice. When GPR43-deficient mice were exposed to chronic inflammation, MAPK-dependent neutrophil migration was defective, which resulted in milder inflammation. However, GPR43-deficient mice were more susceptible to acute DSS colitis than WT mice, due to the disruption of gut integrity (37). Our group also reported the role of GPR41 and GPR43 in ethanol- or TNBS-induced colitis. In GRP41- or GPR43-deficient conditions, leukocyte recruitment was impaired and mice developed milder inflammation. However, due to the defective function of SCFA-receptors, GPR41- or GPR43-deficient mice were unable to clear infected bacteria and intestinal permeability was damaged (38).

SCFAs directly regulate intestinal inflammation through epigenetic modification. SCFA-mediated histone acetylation regulates immune cell differentiation and controls intestinal inflammation. In experimental colitis models, HDAC inhibitors showed protective effects against DSS- or TNBS-induced colitis. HDAC inhibitor treatment with SAHA or ITF2357 ameliorated intestinal inflammation by suppressing inflammatory cytokine production (39, 40). HDAC inhibitors act through various cell types to control

inflammation. Deletion of intestinal epithelial HDAC1 and HDAC2 changed the function and structure of epithelial cells. In neutrophils, SCFAs suppressed TNFα expression and inhibited the Nf-κB pathway, which is linked to HDAC inhibition. In macrophages, the anti-inflammatory effect of SCFAs was suggested as well. C4 treatment suppressed inflammatory cytokine expression in colonic macrophages both in vivo and in vitro. Authors provided a mechanism for C4 enhanced histone 3 lysine 9 (H3K9) acetylation of *Nos2*, *Il6*, and *Il12b* promoter regions in bone marrow derived macrophages (BMDM) (41-43).

The T cell is a major cell type involved in intestinal inflammation. Previously, we discussed that SCFAs control T cell differentiation through HDAC activation in GPR41- and GPR43- independent manners. Then, we examined the effect of SCFAs in T cell-mediated colitis. In a T cell adoptive transfer model, SCFA-treated T cell showed less inflammatory action. Oral SCFA administration decreased the inflammatory response to anti-CD3 in a IL-10 dependent fashion (44). A different study reported that colonic $FoxP3^+$ T cells, which have anti-inflammatory functions, were enhanced by SCFAs treatment independent of GPR109a. Furthermore, SCFA induced histone H3 acetylation in *FoxP3* promoter and the *FoxP3* enhancer-conserved non-coding sequence 1 (CNS1) was required in SCFA-mediated $FoxP3^+$ T cell generation (30). A similar study showed the beneficial role of SCFAs in T cell-mediated colitis. The adoptive transfer of naïve $CD4^+$ T cell into a C4-diet fed RAG1-deficient host resulted in less inflammation than mice with standard diet. $FoxP3^+$ T cells expanded in the colonic lamina propria of C4-diet fed mice; however C2 or C3 feeding was unable to ameliorate T cell-mediated inflammation (29). We demonstrated that GPR43 was neither detected in splenic nor colonic $CD4^+$ T cells, and that SCFAs

enhanced T cell differentiation independent of GPR43. However, a study suggested that SCFAs ameliorate T cell-mediated colitis in a GPR43-dependent manner. T cells of WT mice suppressed naïve T cell induced colitis in SCFA-fed RAG1-deficient hosts, while cells from GPR43-deficient mice did not suppress intestinal inflammation (31).

1.2 Immune cell regulation of renal disease development and its underlying mechanisms.

1.2.1 The role of T cell and cytokines in renal inflammation.

The T cell is a major regulator of renal inflammation, and a number of renal disease models demonstrate the critical role of the T cell. In the unilateral ureteral obstruction (UUO) model, the essential role of the $CD4^+$ T cell was reported. $CD4^+$ T cell depletion or RAG1-deficiency, protected mice from UUO-induced inflammation and fibrosis. There was reduced collagen accumulation in the interstitial area of SCFA-treated mice (45). Similarly, our study showed that αβ-T cell deficiency inhibited gut metabolites-induced ureteral obstruction and inflammation (46). Antigen stimulation activates effector T cell generation, which promotes inflammatory cytokine secretion. T cell-mediated inflammatory cytokines, such as IL-17 and IFNγ are responsible for renal inflammation. The role of renal T cells was demonstrated in the anti-glomerular basement membrane (GBM) glomerulonephritis as well. Effector $CD4^+$ or $CD8^+$ T cells, which produce IL-17 or IFNγ, accumulated in the tubulointerstitial region of the inflamed kidneys (47). The concise action of effector T cells was confirmed in an antigen specific glomerulonephritis model. Th1 or Th17 cells from OVA-specific OT-II mice induced proliferative renal

inflammation in OVA-bearing RAG-deficient mice (48). The role of IL-17 was also identified in fatal lupus glomerulonephritis. In lupus-prone mice, IL-17 deficiency protected fatal glomerulonephritis (49). T cells are stimulated by other immune cells, such as antigen-presenting cells (APCs) that provide inflammatory cytokines. For instance, dendritic cell (DC) produced IL-1, which induces of IL-17A production by renal T cells (46, 50). In obstructed kidneys, T cells and DCs were collated and induced Th1 or Th17 cells (51). In addition, renal resident cells, tubular epithelial cells interacted with T cells and affected effector T cell generation in kidney tissues (52). These findings support the role of the T cell and the mutual interaction between T cell and APCs in renal inflammation pathogenesis.

1.2.2 mTOR signaling and the effect of mTOR inhibition in renal disease

mTOR signaling has a critical function in immune cell proliferation and differentiation. mTORC1, a downstream signal of mTOR, is required for effector $CD4^+$and $CD8^+$ T cell differentiations (53, 54). mTOR activation also regulates IL-10^+ T cell generation (44). Besides, mTOR signals control non-T cell regulation, such as B cell or DC maturation (55, 56). Because antibody or cytokine production from these non-T cells affects T cell differentiation (57),better understanding of mTOR regulation in immune cells is required to control inflammatory disorders.

In this regards, the mTOR pathway is involved in the development of a number of renal diseases. Our group reported that increased mTOR activity in renal $CD4^+$ T cells resulted in hydronephrosis (46). In mice with polycystic kidney disease (PKD), the mTOR-

S6K pathway, a key downstream of mTOR, was activated (58). mTORC2 is a mTOR kinase component and its deletion abrogated TGFβ1-dependent kidney fibrosis (59). Because mTOR activation leads to renal inflammation, an mTOR inhibitor, rapamycin, was utilized in various kidney disease models. In an UUO model, the rapamycin application protected host mice from diseases, by reducing the infiltration of collagen fiber, macrophages, and effector T cells in kidney tissues (46, 60, 61). Rapamycin also inhibited mTOR activity in PKD mice, which blocked renal cyst formation and recovered renal function. In Han:SPRD rats, a PKD-prone strain, rapamycin prohibited PKD pathogenesis, via reducing kidney cyst volume density and blood urea nitrogen (BUN) levels. Rapamycin treatment protected rodents from anti-GBM antibody-induced glomerulonephritis by suppressing inflammatory immune cell infiltration and proteinuria (62, 63).Because mTOR activation is responsible for renal inflammation development, many renal disorders can be prevented or relieved with mTOR pathway inhibition.

Although the beneficial impact of rapamycin on renal disease is clear, how mTOR signaling controls intracellular processes is still a question of interest. mTOR pathways regulate endoplasmic reticulum (ER) stress and ER stress is associated with renal diseases. A recent study suggests that mTOR signaling increases ER stress, which promotes tubular cell apoptosis(64, 65). In the rat minimal-change disease (MCD) model, mTORC1 activation enhanced ER stress, which resulted in glomerular podocyte damage and proteinuria(66). Accordingly, it is worth studying whether or not mTOR activation regulates ER stress-induced apoptosis in renal immune cells and mediates kidney diseases.

1.2.3 Involvement of HDAC in renal disease

In the previous section, we discussed that SCFA-mediated HDAC inhibition has beneficial effects on intestinal inflammation. A number of HDAC inhibitors are also applied to control renal inflammation in both human patients and animal research. Trichostatin A (TSA) is a pan-HDAC inhibitor, which has inhibitory effects on HDAC class I and II. TSA treatments were applied to renal disease models, which attenuated fibronectin expression in UUO mice. In addition, suppressed STAT3 activity and cellular apoptosis were observed in TSA-treated mice (67). A later study investigated the effect of HDAC class I-specific inhibitor in obstructed kidneys. An intraperitoneal injection of HDAC I inhibitor controlled fibrosis and TGFβ1 expression. Moreover, epidermal growth factor receptor (EGFR) activity was suppressed by HDAC I inhibitor followed by Smad-3 abrogation (68). The beneficial effects of HDAC inhibitors on renal diseases were confirmed in an acute kidney injury model as well. Pre-treatment application of valproic acid or acetate supported regular renal function and protected against ischemia-reperfusion injury (69, 70).

In addition, the therapeutic potential of HDAC inhibitors is suggested as follows. When methyl-4-(phenylthio) butanoate was administrated one day after ischemia-reperfusion injury, tubular epithelial apoptosis and fibrosis were attenuated (71). Although it is uncertain whether or not HDAC inhibitors protect disease through histone acetylation or other pathways, HDAC inhibitors are a promising tool for the maintenance of various renal diseases.

1.2.4 The role of gut microbiota and metabolite in renal disease

The human body accommodates more than 100 trillion microbiota, collectively considered an internal organ due to its essential role. When the homeostatic composition of microbiota is disrupted, the human body is vulnerable to diseases including renal failure. Healthy people had more diverse bacterial populations than end-stage renal disease (ESRD) patients, who had decreased compositions of Firmicutes, Actinobacteria, and Proteobacteria. Rats with Chronic kidney disease (CKD) had less Lactobacillaceae and Prevotellaceae than the healthy control population (72). As pathobionts expanded, intestinal toxic metabolites disorganize gut junction and barrier function. In CKD rats, the level of gut junction proteins, such as ZO-1, occludin, and claudin-1 were reduced (73). As a result, gut permeability was increased and hosts were more vulnerable to kidney diseases. In addition, urase-processing bacteria was increased in ESRD patients and induced urea accumulation in the intestinal tract (74).

It is possible that a growing pathogenic bacteria population relates to diet. Food restriction protected PKD-prone mice from cellular injury, cyst formation, and helped normal kidney function (58). To treat microbial-induced renal diseases, many studies applied antibiotics. Our recent study also showed that oral vancomycin feeding prevented ureteral obstruction (46, 75, 76). However, the risk of antibiotic treatment on renal diseases was also demonstrated. Broad-spectrum antibiotics treatment elongated renal failure in human patients. Moreover, oral administration of fluoroquinolone increased the risk of acute kidney injury by about two times (77-79).

To overcome the adverse effect of antibiotics, benign gut metabolites were applied to treat renal diseases. A couple of studies demonstrated the beneficial effect of SCFAs on acute kidney injury (AKI). SCFA treatment inhibited NFκb activation and inflammatory cytokine accumulation. Delivering SCFA-producing bacteria, such as Bifidobacterium restored renal function after AKI as well (76, 80). Butyrate treatment attenuated TGF-β1 and Smad3 activation in renal epithelial cell cultures, which suppressed renal fibrosis (81). RA, a metabolite of the small intestine, inhibited fibrosis in UUO mice by ameliorating TGF-β1 expression and collagen deposition (82). While SCFAs have beneficial effects, our results indicate that they can induce inflammatory responses of chronically elevated concentrations (46).

CHAPTER 2. IMPACT OF GUT METABOLITES SHORT CHAIN FATTY ACIDS ON EFFECTOR AND REGULATORY T CELL DIFFERENTIATION

2.1 Introduction

From an immunological perspective, a healthy life means maintaining the balance of the immune system. T cells are a major player in the immune system because they control inflammation and host immunity. T cells are produced in the thymus and stored in lymphoid tissue in a naïve form. When naïve T cells are stimulated by several signals, such as cytokines and co-stimulatory molecules, they differentiate into effector T cells or regulatory T cells. Effector T cells secrete inflammatory cytokines, fight against invading pathogens, and induce inflammation. On the other hand, regulatory T cells have anti-inflammatory or immune suppressive functions.

Food significantly affects healthy life because gut microbial metabolites regulate the immune system and control the homeostasis of body. Short chain fatty acids (SCFAs) such as acetate (C2), propionate (C3), or butyrate (C4) are major microbial metabolites produced by the fermentation of dietary fiber. SCFAs have various functions and contribute to healthy physiological condition by regulating gut mobility and providing an energy source to intestinal cells.

In this study, we investigated the role of SCFAs in T cell regulation and intestinal inflammation. We found that SCFAs promoted regulatory T cells. At the same time,

SCFAs enhanced effector T cell differentiation. SCFA-treated T cells showed suppressive function in T cell-dependent inflammation and promoted anti-bacterial immunity. In addition, our study suggests the mechanisms by which SCFAs shape T cell differentiation. We propose that SCFAs inhibit histone deacetylases and increase mTOR activity in T cells, which is required for generation of both effector and regulatory T cells.

2.2 Materials and methods

Mice

C57BL/6 mice were from Harlan. CD45.1 C57BL/6 mice, Rag1(-/-) (B6.129s7-Rag1 ^{tm1Mom}/J) mice, and IL-10(-/-) mice were from the Jackson laboratory. GPR43(-/-) mice were from Deltagen (San Mateo, CA), and GPR41(-/-) mice were obtained from Dr. M. Yanagisawa (UT Southwestern Medical Center at Dallas). All mice were kept at Purdue University for at least 12 months before use. All experiments with animals in this study were approved by the Purdue Animal Care and Use Committee (PACUC).

T cell isolation

For Naïve $CD4^+$ T cell isolation, total $CD4^+$ T cells were isolated from the spleen and lymph nodes, using the $CD4^+$ T cell isolation kit (Miltenyi). For further depletion, PE-conjugated antibodies to CD8 (clone 53-6.7), CD19 (clone 6D5), CD25 (clone 3C7), CD44 (clone IM7), and CD69 (clone H1.2F3) and anti-PE microbeads were applied. $CD8^+$ cells were isolated by the $CD8^+$ T cell isolation kit (Miltenyi), and cells expressing CD4, CD19, CD25, CD44, and CD69 were further depleted as described for naïve $CD4^+$ T cells.

GPR41 and GPR43 expression in various cell types

For qRT-PCR and conventional PCR analysis of GPR41 and GPR43 in different cell types, colonic epithelial cells were positively selected by biotin conjugated anti-CD326 (clone Ep-CAM) and anti-biotin microbeads. To collect colonic T cells, non-T cells were deleted by biotin conjugated anti-CD11c (clone N418), CD19 (clone 6D5), CD326 (clone Ep-CAM), and Gr-1 (clone RB6-8C5) antibodies and anti-biotin microbeads. Total $CD4^+$ cells were isolated using PE-conjugated anti-CD4 antibody and anti-PE microbeads. Marrow $Gr\text{-}1^+$ cells were positively isolated from total bone marrow cells by biotin-labeled anti-GR-1antibody (clone RB6-8C5) and anti-biotin microbeads. The purity of the isolated each cell types was higher than 95%. Conventional PCR was performed with 28 cycles for β-actin and 35 cycles for GPR41 and GPR43 at 55°C annealing temperature.

T cell differentiation *in vitro*

Naïve $CD4^+$ or $CD8^+$ T cells from wild type, GPR41(-/-), and GPR43(-/-) mice were activated with plate-bound anti-CD3 (1-5 μg/ml) and soluble anti-CD28 (2 μg/ml) for 3-6 days in the presence or absence of Sodium Acetate (C2), Sodium Propionate (C3), or Sodium Butyrate (C4) at indicated concentrations (0.1-10 mM). Effector or regulatory T cells were induced in following polarizing conditions in normal RPMI 1640 medium (10% FBS). For the non-polarized condition (Tnp), hIL-2 (100 U/ml) was used. For Th17/Tc17 cells, hTGF-β1 (5 ng/ml), mIL-6 (20 ng/ml), mIL-1β (10 ng/ml), mIL-23 (10 ng/ml), mIL-21(10 ng/ml), mTNF-α (20 ng/ml), anti-mIL-4 (11B11, 10 μg/ml), and anti-mIFN-γ (XMG1.2, 10 μg/ml) were used. For Th1/Tc1 cells, hIL-2 (100 U/ml), mIL-12 (10 ng/ml), and anti–mIL4 (10 μg/ml) were used. For $IL\text{-}10^+$ T cells, hIL-2 (100 U/ml) and mIL-27 (50

ng/ml) were used. Rapamycin (25 nM), metformin (1,1-dimethylbiguanide hydrochloride, 1 mM), or TSA (trichostatin A, 10 nM) was used for the T-cell culture.

Flow cytometry

For intracellular staining of IL-10, IL-17 and IFNγ, cells were stained first for surface antigens with antibodies (e.g. RM4-5 for CD4 or 53-6.7 for CD8) and then activated in RPMI 1640 (10% FBS) with PMA (50 ng/ml), ionomycin (1 μM), and monensin (2 mM; Sigma-Aldrich) for 4 hours. Cells were then fixed, permeabilized, and stained with antibodies to mIL-10 (JES5-16E3), mIL-17A (TC11-18H10.1), or IFN-γ (XMG1.2). Cells were stained with an antibody to mouse FoxP3 (FJK-16s), T-bet (eBio4B10), or RORγt (AFKJS-9) according to the manufacturer's protocol. For co-staining of IL-10 and FoxP3, cells pre-stained with anti-CD4 (RM4-5) were activated with PMA (50 ng/ml), ionomycin (1 μM), and Brefeldin A (25 μg/ml) for 4 hours. Activated cells were fixed, permeabilized and stained with antibodies to IL-10 (JES5-16E3) and FoxP3 (FJK-16s).

For the assessment of mTOR activation and STAT3 activation, isolated mouse $CD4^+$ cells were prepared. Cells were activated for up to 60 hours in complete RPMI-1640 medium with an immobilized antibody to CD3 (5 μg/ml) and soluble antibody to CD28 (2 μg/ml) in the presence of C2 (0-20 mM), C3 (0-1 mM) or C4 (0-0.5 mM). Antibodies to phosphorylated rS6 (Ser235/236; D57.2.2E), phosphorylated STAT3 (Y705; D3A7), and phosphorylated MAPK (Erk1/2) (Thr202/Tyr204; 137F5) were used for flow cytometry.

Microarray analysis

The microarray study was performed using Mouse 430 2.0 chips (Affymetrix, Santa Clara, CA) as described previously (83). Raw intensity signals were obtained with GeneChip Operating Software (Affymetrix) and normalized with the signals of a housekeeping gene (*β-actin*). The heatmap plot of up- or down-regulated genes was drawn using Treeview (http://rana.lbl.gov/EisenSoftware.htm). The microarray data have been deposited to the Gene Expression Omnibus site (accession number: GSE31585).

Quantitative real-time PCR analysis and ELISA

Total RNA was extracted with TRIzol® (Invitrogen), and cDNA synthesis was performed with SuperScript® II Reverse Transcriptase (Invitrogen). Quantitative real-time PCR (qRT-PCR) was performed with Maxima® SYBR Green/ROX qPCR Master Mix (2X) (Fermentas).

The primers used were:

IL-10 (CCA.GCT.GGA.CAA.CAT.ACT.GCT and

CAT.CAT.GTA.TGC.TTC.TAT.GCA.G);

IL-17A (GAC.TCT.CCA.CCG.CAA.TG and CGG.GTC.TCT.GTT.TAG.GCT);

IL-17F (CCA.TGG.GAT.TAC.AAC.ATC.ACT.C and

TTG.TAT.GCA.GCG.TTG.TCA.G);

RoRγt (AGC.CAC.TGC.ATT.CCC.AGT.TTC.T and

TGA.AAG.CCG.CTT.GGC.AAA.CT);

RoRα (GTG.GCT.TCA.GGA.AAA.GGT and GCG.CGA.CAT.TTA.CCC.AT);

IFN-γ (AGA.CAA.TCA.GGC.CAT.CAG.CA and
CGA.ATC.AGC.AGC.GAC.TCC.TTT);
T-bet (ATG.CCG.CTG.AAT.TGG.AAG.GT and
ACC.TCG.CAG.AAA.GCC.ATG.AAG.T).
Gene expression levels were normalized by β-actin levels. ELISA of secreted IL-10 was performed with anti-mIL-10 antibody (JES5-2A5) and a biotinylated anti-mIL-10 antibody (JES5-16ES).

Assessment of in vitro suppressive activity

Naïve $CD4^+$ T cells were cultured for 5-6 days in a Th1 condition in the presence (C2-treated cells) or absence (control cells) of C2. Suppression activity on freshly isolated $CD4^+$ $CD25^-$ T cells was examined. Responder cells, $CD4^+$ $CD25^-$ T cells (5×10^4/well) were isolated from the spleen of CD45.1 congenic mice, and cultured T cells (suppressors) were co-cultured in U-bottomed 96-well plates for 3 days at the indicated ratios in the presence of anti-CD3 (2.5 μg/ml) and 10^4 irradiated T cell-depleted splenocytes as antigen presenting cells (APCs). Dilution of carboxy fluorescein diacetate succinimidyl ester (CFSE) was assessed by flow cytometry.

T cell mediated colitis in Rag1(*-/-*) mice

The control and C2-treated T cells (prepared in a Th17 or Th1 condition) were separately injected i.p. into Rag1-deficient (B6.129s7-Rag1 ^{tm1Mom}/J) mice (1 million cells/mouse). The mice were monitored daily for weight change and activity. All mice were sacrificed once some mice experienced 20% weight loss or were moribund. Intestine and

other tissues were examined for the frequencies of Th1, Th17, and FoxP3$^+$ T cells by flow cytometry. Intestinal tissues were embedded in paraffin, cut into 6 μm-thick sections, and stained with hematoxylin and eosin. Tissue inflammatory scores were assessed based on the degree of leukocyte infiltration and mucosal hyperplasia on a scale of 0–4. The histological images were obtained with a wide field Leica microscope equipped with a color camera at 100× magnification (scale bar: 200 μm).

C2 feeding effect on effector and regulatory T cell subsets in vivo.

WT C57BL/6, GPR43(-/-), and GPR41(-/-) mice were kept on drinking water containing C2 (200 mM, pH 7.5) from 3 weeks of age for 6-8 weeks. Drinking water was replaced once a week. Frequencies of indicated T cell subsets in various organs were determined by flow cytometry. To boost T cell activity, C2-fed WT or IL10-deficient mice were injected with anti-CD3 (15 μg/mouse, clone 145-2C11) at twice (0 and 48 h) and were sacrificed at 52 h after the first injection of anti-CD3. Alternatively, mice were infected with *C. rodentium* (DBS100, 10^{10} CFU/mouse) via oral gavage as described previously (38). After 2 weeks, infected mice were sacrificed, and indicated tissues were examined for frequencies of T cell subsets with flow cytometry. Intestinal inflammation was accessed based on the degree of leukocyte infiltration, mucosal hyperplasia, and loss of villi on a scale of 0–5.

Cell-based HDAC inhibitor assay and assessment of S6K acetylation in T cells

SCFA-induced HDAC activity in T cell was assessed with an HDAC Cell-Based Activity Assay Kit (Cayman Chemical). Naïve CD4$^+$ T cells were prepared from WT,

GPRs-KO mice and were pre-activated with plate-coated anti-CD3 (5 μg/ml) and soluble anti-CD28 (2 μg/ml) for 2 days. The activated T cells were incubated with C2, C3, or TSA for 2 hours and the cellular HDAC activity was determined according to the manufacturer's protocol.

$CD4^+$ T cells were activated with anti-CD3/CD28 and hIL-2 (100 U/ml) in the presence or absence of C2 (10 mM), C3 (1 mM), or TSA (10 nM) for 3 days. Cultured cells (1×10^7 cells) were lysed, pre-cleared by Protein A agarose beads, and incubated with acetylated-lysine antibody (# 9441, Cell Signaling Technology) overnight at 4ºC. Antigen-antibody complexes were precipitated with Protein A agarose beads. Immunoprecipitates or total cell lysate (40 μg of protein/well) were separated with SDS-polyacrylamide gels and then transferred onto nitrocellulose membranes (Bio-Rad). After blocking 1 h in a nonfat dried milk, membranes were incubated with mAb to p70 S6 Kinase (49D7, biotinylated, Cell Signaling Technology) overnight at 4ºC. The membranes were developed with HRP Streptavidin (Biolegend) and the ECL detection system (GE Healthcare) using a G:BOX (Syngene).

Measurement of SCFAs concentrations in C2-fed mice

Intestine tissues and cecal content (100 mg) were collected from normal or C2-water fed mice and homogenized in 900 μl of water and 1.4 mm ceramic beads using a Precellys®24 homogenizer. The homogenates were labeled with regular aniline ($^{12}C_6$), and external SCFA standard solution (10 mg/ml of C2, C3, and C4) was labeled with aniline-$^{13}C_6$ using N-(3-Dimethylaminopropyl)-N′-ethylcarbodiimide hydrochloride (EDC, 2 mg/sample). Crotonic acid (0.1 mg/ml) was used as an internal standard. The labeling

mixture was incubated for 2 h, and triethylamine (TEA) was added to stop the labeling reaction. The samples and standard reaction solution were mixed (1:1) and analyzed with an Agilent 6460 Triple Quad LC/MS System (Agilent Technologies). SCFAs were separated with a CN column (4.6×150 mm) at gas temperature of 325^{o}C, gas flow rate of 8 L/min, nebulizer pressure of 45 psi, sheath gas temperature of 250^{o}C, sheath gas flow rate of 7 L/min, capillary voltage of +3500V, and nozzle voltage of +1000V. SCFA concentrations in samples were determined based on peak areas of the internal and external standards.

Statistical analysis

Student's paired *t* test (2-tailed) was used to determine the significance of the differences between two the groups. Mouse weight change data was analyzed with a repeated measures analyses of variance (ANOVA, SAS, version 9.2, SAS Institute Inc. Cary, NC.). *P* values < or = 0.05 were considered significant.

2.3 Results

Major SCFAs acetate (C2) and propionate (C3) promote naïve T cell differentiation into Th1 or Th17 effector T cells

Toexplore the role of SCFAs in effector T cell differentiation, we cultured naïve $CD4^{+}$ T cells in Th1 and Th17 polarizing conditions in the presence of C2 or C3. Effector T cell differentiation into Th1 or Th17 cells were increased by C2 or C3 in a dose-dependent manner (Fig. 2.1). Next, we examined the regulation of transcription factors and

signature genes of Th1 or Th17 cell by SCFAs. Both C2 and C3 elevated the expression levels of *IL-17A, IL-17F, RORα, RORγt, T-bet,* and *IFNγ* at mRNA level (Fig. 2.2A). Regulation of transcription factors by SCFAs was further verified in various T cell-activating conditions. Naïve CD4+ T cells were activated with standard anti-CD3 (5μg/ml) or low anti-CD3 (1 μg/ml) in the presence of C2 or C2, and expressions of RORγt, T-bet, and FoxP3 were determined. While C2 and C3 increased frequencies of RORγt$^+$ and T-bet$^+$ cells, FoxP3$^+$ cells were unaffected (Fig. 2.2B). However, FoxP3 expression combined with RORγt was enhanced by C2 or C3 in a weak anti-CD3 (1 μg/ml) activation condition (Fig. 2.3).

To investigate the function of SCFA-induced effector T cells, we examined the colitis-inducing activity of T cells. We cultured Th17 cells in the presence or absence of C2 (C2-Th17 or Th17 cells) (Fig. 2.4A) and transferred cultured T cells into Rag1-deficient mice. Unexpectedly, the control Th17 cell-injected mice started to lose more weight 15 days after administration. Despite a higher frequency of IL-17$^+$ T cells, C2-Th17 cells were unable to induce colitis as severely as control Th17 cells (Fig. 2.4). In line with low anti-CD3 activation conditions (Fig. 2.3B), the increased frequency of FoxP3$^+$ T cells was observed in the colon of the mice injected with C2-treated T cells (Fig. 2.4C). Additionally, we examined the function of C2-treated Th1 cells in colitis. Similar to Th17 cells, cultured Th1 cells induced less inflammation despite increased IFNγ$^+$ T cell frequencies (Fig. 2.5). These results indicate that C2-treated T cells have anti-inflammatory functions in vivo; however their inflammatory cytokine expressions and transcription factors are promoted by C2 in vitro.

C2 and C3 promote IL-10-producing regulatory T cells

Because C2-promoted effector T cells were not inflammatory, we asked to determine the factor that regulates inflammation. To answer this question, we performed a microarray analysis. Gene expressions in Th17 and Th1 cells were compared in the presence and absence of C2. Among a number of genes that are regulated by C2 treatment, we found IL-10 expression was consistently upregulated by C2 in both Th17 and Th1 cells (Fig. 2.6). This led us to investigate the differentiation of naïve $CD4^+$ T cells into IL-10^+ T cells in response to SCFAs. We cultured naïve T cells in Tnp, Th1, and Th17 polarizing conditions with SCFAs. With each condition, IL-10^+ T cells expanded as in a SCFA-dose dependent manner. In addition, C2 or C3 increased T cell subsets that express both IL-10 and IFNγ (Fig. 2.7 A and B). Upregulated IL-10 secretion by SCFAs in culture media was verified at protein level with ELISA and at mRNA level by qRT-PCR (Fig. 2.7 C and D). Although it has been reported that SCFAs enhance both IL-10^+ and $FoxP3^+$ T cells (29, 31), we were unable to reproduce SCFA-dependent IL-10^+ $FoxP3^+$ T cell increase by standard anti-CD3 (5 μg/ml) activation. However, those subsets were expanded by low anti-CD3 (1 μg/ml) activation (Fig. 2.8).

SCFAs stimulated both effector and regulatory T cell differentiation, and these cells showed anti-inflammatory function in a colitis model. To examine the regulatory activity of SCFAs in T cells, we performed an in vitro suppression assay. When we cultured activated T cells with CSFE-labeled $CD4^+CD25^-$ T cells, C2-treated T cells suppressed the proliferation of responder T cells more efficiently than control-T cells. However, C2-treated T cells from IL10-deficient mice did not show suppressed activity (Fig 2.9). This indicates that the SCFA-mediated suppressive function is IL-10 dependent.

So far, we examined the effect of SCFA on $CD4^+$ T cells. Next, we asked if other T cells, such as $CD8^+$ T cells have similar responses to SCFAs. When we cultured $CD8^+$ T cells with SCFAs, we found that IL-10, IFNγ, and IL-17 expressions were also significantly increased in both Tc1 and Tc17 polarizing conditions (Fig. 2.10).

Then, we investigated the impact of SCFAs in vivo by providing C2-containing water to mice. First, we examined the concentration of the major SCFA-C2, C3, and C4- in intestinal tissues and cecal contents. C2 administration significantly increased C2 concentration in cecal contents and colon tissues, whereas the effect on C3 and C4 concentrations was minimal (Fig. 2.11). In line with increased concentration, C2 feeding increased the frequency of IL-10^+ T cells in cecum, while it did not affect cells in secondary lymph nodes (Fig 2.12). We previously reported the impact of C2 feeding on the clearance of *C. rodentium* (38). To examine the regulation of C2 on T cells in bacteria infected conditions, we evaluated the change of effector T cells following C2 feeding. Frequencies of Th1 and Th17 cells were elevated in secondary lymph nodes as well as in cecum, but IL-10^+ T cells were consistent (Fig 2.12). These results explain the dual roles of SCFAs in T cell differentiation. In a steady state, SCFAs promote regulatory T cells but boost effector T cells and enhance immunity in bacteria infected conditions.

Because SCFAs promote different T cell subsets depending on immune stimulation, we applied an anti-CD3 injection (i.p.) model, which induces inflammation in the intestine and increases IL-10^+ T cells (84, 85). In systemic organs, such as the spleen and MLN, both IL-10^+ T cells and effector T cells were expanded via C2 administration. In the intestinal tissues, C2 did not stimulate the frequency and number of IL-10^+ and effector T cells (Fig 2.13 A,B, and C). Histological analysis revealed that C2 feeding ameliorated

anti-CD3 induced inflammation in terminal ileum in an IL-10 dependent manner (Fig 2.13 D).

The SCFA effect on T cells is independent of GPR41 or GPR43

To define the role of GPRs in SCFA-promoted T cell differentiation, first we compared the expression levels of GPR41 and GPR43 between T cells and non-T cells. Cultured T cells or isolated T cells from fresh colons or spleens showed minimal expressions of *Gpr41* and *Gpr43* at mRNA level compared to colonic epithelial cells, and Gr^+ cells (Fig 2.14). To investigate if GPRs are required for SCFA-enhanced T cell differentiation, we prepared naïve $CD4^+$ T cells from GPR41-and GPR43-deficient mice, then cultured in the presence of C2 or C3. Deficiency of GPR41 and GPR43 in the T cells did not affect SCFAs-enhanced Th1, Th17 or IL-10^+ T cell differentiation (Fig 2.15). Next, we examined the role of GPR41 and GPR43 in T cell regulation in vivo. Compared to WT mice, frequencies of IL-17^+, IFNγ^+, and IL-10^+ T cells in GPR-deficient mice were not significantly changed in the spleen, MLN, or colon tissues (Fig 2.16). We further examined effector and IL-10^+ T cell changes by C2-feedingin GPR41- and GPR43-deficient mice. C2 administration promoted frequencies and cell numbers in the colon tissues of both WT and GPR-deficient mice (Fig 2.17). These data suggest that GPR41 and GPR43 expressions are not required for SCFA-dependent T cell differentiation.

SCFAs inhibit HDACs and increase mTOR pathway in T cells

SCFAs are known as histone deacetylases (HDAC) inhibitors and SCFA-mediated HDAC activity is involved in immune cell regulation (86, 87). A recent study reported

that HDAC activity could be regulated in a GPR43-dependent manner, although the direct action of SCFA on T cells was not demonstrated (88). To verify if SCFAs directly affect HDAC activity in T cells, we performed a cell-based HDAC assay, which is designed for SCFAs to enter T cells and inhibit HDAC activity. We compared HDAC activity to SCFAs in activated T cells from WT-, GPR41-, and GPR43-deficient mice. HDAC activity gradually declined as higher concentrations of SCFAs were applied. Interestingly, SCFAs-mediated HDAC inhibition was not influenced by GPR41 or GPR43 expression (Fig. 2.18). Since we verified that SCFAs suppress HDAC activity in T cells, we asked if SCFAs upregulate T cell differentiation via HDAC inhibition. We compared the effect of SCFAs on T cell differentiation to TSA, a class HDAC I and II inhibitor. Similar to C2 or C3, TSA promoted both effector and IL-10^+ T cell differentiation in each polarizing condition (Fig. 2.19).

mTOR-signaling activation is required for not only cellular metabolism, but also for effector or IL-10^+ T cell differentiation (89-91). Because both SCFAs and TSA affected T cell differentiation, we examined their effect on mTOR activity. When $CD4^+$ T cells were activated with SCFAs or TSA, phosphorylation levels of ribosomal protein S6 (rS6), a major target of the mTOR pathway, was increased (Fig 2.20A). Thus, we found that C2 and C3 maintain mTOR activity up to 60 hours and promote mTOR activity in a dose-dependent manner (Fig. 2.20 B). To confirm if SCFA-induced mTOR activity opens doors to T cell differentiation, we inhibited the mTOR pathway with rapamycin (an mTOR inhibitor) and examined if SCFAs were still able to increase IL-10^+ T cell induction. Rapamycin effectively suppressed the frequency and number of effector and IL-10^+ T cells and blocked IL-10 secretion from SCFA-treated T cells (Fig. 2.21). The impact of SCFA-

mediated mTOR activity on T cell differentiation was also verified with AMP kinase (AMPK) activity in T cells. AMPK is involved in cellular metabolism and suppresses mTOR pathways (92-94). We cultured T cells with C2 or C3 in the presence of an AMPK activator, metformin. Metformin treatment, which can suppress mTOR pathways, abolished SCFAs-dependent IL-10^+ T cell increases (Fig. 2.22).

So far, we have investigated the role of C2 and C3 in T cell regulation. Butyrate (C4) is another major SCFA and well recognized as a HDAC inhibitor. We asked if C4 has comparable effects on mTOR activity and T cell differentiation as C2 or C3. C4 promoted mTOR activity and T cell differentiation in dose-dependent manners (Fig. 2.23).

The importance of HDAC inhibition and mTOR activation in SCFA-mediated T cell differentiation was examined. We further investigated the involvement of HDAC inhibition and mTOR pathway. rS6 is a substrate of S6 kinase (S6K) and one study reported that TSA treatment induced the acetylation of S6K (95). We found that C2, C3, and TSA facilitated acetylation of S6K in activated T cells (Fig 2.24). Comprehensively, these results demonstrate the intracellular mechanisms of SCFA-dependent T cell differentiation. SCFAs regulate mTOR activity and HDAC inhibition in T cells, which lead to the acetylation of S6K.

SCFAs also regulate mTOR-related intracellular pathways in T cells

Activated mTOR pathway promotes IL-10 expression through signal transducer and activator of transcription 3 (STAT3) (96). C2 or C3 enhanced phosphorylation of STAT3 in T cells and its boosting effect was similar to IL-6 (Fig. 2.25). However, SCFAs

did not change the activity of extracellular signal-regulated kinase (ERK) pathways (Fig. 2.26), which are involved in IL-10 expression of T cells (97).

2.4 Discussion

We report the role of gut metabolites SCFAs in T cell differentiation and T cell-dependent intestinal inflammation. Major SCFAs, C2, C3, and C4 directly support naïve T cell differentiation into both effector and regulatory T cells. They showed regulatory function and anti-inflammatory effects. The action of SCFAs is not dependent on their receptors, GPR41 or GPR43. Rather, SCFAs directly induced mTOR activation and HDAC inhibition in T cell differentiation. In particular, SCFAs promoted acetylation of the mTOR-S6K molecule. Besides, downstream pathways of mTOR activation were also enhanced by SCFAs.

SCFAs are generated by microbial fermentation in the gut. GPR41 or GPR43 are major SCFA receptors. SCFAs activate these receptors and regulate various immune responses. However, the role of GPR41 or GPR43 is intriguing because their expressions are variable in different cell types. In our study, we demonstrated the minimal expression of GPR41 and GPR43 in both splenic and colonic T cells. SCFA-mediated T cell differentiation was independent of GPR41 and GPR43 in vitro and in vivo.

Instead, we discovered the intracellular mechanisms of SCFA influence on T cell differentiation. Activation of mTOR pathways is required for effector and $IL10^{+}$ T cell differentiation (96). Accordingly, we found that SCFAs promoted mTOR activity in control of T cell differentiation. On the other hand, blocking mTOR activity with

rapamycin or AMPK activator abolished the effect of SCFAs on T cell differentiation. STAT3 signaling is downstream of mTOR pathways and their activation modulates effector and IL-10^+ T cell generation (98, 99). In this regard, we examined STAT3 activation and glucose uptake levels in SCFA-treated T cells. C2 and C3 enhanced STAT3 phosphorylation. Histone acetylation regulates gene transcription and determines the function of T cells (100). SCFAs are HDAC inhibitors, and recent studies reported that SCFA-mediated HDAC inhibition promotes regulatory T cell expansion (29-31). In this study, we examined the effect of SCFAs on HDAC activity in activated T cells. We found that C2, C3, and C4 directly inhibited HDAC activity in a GPR41- and GPR43-independent manner. C2 and C3 showed comparable effect on effector or IL-10^+ T cell differentiation as TSA, a HDAC I and II inhibitor. So far, we have showed that SCFAs regulate T cell differentiation through two intracellular pathways, mTOR activation and HDAC inhibition. In order to fill the gap between the suggested mechanisms, we validated that SCFAs enhance mTOR-S6K acetylation, which can be a regulatory point of T cell differentiation.

It has been thought that SCFAs mainly affect regulatory T cell differentiation and anti-inflammatory cytokine expression (29-31). A compelling observation was that SCFA-induced amixed T cells express both regulatory and effector cytokines. SCFA-treated T cells alleviated colitis and suppressed other T cell proliferation. Our results imply that SCFAs regulate T cell differentiation by immunological stimulation and cytokine milieu. In mice, SCFA administration augmented IL-10^+ T cells in regular conditions. Upon anti-CD3 stimulation or bacterial infection, however, effector T cells expanded but regulatory T cells did not. We also found that the level of TCR-activation directs SCFA-mediated T

cell differentiation. In a weaker TCR-activation conditions, SCFAs induced more FoxP3^{+} T cells.

Our study emphasizes the importance of gut metabolites in the immune system and homeostasis. SCFAs, major gut bacterial products, control adaptive immunity by regulating T cell differentiation. These results also provide an example of how the host immune system harnesses commensal bacterial metabolites for the induction of specialized effector and regulatory T cells. Hence, SCFA levels and the immunological context control T cell differentiation. Overall, this study has many practical ramifications in the regulation of tissue inflammation and immunity.

2.5 Summary and future directions

2.5.1 Summary

We investigated the impact of SCFAs on T cell regulation and T cell mediated inflammation and immunity. SCFAs promote both effector and regulatory T cells. In vitro and in vivo studies revealed that SCFA-induced T cell has suppressive activity on responder T cells and ameliorated T cell-mediated colitis. In addition, SCFA administration enhanced Th17 cell response to *C. rodentium* infection and efficiently cleared invading pathogens. Interestingly, indicated functions of SCFAs were GPR41- and GPR43-independent. In splenic or colonic T cells, gene expressions of these receptors were rarely detectable. SCFAs are known as HDAC inhibitors and we demonstrated that SCFAs suppressed HDAC activity in T cells. SCFAs increased the phosphorylation of rS6, which indicates mTOR activation. The acetylation of p70 S6 kinase was also enhanced by SCFAs.

2.5.2 Future direction

The more intricate mechanism by which SCFAs regulate mTOR or HDAC activity in T cell need to be studied. First, we will examine how SCFAs regulate mTOR activity. AMPK activation is known to block mTOR pathways and affect T cell differentiation (92), and we demonstrated that the AMPK activator metformin inhibited SCFA-mediated IL-10^+ T cell induction. To verify the effect of SCFAs on mTOR upstream molecules, we will examine the AMPK activity level in SCFA-treated T cells. In the case that AMPK activity is suppressed by SCFA, we will further examine if SCFAs control AMPK upstream signal. The liver kinase B1 (LKB1) is a serine/threonine kinase that signals for AMPK activation and control T cell regulation (101). We will first measure mRNA and protein expression of LKB1 in SCFA-treated T cells. Then, we will culture T cell with LKB1-siRNA in the presence or absence of SCFAs (102), and examine whether SCFAs-induced mTOR activation or IL-10^+ T cells.

Next, we will ask how SCFAs regulate HDAC activity in T cells. We found that the*Hat1* gene was upregulated by SCFAs in different T cell polarized condition by microarray analysis (data not shown). HAT represses HDAC activity (103), and we will examine if SCFAs enhance histone acetylation via HAT activation. We will utilize a HAT activity assay kit that detects NADH, released by HAT activated conditions. Next we will ask if SCFA-induced HAT activity regulates IL-10 producing T cells. Among several co-activators of HATs, CBP and p300 induce hyper-acetylation in histone N-terminal tail lysine in T cells. We will investigate the role of SCFAs in p300 mediated IL-10 expression with a luciferase reporter assay. WT p300 or mutant p300 plasmids will be co-transfected

with the IL-10 promotor gene inserted reporter plasmid (pGL4.10-IL10) into naive T cell or T cell lines. Transfected cells will be cultured in the presence of SCFAs and IL-10 promotor activity will be determined.

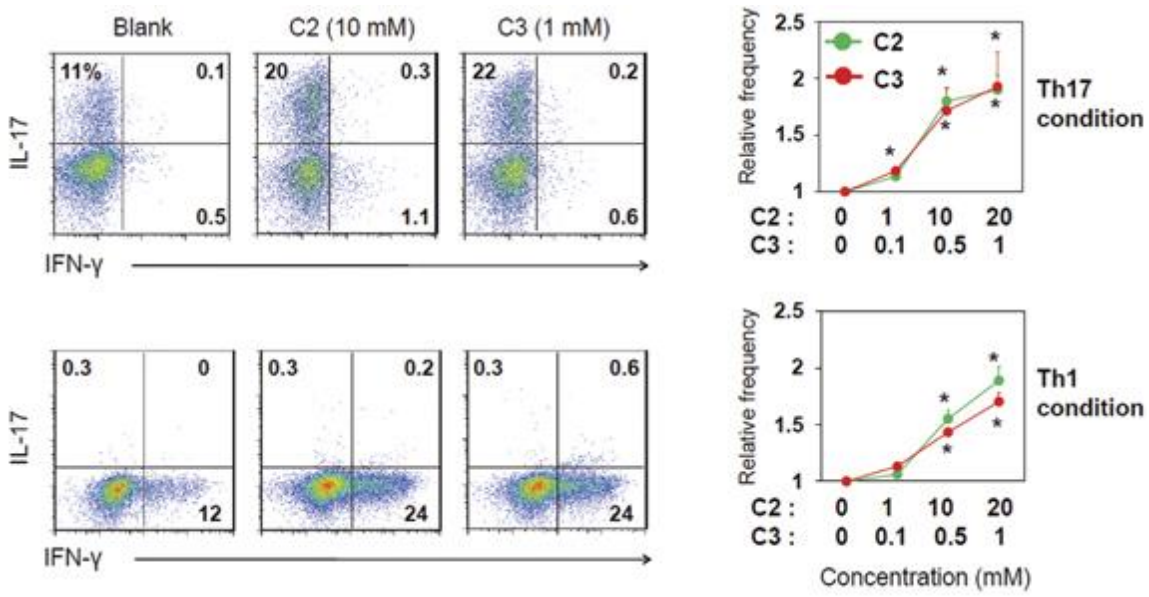

Figure 2.1 Effect of Short chain fatty acids (SCFAs) on effector T cell (Th17 and Th1 cells) differentiation in a dose dependent manner.

Major SCFAs acetate (C2) and propionate (C3) promoted naïve $CD4^+$ T cell differentiation into Th17 and Th1 cells. Naïve T cells were isolated and activated with anti-CD3/CD28 in the presence of various concentrations of C2 or C3. Th17 cell differentiation was determined after a five or six day culture with IL-1β, IL-6, IL-21, IL23, TGFβ1, anti-IL-4 and anti-IFNγ. Th1 cell differentiation was determined after five or six day culture in Th1 conditions (IL-12, IL-2, and anti-IL-4). *Significant differences resulted from blank groups (no treatment with C3 or C3 ≤ 0.05).

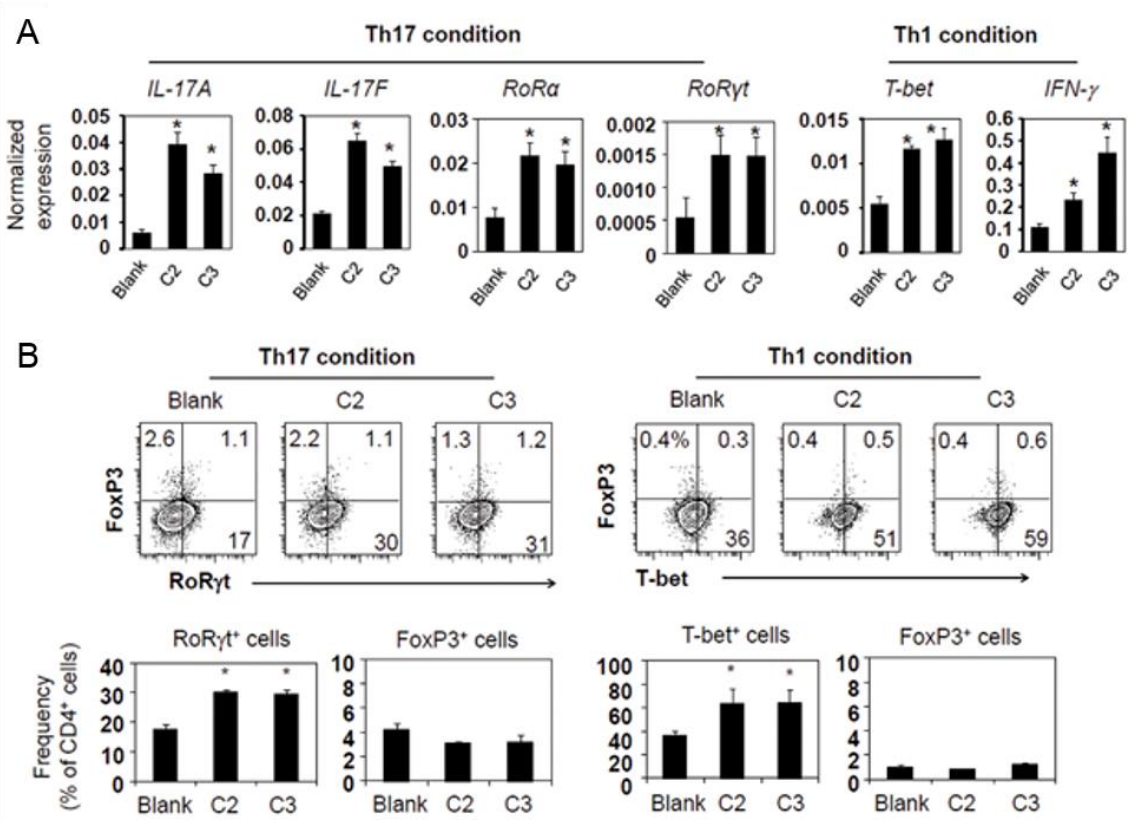

Figure 2.2 Regulation of signature genes and transcription factors by SCFAs in Th17 and Th1 cells.

(A) mRNA expression level of selected genes and transcription factors were determined by quantitative real-time PCR. Naïve T cells were isolated and cultured with SCFAs for 3 days in Th17- or Th1-polarizing conditions. (B) Expression of FoxP3, RoRγt, and T-bet were examined in Th17 or Th1 cells. Naïve T cells were cultured with C2 or C3 for five or six days. *Significant differences resulted from blank groups (no treatment with C3 or C3, $P \leq 0.05$).

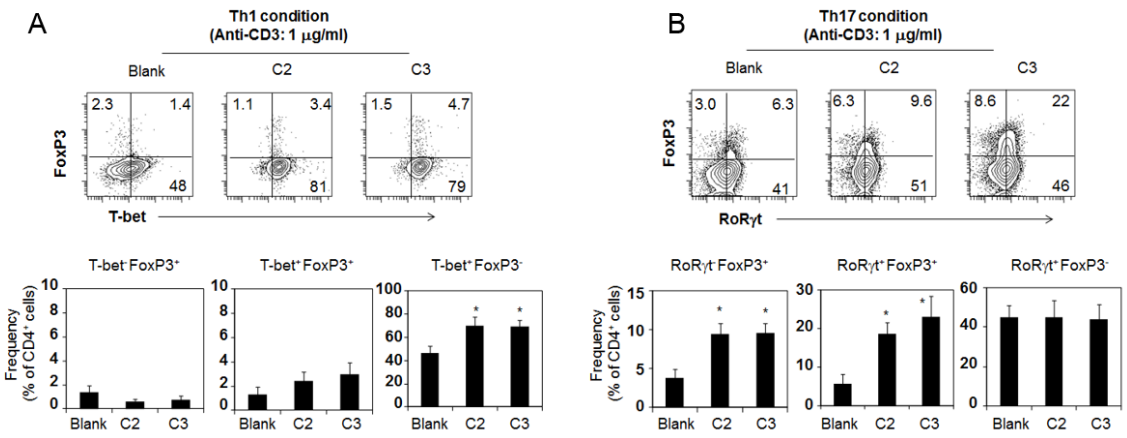

Figure 2.3 FoxP3 expression in T-bet$^+$ or RORγt$^+$ T cells with a weak anti-CD3 (1 μg/ml) activation.

Naïve T cells were cultured in Th-1 or Th17-polarized conditions for five or six days. Cell were activated with a low dose of anti-CD3 (1 μg/ml) in combination with C2 (10 mM) or C3 (1 mM). Frequencies of FoxP3$^+$ in T-bet$^+$ T cells (A) or RORγt$^+$ cells (B) were determined. Representative or pooled data of three experiments are shown. *Significant differences from blank groups ($P \leq 0.05$).

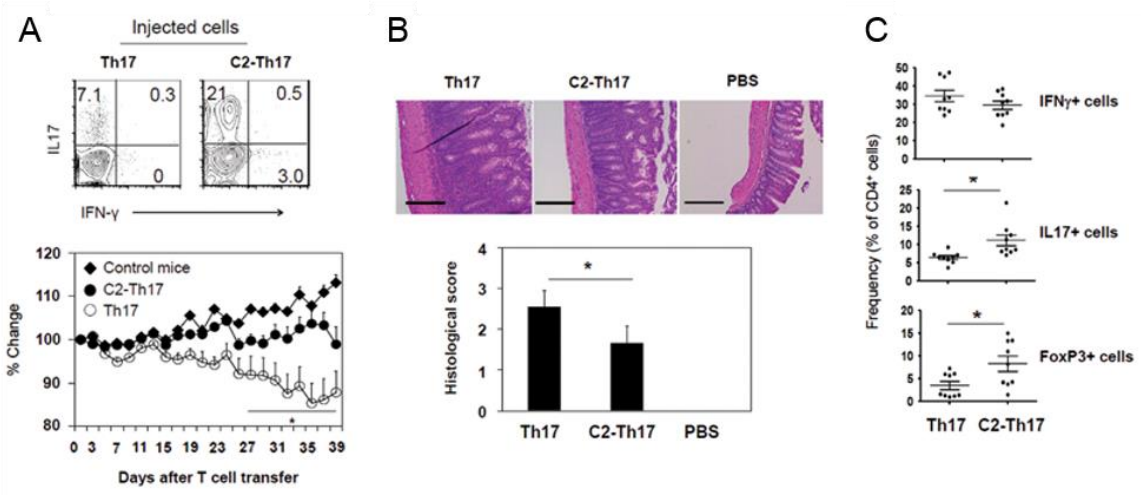

Figure 2.4 Role of SCFA-treated Th17 cells in T cell-mediated colitis.

(A) Phenotype of injected Th17 cells and body weight changes in host mice. Naïve T cells were cultured with C2 in Th17 condition for five or six days. (B) Histological changes in the distal colon were determined by HnE staining (x 100 original magnification; scale bar = 200 μm). (C) Frequencies of T cell subsets (Th1, Th17 and FoxP3$^+$ T cells) were examined in the distal colon by flow cytometry. Representative or pooled data from two or three experiments are shown (n=5-10 for A, B, or C). *Significant differences from indicated groups ($P \leq 0.05$).

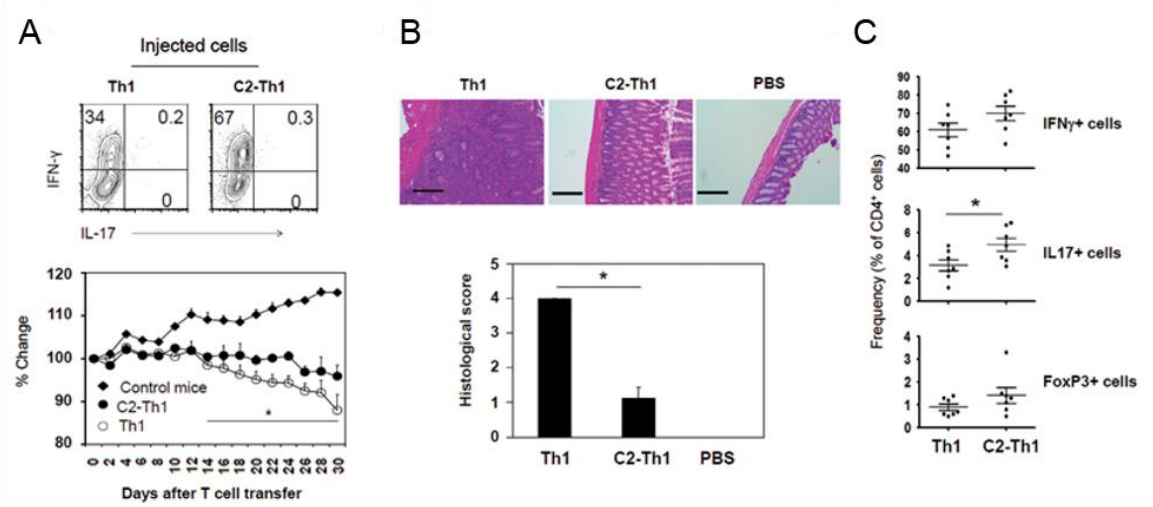

Figure 2.5 Role of SCFA treated Th1cell in T cell-mediated colitis.

(A) Phenotype of injected Th1 cells and body weight changes in host mice. Naïve T cells were cultured with C2 in Th1 condition for five or six days. (B) Histological changes in distal colon were determined by HnE staining (x 100 original magnification; scale bar = 200 μm). (C) Frequencies of T cell subtypes (Th1, Th17 and FoxP3^{+} T cells) were examined in the distal colon by flow cytometry. Representative or pooled data from two or three experiments are shown (n=4-7 for A, B, or C). *Significant differences from indicated groups ($P \leq 0.05$).

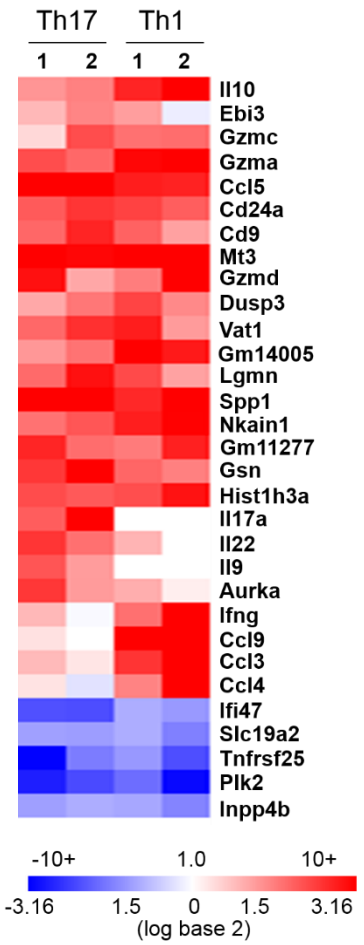

Figure 2.6 SCFA-mediated gene expression in T cells.

Microarray analysis identified genes that are regulated by SCFAs**.** Naïve T cells were isolated and cultured with C2 for three days in Th17 or Th1 polarizing conditions. Data from the two experiments are shown.

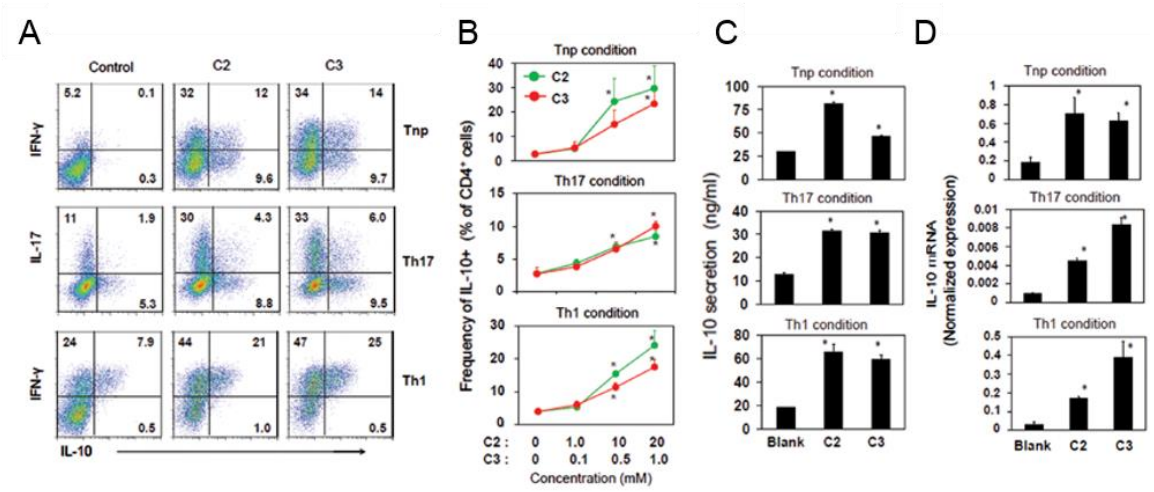

Figure 2.7Effect of SCFAs on IL-10 expression in T cells.

(A) Changes in cytokine expressions were determined by flow cytometry. Naïve $CD4^+$ T cells were cultured with SCFAs in Tnp, Th17, and Th1 conditions. (B) SCFA-induced IL-10 expression in each T cell subset in a dose dependent manner. Secreted IL-10 was examined using a conditioned media by ELISA (C), and IL-10 mRNA level was determined by quantitative real-time PCR (D). *Significant differences from blank groups or between indicated groups ($P \leq 0.05$).

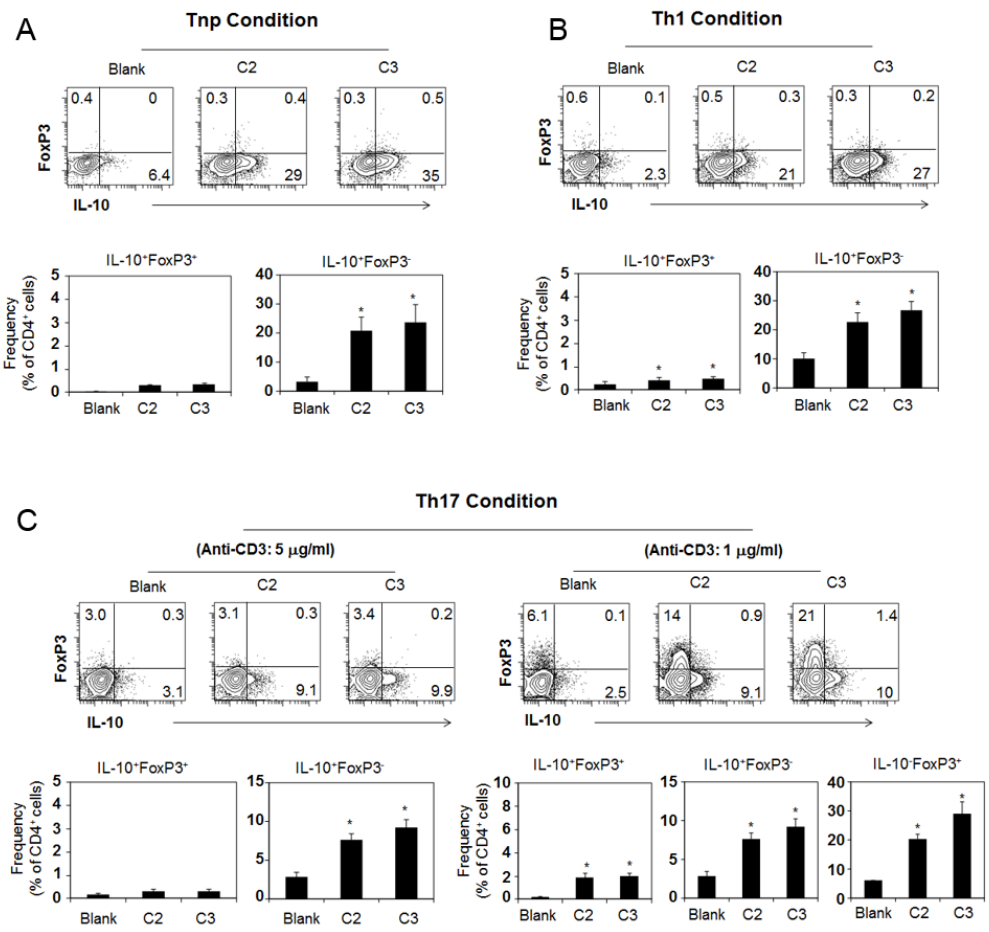

Figure 2.8 SCFA-enhanced FoxP3$^+$ and IL10$^+$ T cells.

Naïve T cells were cultured in Tnp (A), Th1 (B), or Th17 (C) polarized conditions for five to six days. Cell were activated with two different doses of anti-CD3 (1 and 5 μg/ml) in the presence of C2 (10 mM) or C3 (1 mM). Frequencies of FoxP3$^+$ and IL-10$^+$ T cells were determined by flow cytometry. Representative or pooled data of the three experiments are shown. *Significant differences from blank groups ($P \leq 0.05$).

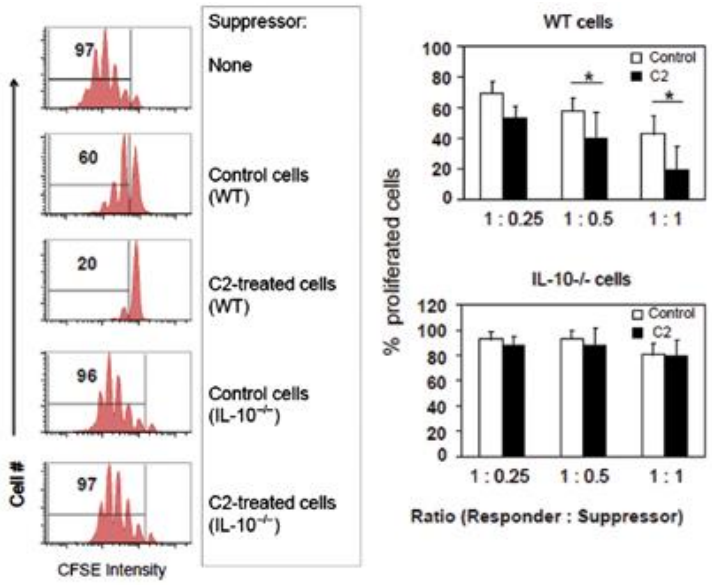

Figure 2.9 Suppressive functions of SCFA-enhanced IL-10 in T cell proliferation.

$CD4^+$ T cells were isolated from WT or IL10-deficient mice and cultured in the presence or absence of C2 in Th1 polarizing condition. C2-treated suppressor T cells were co-cultured with responder cells (CFSE-labeled $CD4^+CD25^-$ T cells) for three days. Suppressive activity of C2-treated T cells was evaluated by flow cytometry. *Significant differences from control groups ($P \leq 0.05$).

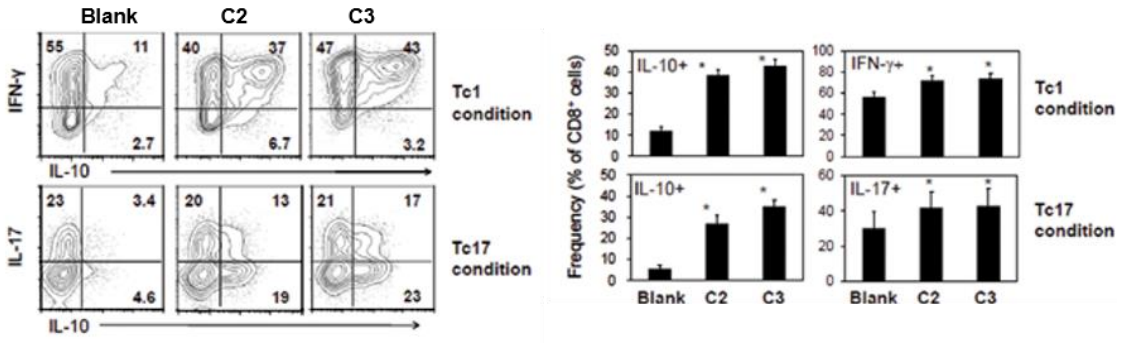

Figure 2.10 SCFA-enhanced IL-10 in CD8$^+$ T cells.

Total CD8$^+$ T cells were isolated and cultured with C2 (10 mM) or C3 (1 mM) in Tc1 (IL-2, IL-12, and anti-IL-4) or Tc17 (IL-1β, IL-6, IL-21, IL23, TGFβ1, anti-IL-4 and anti-IFNγ) polarizing conditions. After a five or six day culture, frequencies of IL-10, IL-17, or IFNγ$^+$ cells were determined with flow cytometry. *Significant differences from blank groups or between indicated groups ($P \leq 0.05$).

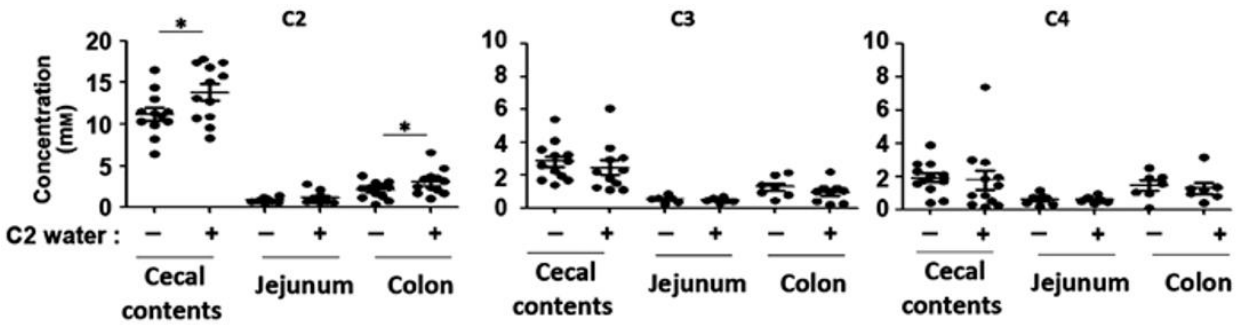

Figure 2.11 Changes of SCFA concentrations in cecal contents and intestinal tissues by C2 feeding.

Mice were administered C2-infused (200 mM) drinking water. The cecal material, jejunum, and colon tissues were collected from C2-fed or control mice. Concentrations of C2, C3, and C4 were determined by liquid chromatography-mass spectrometry. *Significant differences between indicated groups ($P \leq 0.05$).

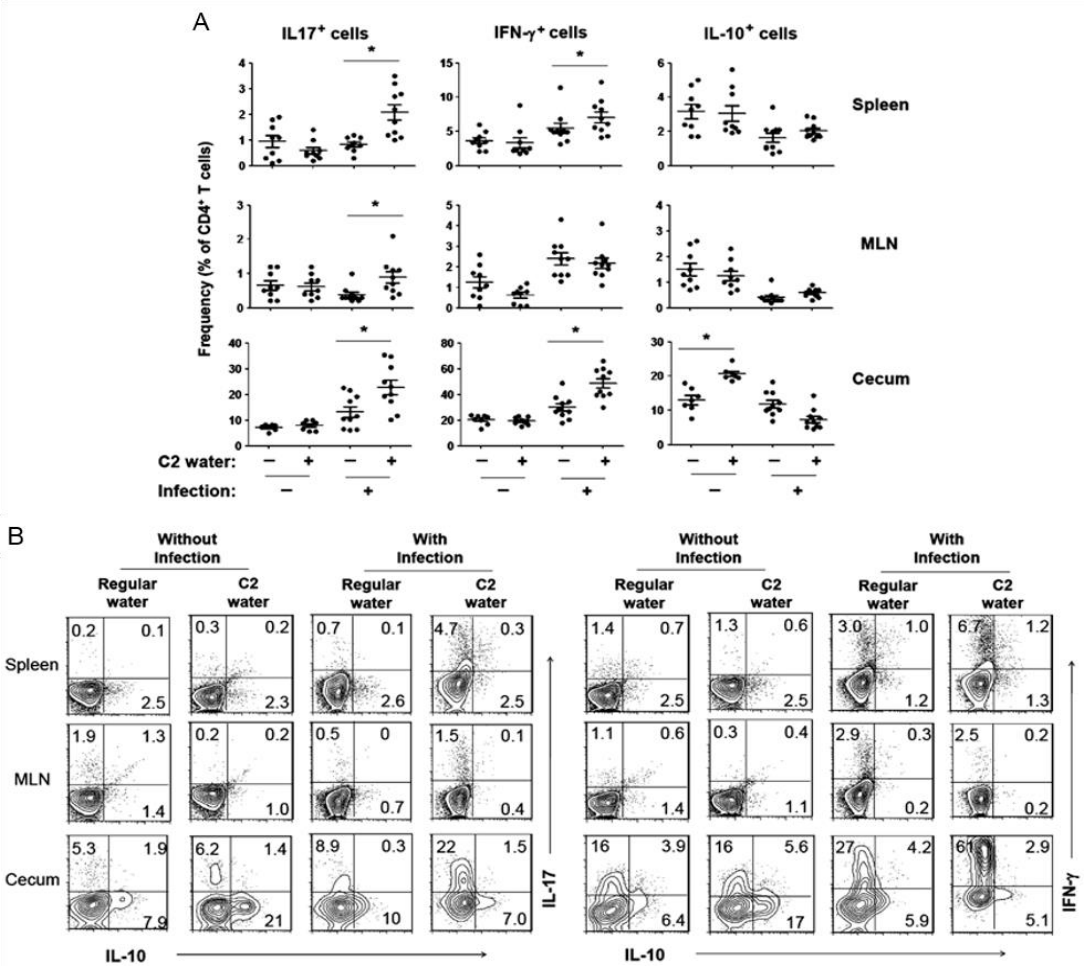

Figure 2.12 The distinct effect of SCFAs on effector or IL-10$^+$ T cells from a bacterial infection.

Mice were fed normal or C2-containing water. Indicated mice were infected with *Citrobacter rodentium*. Changes of Th1, Th17 and IL-10$^+$ T cells were examined in the spleen, MLN, or cecum by flow cytometry fourteen days of post infection. (A) Pooled data (n=7-9) or (B) representative dot plots are shown. *Significant differences between indicated groups ($P \leq 0.05$).

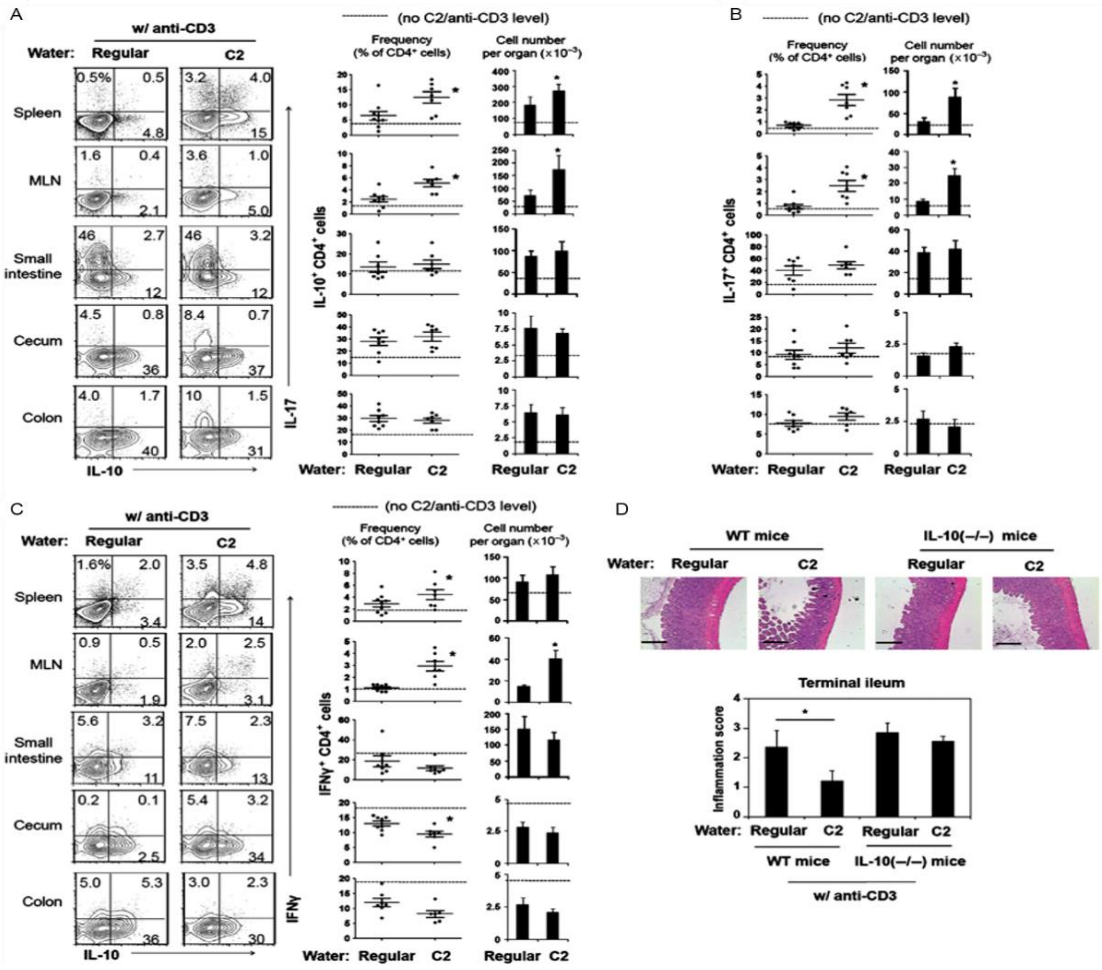

Figure 2.13 Anti-inflammatory role of SCFAs in anti-CD3 induced colitis.

Mice were fed normal or C2-containing water, followed by an anti-CD3 antibody (145-2C11) injection. Mice were euthanized 52 hours later and frequencies or numbers of IL-10^+ T cells (A), Th17 cells (B), or Th1 cells (C) were determined by flow cytometry (n=6-9/group). (D) Inflammation severity was compared between WT and IL10-deficient mice after anti-CD3 injection and C2 feeding. *Significant differences from regular water fed mice and indicated groups ($P \leq 0.05$).

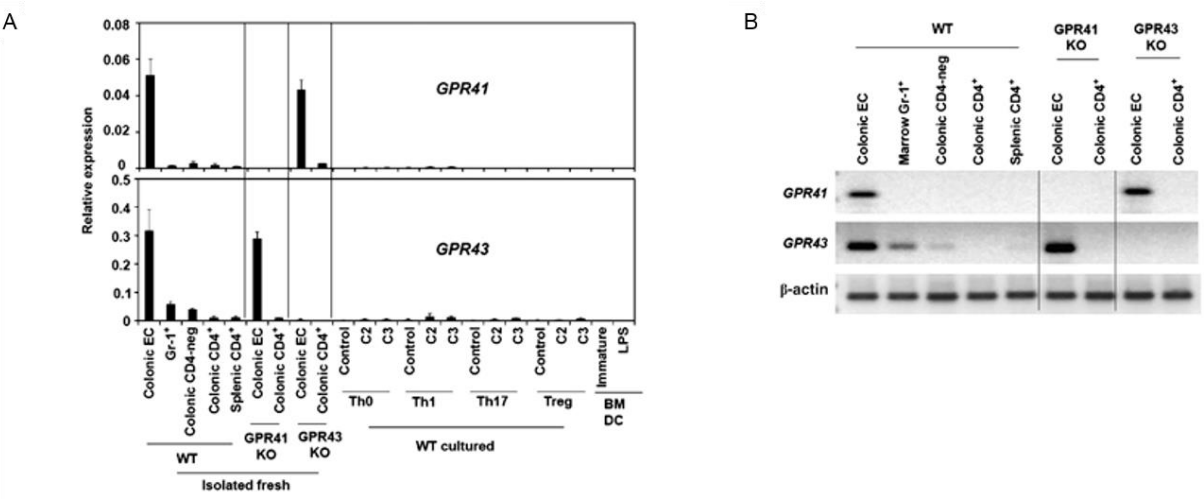

Figure 2.14 Expression of SCFA receptors, GPR41 and GPR43 in T cells and other subtypes.

Cultured or splenic $CD4^+$ T cells, colonic epithelial cells ($CD326^+$), $CD4^+$ or $CD4^-$ T cells of colon, bone marrow $Gr1^+$cells, and cultured BM-DCs were prepared from WT-, GPR41-, or GPR43-deficient mice. mRNA levels of *GPR41* or *GPR43* was determined by quantitative real time-PCR (A) or conventional PCR (B).

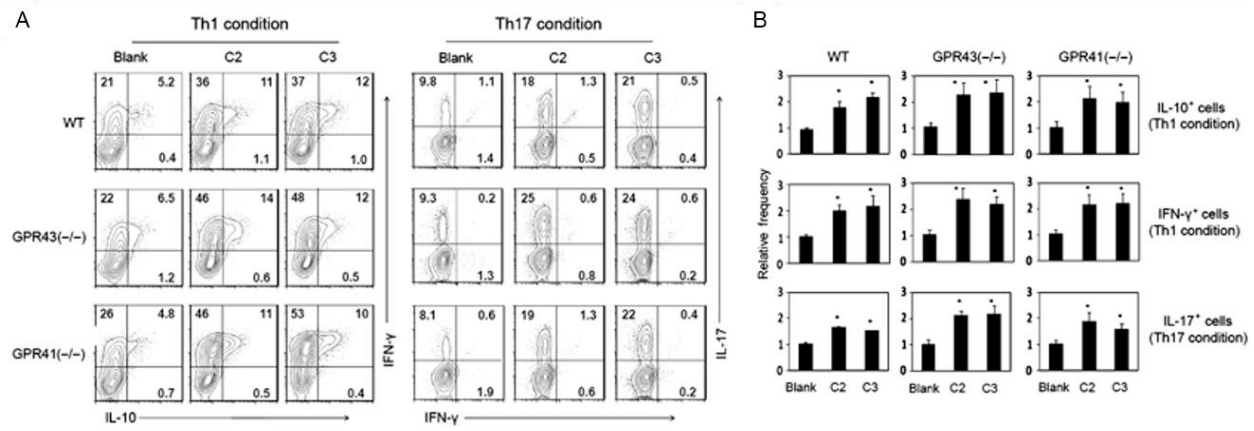

Figure 2.15 SCFA-promoted T cell differentiations in GPR41- or GPR43-deficient CD4+ T cells.

Naïve $CD4^+$ T cells were isolated from WT, GPR41-, or GPR43-deficient mice and cultured in Th1 or Th17 polarizing conditions in the presence of C2 or C3. After five to six days of culture, frequencies of IL-10, IL-17, or $IFN\gamma^+$ cells were determined by flow cytometry. Representative dot plots (A) and pooled data from three individual experiments are shown (B). *Significant differences from blank groups ($P \leq 0.05$).

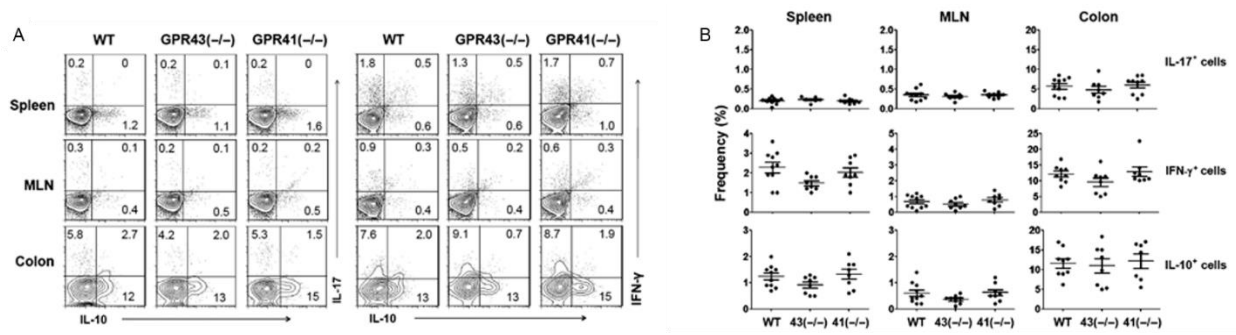

Figure 2.16 Normal population of effector and IL-10$^+$ T cells in GPR41- and GPR43-deficient mice.

WT-, GPR41-, and GPR43-deficient mice of six to nine weeks of age were prepared and cells were collected from indicated organs. Frequencies of Th17, Th1, or IL-10$^+$ T cells were shown from WT- and GPR-deficient mice. *Significant differences from WT groups ($P \leq 0.05$).

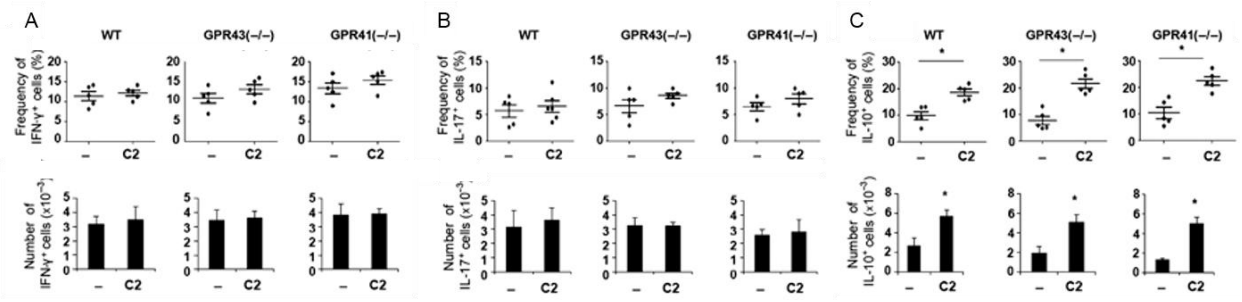

Figure 2.17 Induction of IL-10$^+$ T cells in SCFA-fed WT-, GPR41-, and GPR43-deficient mice.

WT-, GPR41-, and GPR43-deficient mice were given C2-containing water for six to eight weeks and colonic cells were collected. Frequencies and numbers of Th1 (A), Th17 (B) or IL-10$^+$ T cells (C) were shown in WT and GPR-deficient mice. Pooled data (n=7-10) are shown. *Significant differences from WT groups ($P \leq 0.05$).

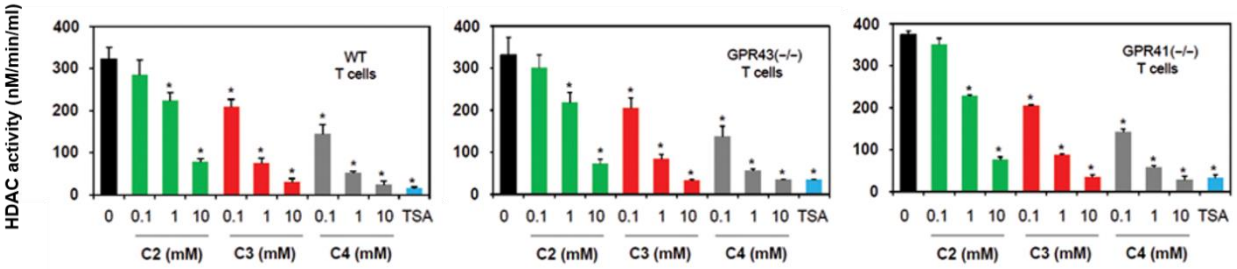

Figure 2.18 Inhibition of histone deacetylases (HDACs) by SCFAs in GPR41- and GPR43-independent manners.

Cell-based HDAC activity by SCFAs was measured in WT, GPR41-, and GPR43-deficient T cells. Naïve $CD4^{+}$T cells were cultured for two days, followed by additional incubation with SCFAs or trichostatin A (TSA) for two hours, and assayed for the HDAC activity. *Significant differences from WT groups ($P \leq 0.05$).

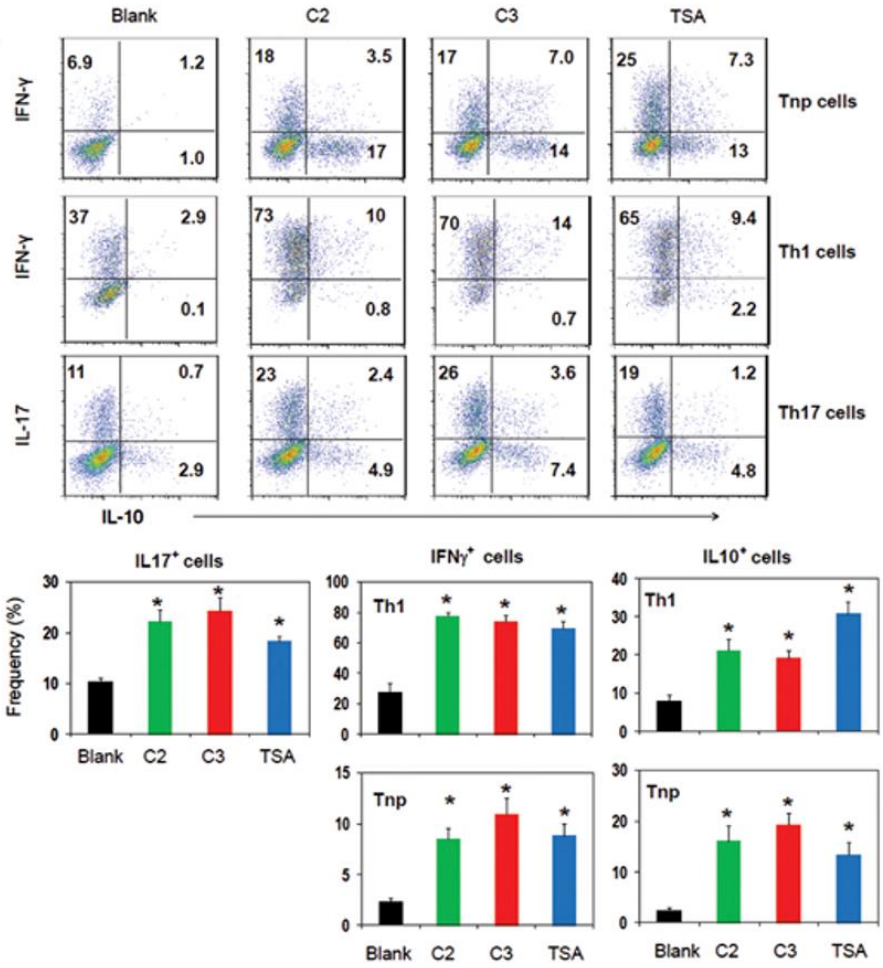

Figure 2.19 Comparison of SCFAs and TSA in regulating T cell differentiation.

Naïve $CD4^+$ T cells were cultured in Tnp, Th1 or Th17 polarizing conditions in the presence of SCFAs or TSA. After a five to six day culture, frequencies of IL-10, IL-17, or $IFN\gamma^+$ T cells were examined by flow cytometry. Representative dot plots (A) and pooled data from three individual experiments are shown (B). *Significant differences from blank groups ($P \leq 0.05$).

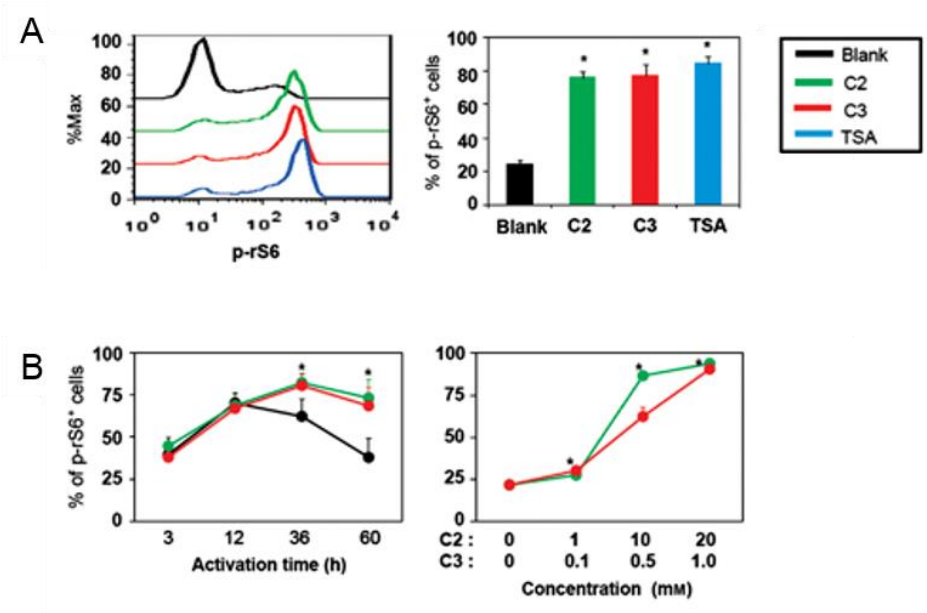

Figure 2.20 SCFA-mediated mTOR activity in T cells.

(A) T cells were activated with anti-CD3/CD28 for three days in the presence of SCFAs or TSA. For mTOR activity, the phosphorylation of rS6 was evaluated. (B) Kinetics (0-60 hours) of mTOR activity (left) and SCFA dose-dependent mTOR activity (right) in T cells were examined by flow cytometry. *Significant differences from blank groups ($P \leq 0.05$).

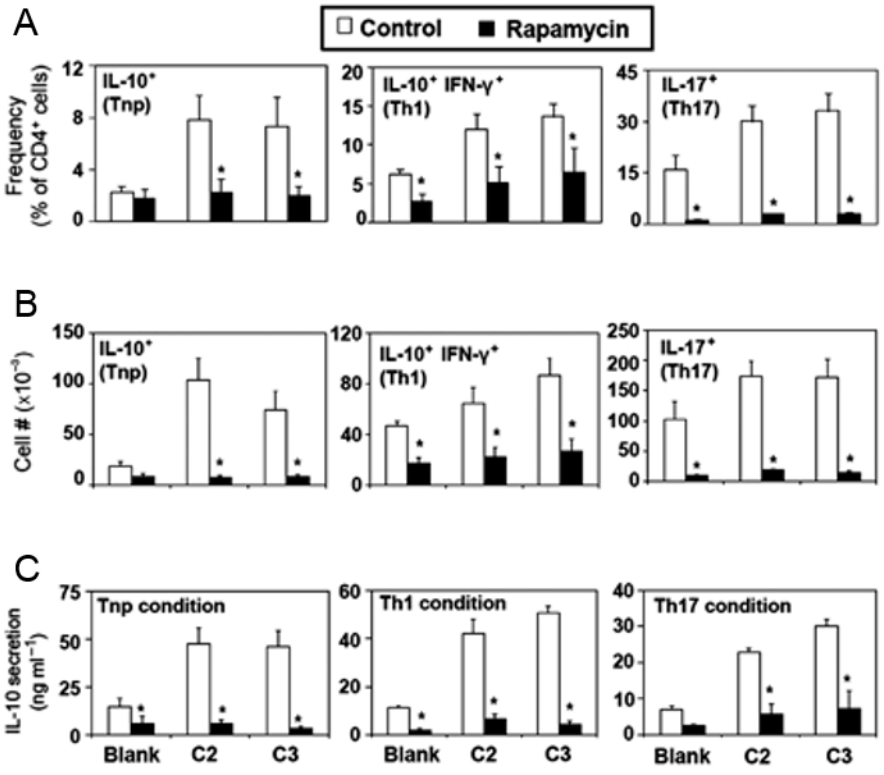

Figure 2.21 Effect of mTOR inhibition on SCFA-promoted T cell differentiation.

Naïve $CD4^+$ T cells were cultured in Tnp, Th1 or Th17 polarizing conditions in the presence of SCFAs and rapamycin (25 nM). After a five to six day culture, frequencies (A) and cell numbers (B) of IL-10, IL-17, or $IFN\gamma^+$ T cells were examined by flow cytometry. (C) Secreted IL-10 from cultured media was determined by an enzyme-linked immunosorbent assay (ELISA) assay. Pooled data from at least three different experiments are shown. *Significant differences from control groups ($P \leq 0.05$).

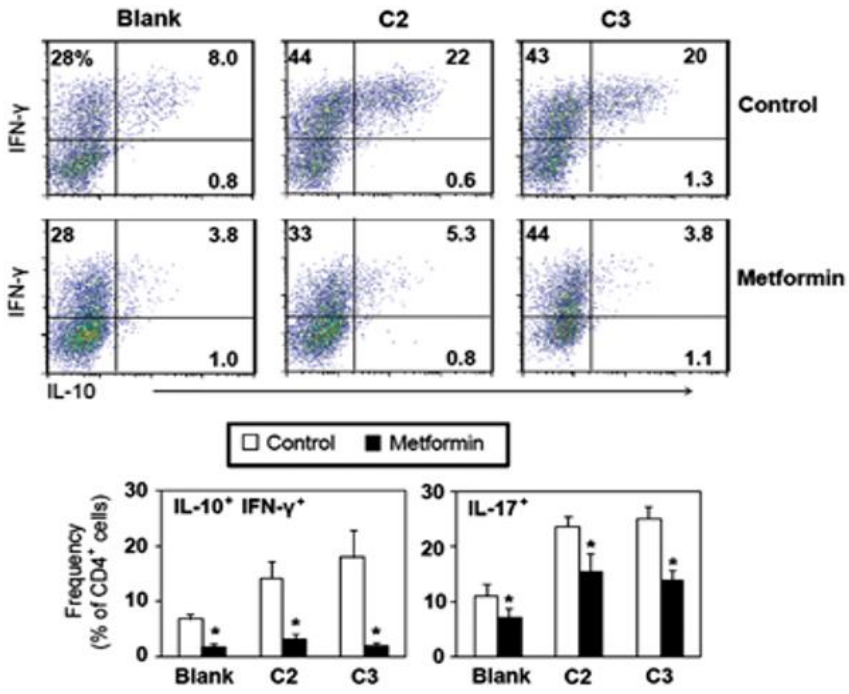

Figure 2.22 Effect of AMPK activation on SCFA-promoted T cell differentiation.

Naïve $CD4^+$ T cells were cultured for five to six days in Th1 or Th17 polarizing conditions in the presence of SCFAs and metformin (1mM). Changes in frequencies of $IL\text{-}10^+IFN\gamma^+$ cells and $IL\text{-}17^+$ T cells were examined by flow cytometry. Representative and pooled data are shown from at least three different experiments. *Significant differences from blank groups ($P \leq 0.05$).

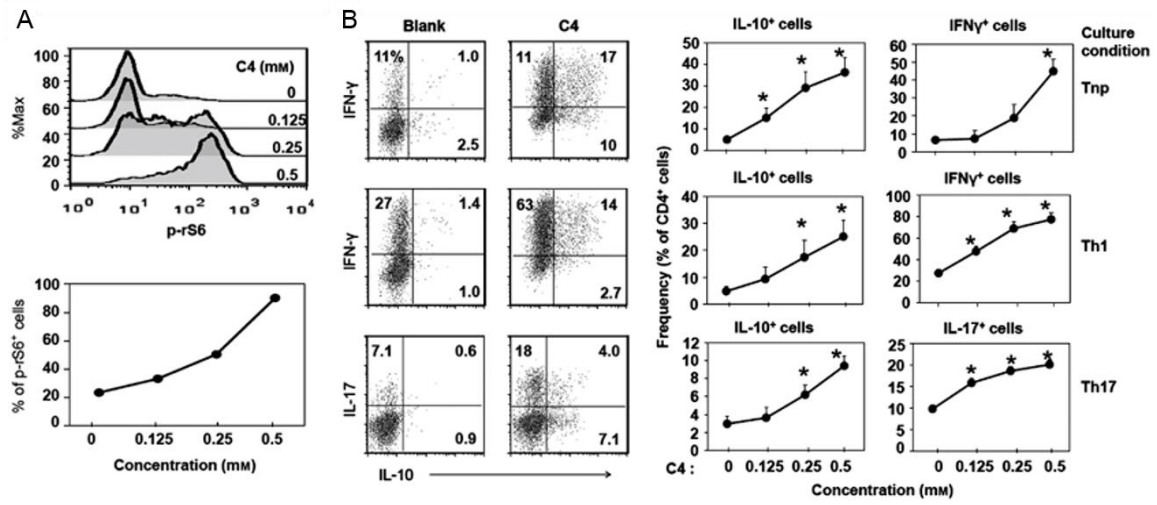

Figure 2.23 Butyrate (C4) effect on mTOR activity and T cell differentiation.

Naïve $CD4^+$ T cells were activated with aCD3/CD28 in Tnp conditions for three days (A) or five to six days (B) with indicated concentrations of C4. (A) mTOR activity in T cells was examined with antibody to rS6 phosphorylation. (B) T cell differentiation in Tnp, Th1, and Th17 polarizing conditions was determined by flow cytometry. Representative and pooled data from three different experiments are shown. *Significant differences from blank groups ($P \leq 0.05$).

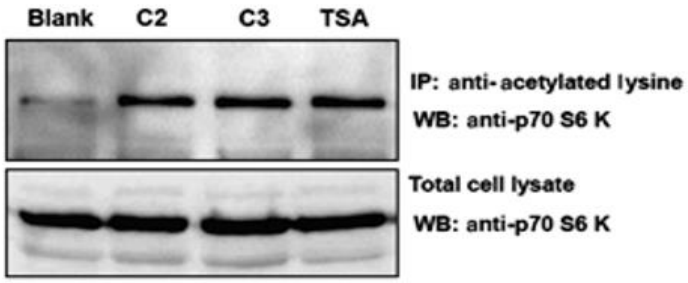

Figure 2.24 SCFA-mediated acetylation of S6K in T cell.

T cell lysates were prepared after three-day activation with anti-CD3/CD28 in the presence of SCFAs or TSA. The lysates were precipitated with an anti-acetylated lysine antibody. To evaluate the acetylation of S6K, immunoprecipitates of acetylated lysine were incubated with an anti-S6K antibody and detected with the western blotting method (upper). In addition, the S6K activity in the total cells were determined (lower). Representative data from the three individual experiments are shown.

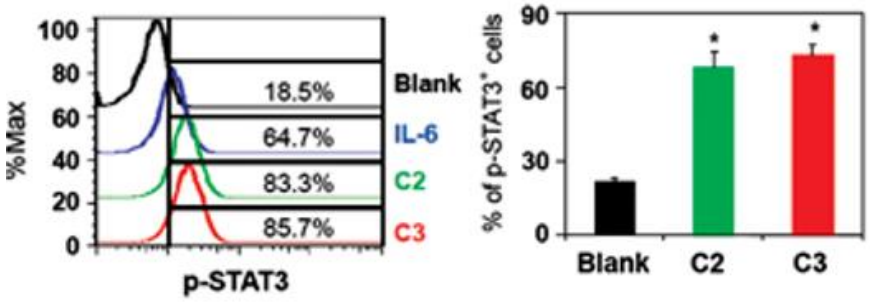

Figure 2.25 Effect of SCFAs on STAT3 activation in T cells.

Naïve $CD4^+$ T cells were activated with aCD3/CD28 and hIL-2 in the presence of SCFAs. After three days, antibody to phosphorylation of STAT3 was used and determined the activity of STAT3 by flow cytometry. Representative and pooled data from at least three different experiments are shown. *Significant differences from blank group ($P \leq 0.05$).

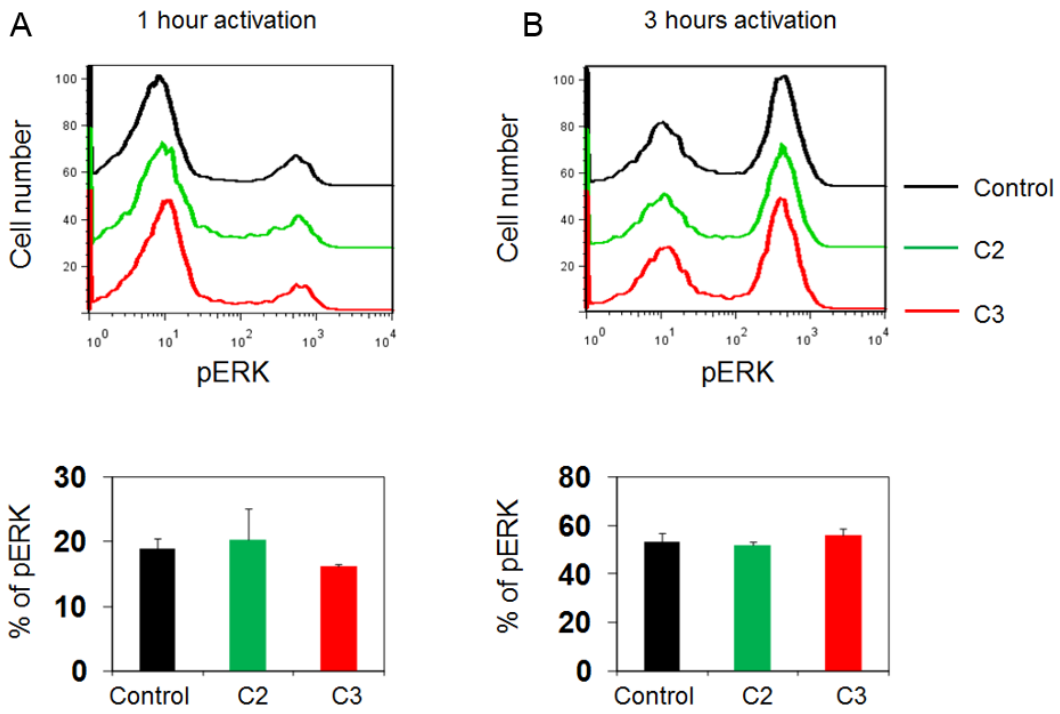

Figure 2.26 Effect of SCFAs on ERK activation in T cells.

Naïve $CD4^+$ T cells were activated with aCD3/CD28 in the presence of SCFAs for one hour (A) or three hours (B). After the activation, an antibody to phosphorylation of MAPK (Erk1/2) was applied and examined the activity of ERK pathways by flow cytometry. Representative and pooled data from three different experiments are shown. *Significant differences from control groups ($P \leq 0.05$).

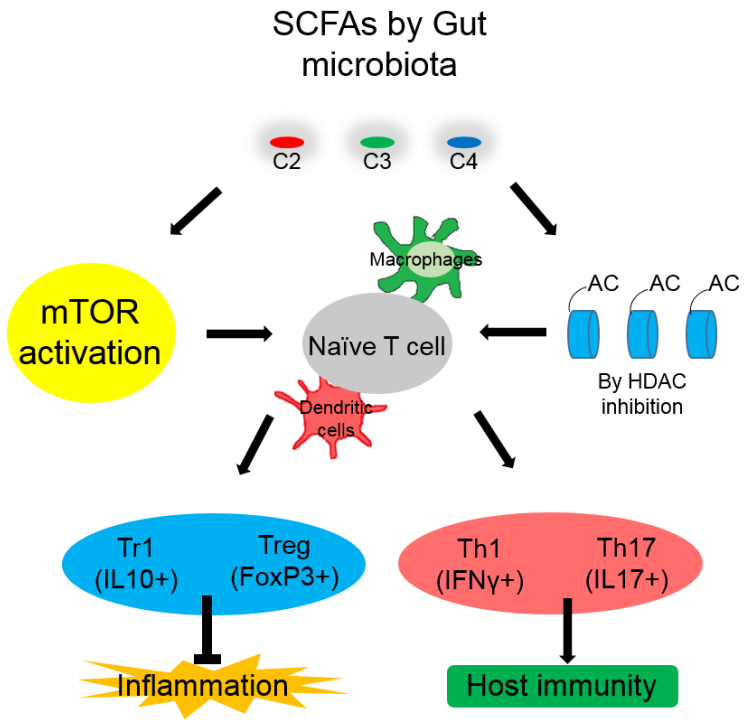

Figure 2.27 Regulation of SCFAs during T cell differentiation and underlying intracellular mechanisms.

SCFAs promote both regulatory and effector T cells differentiation. These cells have either anti-inflammatory function or support host immunity. SCFAs directly activate mTOR pathways or inhibit the HDAC activity required for T cell differentiation.

CHAPTER 3. PROLONGED EXPOSURE TO SHORT CHAIN FATTY ACIDS PROMOTES URETERAL OBSTRUCTION AND HYDRONEPHROSIS IN A T CELL-DEPENDENT MANNER

3.1 Introduction

Intestinal microbiota is critical to maintaining the homeostasis of the intestines as well as other peripheral organs. Bacterial composition is changed by dietary ingredient and affects gut barrier function. In symbiotic conditions, beneficial metabolites such as SCFAs are produced and support epithelial integrity. SCFAs also provide energy sources and regulate immune responses in SCFA receptor-dependent or independent manners. On the other hand, pathobiont-producing metabolites exacerbate inflammation

In T cells, the expression of SCFAs receptors G protein-coupled receptors (GPCRs), is minimal. Hence, SCFAs inhibit histone deacetylase (HDAC) and activate mTOR pathways that control of T cell regulation. Environmental factors, such as infection or inflammation, direct SCFAs to induce effector or regulatory T cells. In the case of a bacterial infection, SCFAs promote host immunity by increasing effector T cell that fight invading pathogens. Besides, SCFAs expand colonic regulatory T cells in inflammatory conditions. While intestinal SCFA actions are well established, the role of SCFAs in the renal system has not been clearly determined. For this reason, we treated mice with water containing SCFAs and examined immunological changes in the renal tissues.

Unexpectedly, SCFAs feedings for four weeks or longer induced ureteral obstruction and hydronephrosis. We found that T cells and gut microbiota were required for disease development. mTOR pathway was activated in affected mice and the SCFA-induced disease was prevented by the mTOR inhibitor treatment. Results suggest that prolonged exposure to SCFAs has the potential to develop renal inflammation.

3.2 Materials &Methods

Mice and treatments

C57BL/6 mice (originally from Harlan, Indianapolis, IN), Gpr41(-/-) mice (provided by M. Yanagisawa, UT Southwestern Medical Center at Dallas), Gpr43(-/-) mice (Deltagen, San Mateo, CA), and TCRβ-deficient mice (B6.129P2-Tcrbtm1Mom/J, The Jackson Laboratory) were kept at Purdue for at least 12 months before use. Mice were treated with sodium acetate (C2 at 100, 150, or 200 mM, pH 7.5), sodium propionate (C3 at 200 mM, pH 7.5), or sodium butyrate (C4 at 200 mM, pH 7.5) in drinking water from 3 or 32 weeks of age for 2-6 weeks. In the indicated groups, mice were fed with rapamycin (25 μg/ml, LC laboratories) and/or vancomycin (0.5 g/L) in drinking water for same time periods in the presence of SCFAs. Based upon hydronephrosis in the kidney mice were diagnosed as C2RD. For most of the experiments, male mice were used unless indicated as female. For the neutralization of cytokines, antibodies to IL-17A (clone 17F3, BioXcell) or IFNγ (clone XMG1.2, BioXcell) (100 μg/mouse, i.p. once a week) were administered

for 6 weeks. All animal experiments were approved by the Purdue Animal Care and Use Committee (PACUC).

Confocal microscopy and histology

Frozen sections of kidneys or ureters (8 μm) were prepared with Leica CM1860 Cryostat fixed with acetone. Sections were stained with antibody to collagen type IV (rabbit polyclonal antibody) and then stained with fluorescently labeled polyclonal anti-rabbit IgG antibodies and antibodies to CD4 (clone RM4-5), CD11c (clone N418), Gr-1 (clone RB6-8C5), cytokeratin (clone AE1/AE3), and muscle actin (clone HHF35). Fluorescent confocal images of kidney and ureter sections were acquired with a Leica SP5 II laser scanning confocal microscope. For histological analysis, paraffin tissue sections (8 μm) were stained with hematoxylin and eosin.

Analysis of serum and urine

Level of creatinine in serum or urine was determined as described before (104). Briefly, 1 ml of creatinine assay solution was prepared with picric acid, sodium hydroxide, and EDTA disodium salt. The assay buffer was mixed with 0.1 ml of standard solutions, serum, or urine. After 30 and 90 seconds, the absorbance was measured at 492 nm. To measure the concentration of urea, a mixture of acid solution (200 μl, H_2SO_4, H_3PO_4, and H_2O in a ratio of 1:3:7) and 9% alpha-isonitrosopropiophenon solution (10 μl) was reacted with serum, urine, or standard solutions for 30 seconds at 95ºC. The absorbance was

measured at 540 nm. Concentrations of creatinine and urea were calculated based on the absorbance values of standard solutions.

Blood pressure measurement

Systolic and diastolic blood pressures were non-invasively measured by determining the tail blood volume with a volume pressure recording sensor and an occlusion tail-cuff (CODA System, Kent Scientific, Torrington, CT) (105). Maximum cuff pressure was set to 250 mmHg, with 20 seconds for each inflation run, per the manufacturer's recommendations. Each mouse was measured 20 times and averages of all accepted runs were used.

Cell culture and differentiation in vitro

Total cells from renal draining lymph nodes were collected and digested with collagenase type 3 (Worthington Biochemical, Lakewood NJ) at 37^{o}C for 30 min. Cells were activated with coated anti-CD3 (5 μg/ml, clone 145-2C11) in different T cell polarizing conditions: hIL-2 (100 U/ml) for a Tnp condition; hIL-2, mIL-12 (1 ng/ml), and anti–mIL4 (clone 11B11, 10 μg/ml) for a Th1 condition; hTGF-β1 (5 ng/ml), mIL-6 (20 ng/ml), mIL-1β (10 ng/ml), mIL-23 (10 ng/ml), mIL-21(10 ng/ml), mTNF-α (20 ng/ml), anti-mIL-4 (10 μg/ml, clone 11B11), and anti-mIFNγ (10 μg/ml, clone XMG1.2) for a Th17 condition in the presence or absence of SCFAs (C2, 10 mM; C3, 1 mM; C4, 0.5 mM),

and/or rapamycin (25 nM, Enzo). mTOR activation or cytokine expression was determined after 3 or 5 days respectively.

Flow cytometry

Kidney or ureter tissues were digested with collagenase type 3 for 1 hour and the total cells were collected. For intracellular staining, surface antigen of CD4 was stained and cells were activated with RPMI 1640 (10% FBS) with 12-myristate 13-acetate (50 ng/ml), ionomycin (1 μM), and monensin (2 mM) for 4 hours followed by fixation and permeabilization. Antibodies to IL-10 (clone JES5-16E3), IL-17A (clone TC11-18H10.1), IFNγ (clone XMG1.2) and/or anti-FoxP3 (clone FJK-16s) was applied for intracellular staining. To determine the level of rS6 protein phosphorylation, antibody to phosphorylated rS6 (clone Ser235/236; D57.2.2E) was applied. The frequencies of T helper cells were determined from the total lymphocyte and $CD4^+$ gates. The total cell numbers were calculated from frequencies of each cell population and numbers of retrieved cells from each organ (1 spleen, 2 draining lymph nodes, 1 kidney, and 2 ureters).

Measurements of SCFA levels in kidney tissues

100mg of kidney tissues were mixed and homogenized in 900 μl of water using 1.4 mm ceramic beads and Precellys®24 homogenizer. Supernatant of homogenates or SCFAs standard were labeled aniline-C12 or C13 and analyzed with an Agilent 6460 Triple Quad

LC/MS System (Agilent Technologies) as described before (106). Ratio between internal and external standards were used to calculate SCFA concentrations in kidney tissues.

Microarray analysis

Total RNA was prepared from normal or C2RD kidneys and microarray study was assessed by Mouse 430 2.0 chips (Affymetrix, Inc.). Analysis of the gene pattern was processed as described previously (83). The microarray data have been deposited in the GEO database (accession number: GSE69864). For a visualization of the gene expression pattern, the GenePattern genomic analysis platform (www.broad.mit.edu/cancer/software/genepattern), Cluster 3.0, and TreeView 1.6 (Eisen Lab, rana.lbl.gov/EisenSoftware.htm) were utilized. Microarray data of C2RD was compared to the published gene expression. We reclaimed published data from the GEO site: GSE36496 (UUO), GSE48041 (*Mgb*-/-), GSE12024 (Lupus), and GSE24352 (PKD). For conversion of Gene IDs from different microarray plat forms into Agilent ID, DAVID Bioinformatics Resources 6.7 (http://david.abcc.ncifcrf.gov) was utilized.

Quantitative real-time PCR

Using TRIzol® solution (Invitrogen), total RNA was extracted and cDNA was synthesized with SuperScript® II Reverse Transcriptase (Invitrogen). Quantitative real-time PCR (qRT-PCR) was performed with Maxima® SYBR Green/ROX qPCR Master Mix (Thermo Scientific).

The primers used for qRT-PCR were:

*Il6(*CTG.GTC.TTC.TGG.AGT.ACC.ATA.GCandTGC.CGA.GTA.GAT.CTC.AAA.GTG.AC);

*Il10(*CCA.GCT.GGA.CAA.CAT.ACT.GCTandCAT.CAT.GTA.TGC.TTC.TAT.GCA.G);

*Il17a (*GAC.TCT.CCA.CCG.CAA.TG and CGG.GTC.TCT.GTT.TAG.GCT);

*Ifng (*AGA.CAA.TCA.GGC.CAT.CAG.CA and CGA.ATC.AGC.AGC.GAC.TCC.TTT);

Tgfb1(CGC.CAT.CTA.TGA.GAA.AAC.C and GTA.ACG.CCA.GGA.ATT.GT);

Ccl2 (AAG.ATG.TGC.TGG.ACA.GCT.G and TCC.AGG.GCA.CAT.ATG.CAG.AG);

Ccl5 (GCG.GGT.ACC.ATG.AAG.ATC.TC and CAG.GGT.CAG.AAT.CAA.ACC.CT);

Ccl17 (AGG.TCA.CTT.CAG.ATG.CTG.CT and CCC.TGG.ACA.GTC.AGA.AAC.AC);

Ccr2(GTT.TGC.CTC.TCT.ACC.AGG.AAT.CandAAG.AGT.CTC.TGT.CAC.CTG.CAT.G);

Ccr4(CAT.GCT.CAT.GAG.CAT.AGA.CAG.A and AAG.CAC.CAC.GTT.GTA.CGG.CGT);

Ccr5 (CCT.CCT.GAC.AAT.TGA.TAG.GTA.C and ATG.ATG.GCA.AAG.ATG.AGC.CTC.A);

Cxcr3 (CCT.TCC.TGC.TGG.CTT.GTA.TAA.G and CCA.CTA.CCA.CTA.GCC.TCA.TAG);

Gpr41 (CTG.GCT.GTT.GTG.ACG.CTT and CGG.TGA.CAA.ATT.CAG.AAC.TCT); *Gpr43* (CTT.CTT.GCA.GCC.ACA.CTG.CT and CAC.TCC.TTG.GAT.GGC.TCT.TC); The expression levels of genes were normalized by the β-actin levels.

Bacterial DNA analysis

To examine the composition of gut bacteria, cecal content were collected from control or C2RD mice. Bacterial DNA was isolated using a FastDNA® SPIN Kit (MP Biomedicals) according to the manufacturer's protocol. For qPCR, primers were designed according to previous publications (107, 108). Differences (ΔCT) between cycle threshold (C_T) values of eubacteria and each bacterial group were calculated ($2^{-\Delta CT}$). Relative expression of bacterial groups in C2RD was compared to the control groups.

Statistical analysis

Student's *t* test (1 or 2-tailed) or the Mann-Whitney test were used to determine the significance of differences between the two groups. *P* values < or = 0.05 were considered significant.

3.3 Results

Oral administration of C2 induces progressing renal disease

Acetate (C2) is the most abundant SCFAs in the gut. Its concentration is up to 130mM in the colon and 1mM in the blood. To examine the role of SCFAs in the renal system, we kept mice on C2 containing water for six weeks at ~1.5 times (200mM) higher

than normal gut concentration. Compared to normal water, mice did not consume more or less C2 water (Fig. 3.1 A). However, six weeks of C2 feeding significantly increased C2 concentrations in the blood and kidney tissues (Fig. 3.1. B and C). Specifically, C2 feeding elevated concentrations of C2 in kidney tissues from 0.56 ± 0.079 mM to 2.78 ± 1.02 mM. When we examined mice after 6 weeks of C2 water, we found irregularly shaped kidneys. Kidneys were bloated with hydronephrosis in the C2-fed group and we named the kidney disease C2RD. However, the same concentration of NaCl (200mM) hardly affected the kidneys, and we ruled out the role of sodium ion (Na^+) in C2RD (Fig 3.2 A). Kinetic observation showed that about 30% of mice had C2RD after four weeks of C2 feeding and most mice developed C2RD by the sixth week of treatment (Fig 3.2 B). Sectioned kidney tissues revealed that the medulla structure of C2RD mice was severely impaired and the cortex was squeezed (Fig 3.2 C). In addition, we observed that 55% of C2RD was in only one side of the kidney (Fig. 3.2 D). The renal function was evaluated by creatinine and urea levels in the serum or urine. As expected, C2RD mice showed increased concentrations in the serum while urinal levels of creatinine and urea were decreased (Fig. 3.3 A). Systolic blood pressure was also higher in C2RD mice (Fig. 3.3 B).

We titrated minimal C2 concentration that develops C2RD, and found that 150mM of C2 induced disease in 30% of mice but not at 100mM (Fig 3.4). The disease rate of C2RD was about three times higher in males than females (Fig. 3.5), which correlates with sex differences inhuman kidney disease (109). These data indicate that chronic exposure

to augmented C2 developed renal disease and disrupted kidney function in dose-and time-dependent manners.

Change of T cell and gene expression profiles in C2RD kidney tissues

Drastic changes in kidney tissue as a result of C2, prompted us to investigate immune cell profiles of C2RD. Using immunofluorescence microscopy, we found $CD4^+$ T cells and $CD11c^+$ cells were highly infiltrated in C2RD kidney tissues (Fig. 3.6 A). We further examined the kinetics of T cell subsets via C2 water feeding. Four weeks or longer of C2feeding increased the expressions of both effector and regulatory T cells (Fig. 3.6 B). Because the infiltration of inflammatory cells and fibrosis in renal tissues are associated with the secretion of cytokines or chemokines, we examined the expressions of related genes by qRT-PCR. Inflammatory cytokines and chemokines *Il6, Il17a, Ifng, Ccl2*, *Ccl5*, and *Ccl17* were increased at mRNA level. In addition, levels of regulatory or fibrosis-related cytokine genes, such as *Il10* or *Tgfb1*, were also upregulated in the affected kidney tissues (Fig. 3.7).

Changes of immune cells and their signature genes in C2RD showed similar patterns as other renal inflammation (51, 110, 111). To characterize the gene expression of C2RD, we applied a microarray analysis. We compared C2RD with unilateral ureteral obstruction (UUO), congenital obstructive nephropathy in the male megabladder $(Mgb)^{-/-}$, lupus nephritis, and embryonic polycystic kidney disease (PKD) models (112-115). In terms of transcriptome levels, C2RD had adjacent relations to UUO and $Mgb^{-/-}$ models, but less correlation with Lupus or PKD (Fig. 3.8 A). C2RD also showed functional similarity to a UUO model in inflammation, fibrosis, nitric oxide, growth factors, and cell

proliferation (Fig. 3.8 B). The results indicate that C2RD shares immunological changes with other renal diseases, especially obstructive ureter models.

Ureteral obstruction and inflammation in C2RD

Because C2RD showed features analogous to ureteral obstruction disease, we closely investigated the ureteral area in C2RD mice. Histological analysis of kidney tissues showed signs of inflammation in both the cortex and medulla regions as C2RD progressed (Fig. 3.9 A). Ureteropelvic junction (UPJ) obstruction leads to obstructive renal disease in humans and animals (116), and we observed severe hyperplasia and immune cell infiltration in C2RD mice (Fig. 3.9 B). To confirm the ureteral obstruction in C2RD mice, we injected India ink into the kidneys. The ink flow was completely blocked from the pelvic area to the bladder. Moreover, HnE staining revealed obstructed UPJ in C2RD mice (Fig. 3.10 A and B). In the proximal ureter, we observed hyperplasia of tissue via the longitudinal section (Fig. 3.11 A). We measured the thickness changes in epithelium, lamina propria, muscular and adventitia layers. Each compartment was expanded with C2 water administration (Fig. 3.11 B). However, ureteral stones were not detected with a Von Kossa staining method in the affected ureters (Fig. 3.12). These results suggest that C2RD is subsequently caused by ureteral obstruction.

T cell subset changes in C2RD ureter

We previously identified the ureter as the target organ of C2RD. Therefore, we examined the changes in the ureter immune cells. In affected ureters, $CD4^+$ T cells and $Gr\text{-}1^+$ granulocytic cells were infiltrated in the epithelium and adventitia layers. Collagen,

which reflects fibrosis, was also heavily deposited in these area (Fig. 3.13). Then, we found effector (Th1 and Th17) and regulatory (IL-10^+ and $FoxP3^+$) T cell expansion in the C2-fed ureters (Fig. 3.14). Moreover, we examined the increased numbers of effector and IL-10^+ T cells in kidney tissues in a C2-dose dependent manner (Fig. 3.15A). The enlarged renal draining lymph nodes indicate the activation of immune cells in C2RD mice (Fig 3.15B). Additionally, we compared the kinetics of T cell subsets in systemic or renal tissues. Although splenic T cells were unaffected, four weeks or longer ofC2 feeding increased total $CD4^+$, effector, and regulatory T cells in each renal tissue sample (Fig. 3.16). To gain comprehensive information from required C2 administration periods, mice were fed C2-infused water for four weeks and switched to regular water for the following two weeks. Withdrawing C2 after the fourth week protected mice from C2RD (Fig. 3.17). Here, we found that extended exposure to C2 is required for C2RD development, in which renal T cells are augmented.

T cell requirement in C2RD development

So far, we have demonstrated that T cells are plentiful in affected renal tissues. To investigate the role of T cells in C2RD pathogenesis, we attempted to induce C2RD in T cell (αβ-TCR)-deficient mice. Interestingly enough, C2 was unable to promote C2RD development in T cell-lacking conditions (Fig 3.18). Because expressions of effector T cell cytokines increased in the renal tissue of C2RD mice, we investigated the role of these cytokines in C2RD development. We injected neutralizing antibodies of IL-17 or IFNγ along during a six-week-long C2 treatment. Blocking antibodies significantly suppressed the progress of the disease by lowering C2RD rates and kidney weights (Fig. 3.19A).

Frequencies of Th17, Th1, or IL-10^+ T cells decreased after antibody treatment (Fig. 3.19B). Therefore, we determined that T cells and their cytokines are required for C2RD pathogenesis.

Impact of other SCFAs and SCFAs receptors on C2RD

Propionate (C3) and butyrate (C4) are other major SCFAs. We investigated whether like C2RD, C3, or C4 are capable of inducing renal disease. The administration of C3 and C4 at the same concentration (200 mM) developed hydronephrosis as efficiently as C2 (Fig. 3.20A). The populations of effector and IL-10^+ T cells in renal tissues increased after C3 or C4 feedings (Fig 3.20B). We confirmed its similarity to C2-induced disease with histological analysis, which affected kidney structures and ureter hyperplasia (Fig 3.20 C).

SCFAs act as ligands of GPR41 or GPR43, and activate cellular processes in various cell types, such as gut epithelium or neutrophils (37, 38). To examine the involvement of GPR41 or GPR43 in C2RD development, we first determined the mRNA expression levels of *Gpr41* or *Gpr43* in the kidneys and ureter tissues. Compared to colon tissue, expressions of *Gpr41* and *Gpr43* were limited in renal tissues (Fig. 3.21). Thus, C2 administration to GPR41- and GPR43-deficient mice developed C2RD as efficiently as WT mice. Both knockout strains showed increased disease rates, kidney weights, and effector T cells in the affected kidneys (Fig. 3.22A and B).

Gut microbiota and age-dependent C2RD development

Because SCFAs are produced by gut microbiota, we questioned if bacterial composition in C2RD mice fluctuates. Using bacterial 16s rRNA gene PCR, we identified

that C2 administration expanded Bacteroidetes, while segmented filamentous bacteria (SFB) and Actinobacteria were reduced (Fig. 3.23A). To examine the effect of gut microbiota on C2RD pathogenesis, we fed vancomycin (along with) C2 in drinking water. Vancomycin eradicates Firmicutes and Bacteroidetes (117, 118), and the oral feeding of vancomycin plus C2 water completely protected mice from C2RD development (Fig. 3.23B).

In humans, UPJ obstruction rates are higher in younger populations (119), and we investigated if C2RD occurrence is age dependent. We exposed 3- and 32-week-old mice to C2 water for 6 weeks. C2 induced less C2RD in older mice than in younger mice (Fig. 3.24). We provide the evidence that intestinal microbiota and age affect the C2RD pathogenesis.

Impact of SCFAs on mTOR pathway and inflammatory T cells in C2RD

Activation of mTOR pathways supports effector and IL-10^+ T cell differentiation, and we reported that SCFAs stimulate mTOR activity in T cells. Because renal inflammation can be controlled by mTOR inhibition (60-63, 120, 121), we examined whether mTOR-mediated T cell activation is involved in C2RD development. First we cultured the total cells in the renal draining lymph nodes (dLN) in the presence of SCFAs and rapamycin. The phosphorylation level of the ribosomal S6 protein (rS6), a key target of mTOR pathways, were examined in dLN T cells. SCFAs enhanced the activity of rS6, which was abolished with rapamycin addition (Fig. 3.25A). SCFAs also enhancedIL-17^+ or IFNγ^+ T cell differentiation, but SCFA-promoted effector T cell generation was blocked by rapamycin in renal dLN T cells (Fig. 3.25B). Next, we examined the mTOR inhibitory

effects on C2RD development. Rapamycin-infused drinking water effectively blocked C2RD development (Fig. 3.26A). In the affected kidney tissues, rS6 activity and effector T cell generation escalated while rapamycin feeding counteracted C2 effects (Fig. 3.26B and C). These consequences imply that SCFAs regulate effector T cell differentiation in renal tissues and C2RD development through promoting mTOR pathways.

3.4 Discussion

This study demonstrates the inimical effect of SCFAs on the renal system. Unexpectedly, the chronological elevation of SCFA levels induced ureteral obstruction and developed hydronephrosis in T cell-dependent fashions. In affected kidneys, mTOR pathways stimulated the expansion of inflammatory T cells. These results suggest that SCFAs have pro-inflammatory roles in reinforcing effector T cell generation.

SCFAs produced by gut microbiota and C2 concentrations reach up to 130mM in the large intestinal region (3, 4). Feeding 200mM of C2water increased C2 concentration in the blood and kidney by 1.5 and 4 times respectively. Although the same dose of NaCl hardly affected renal tissues, prolonged exposure to C2 induced UPJ obstruction formed a huge sac in the kidneys, which we named C2RD. We compared the transcriptome of C2RD to other kidney diseases including UUO, congenital ureteral obstruction, Lupus, and PKD. We found that C2RD gene expression patterns most closely resemble ureteral obstruction models. In functional groups, C2RD also showed similarities to the UUO model. In humans, a number of causes, including ureter stone, genetic modification or birth defect,

induce ureteral obstruction (122, 123). However, C2RD does not originate from these factors. Von Kossa staining did not detect ureteral stones and C2RD was detected in adult wild-type mice. Indeed, C2RD development was independent of the SCFA receptors, GPR41 and GPR43.

Instead, we found the role of the T cell as a major player in C2RD pathogenesis. In αβ T cell-deficient mice, C2 administration scarcely induced C2RD, which implies that T cells are required for disease development. In ureteral obstruction diseases, effector T cells expanded and their expression of inflammatory cytokines contributes to inflammation (45, 50). In our previous study, we reported that SCFAs facilitate effector T cell differentiation (44). In this regard, Th1 and Th17 cells expanded following SCFA feeding and subsequently developed renal inflammation. This demonstrates the role of SCFAs in renal effector T cell generation. Furthermore, we verified the function of effector cell-producing cytokines by neutralizing IL-17 and IFNγ, which abolished C2RD development. SCFAs also regulate regulatory T cell generation, such as IL-10^{+} or $FoxP3^{+}$ T cells in various organs (11, 29-31, 44). A recent study reported the protective role of SCFAs in lessening inflammatory processes in acute kidney injuries (69). We observed expanded populations of regulatory T cells in C2RD mice, further evidence of the action of SCFAs on regulatory T cells in the renal system. However, we suggest that the increase was due to general activation of T cells in inflammatory conditions (124-126), and increased regulatory T cells were not potent enough to suppress inflammation. As stated in our previous work, SCFAs

regulate T cell differentiation according to the environment (e.g. the intensity of T cell activation or pathogen infection).

mTOR pathways are activated when effector T cells are induced. SCFAs are able to promote both regulatory and effector T cells by stimulating mTOR-S6K signals (44). In many renal diseases, such as UUO, Lupus or PKD, mTOR pathways were activated. In these cases, rapamycin effectively prevented renal inflammation (115, 127, 128). In C2RD, the mTOR activity of renal $CD4^+$ T cells and the population of effector T cells increased. Administration of rapamycin in drinking water prohibited C2RD development by mitigating mTOR activity and effector T cell expansion.

Along with T cells, it is possible that non-T cell or other elements coordinate C2RD pathogenesis. Besides $CD4^+$ T cells, a number of $CD11c^+$ dendritic cells (DCs) were detected in C2RD kidney tissues. The role of DCs in renal inflammation is clearly demonstrated by numerous studies. In DC-depleted conditions, UUO kidneys showed decreased effector T cell populations, and inflammation was suppressed (51).

Intestinal microbiota is recognized as an important player in C2RD development. SCFAs are gut metabolites, and SCFA feedings changed the composition of major microbiota. The role of commensal bacteria in autoimmune diseases, such as multiple sclerosis, colitis, diabetes, or rheumatoid arthritis, was suggested (129-131). In line with previous works, antibiotic feeding completely suppressed C2RD. While underlying mechanisms need to be investigated, we consider that vancomycin treatment abolished C2-induced bacterial composition and blocked C2RD progress. Besides, we observed that age and sex affect C2RD development. In agreement with human kidney studies, C2RD was

more frequent in younger and male mice. This suggests that C2RD has the potential to be used in a human renal disease model. Compare to the UUO model, C2RD does not require surgery to address the artificial ureter obstruction. The natural progress of ureteral obstruction, which leads to hydronephrosis can offer a useful disease model.

To take advantage of this study, prolonged exposure to uplifted-SCFAs can induce Th1 or Th17 cell-mediated inflammation in renal tissue. Oral SCFA delivery regulated mTOR dependent T cell differentiation with the help of gut microbiota. We suggest that SCFAs, along with environmental factors, have the potential to induce renal inflammation via effector T cell generation.

3.5 Summary and future directions

3.5.1. Summary of the study

We reported that prolonged exposure to high doses of SCFAs develops ureteral obstruction and hydronephrosis, which we named C2RD. T cell had essential role in C2RD pathogenesis and SCFAs expand renal effector T cell in a mTOR-dependent manner. Gut microbiota are also required to promote C2RD in combination with SCFAs. In addition, we found age and sex influence the occurrence of C2RD. However, the expression of SCFAs receptors, GPR41 and GPR43 were least significant in renal tissue and not involved in C2RD development.

3.5.1. Future study directions

In this study, we mainly discussed the role of T cells in SCFA-mediated renal inflammation. In affected kidneys, we also found increased population of $CD11C^{+}$ cells, which presumes the role of dendritic cells (DCs) in C2RD development. Kidney resident-DCs activate renal dLN T cells through antigen presentation or cytokine secretion, which develops into kidney inflammation (51, 132). Although the effect of SCFAs on DCs regulation is unclear, a study reported that C4 enhance IL-23 expression in LPS-stimulated bone marrow-derived DCs. Moreover, a co-culture of C4-treated DCs increased IL-17 expression in splenic T cell (133). Accordingly, cytokine expression in SCFA-treated renal DCs need to be examined. These DCs should be co-cultured with T cells and induction of effector T cell will be determined. To confirm the role of renal DCs in C2RD in vivo, CD11c-DTR mice or clodronate liposomes injection methods can be applied in C2RD-inducing conditions (134, 135).

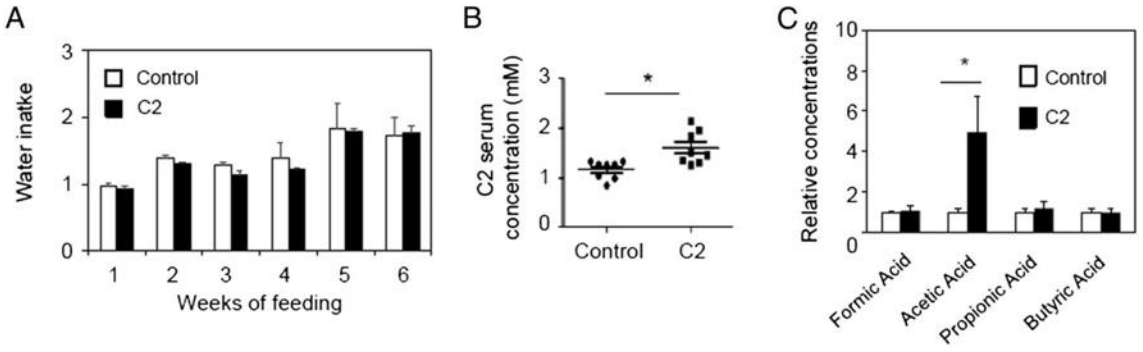

Figure 3.1 Amount of oral acetate (C2) drinking and concentrations of SCFA in blood and kidneys.

(A) Measurement of the consumed water (ml/g body weight/week) in control or C2-allocated group. SCFA concentrations in serum (B) or kidney tissues (C) were determined in normal water and C2-infused water-fed mice. The water treatment was for six weeks. *Significant differences from control groups ($P \leq 0.05$).

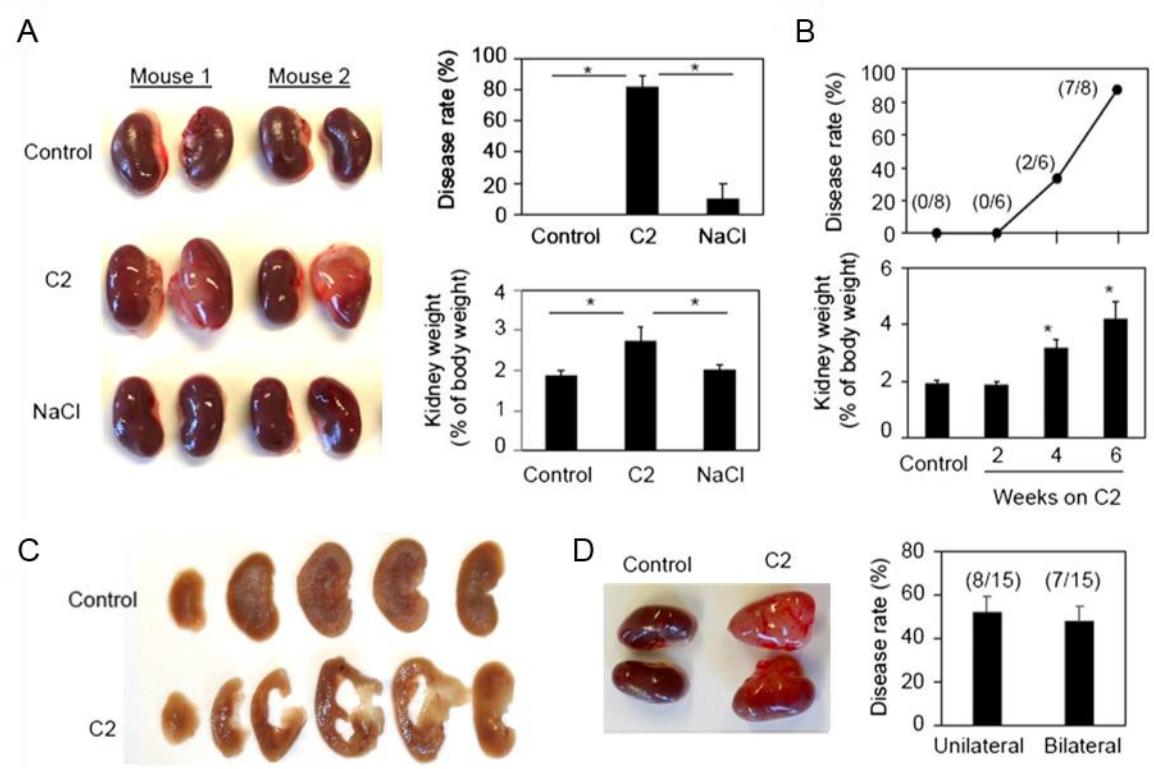

Figure 3.2 Acetate (C2, 200 mM)-infused water induced a renal disease (C2RD).

(A) C2 (200 mM) or NaCl (200 mM) were treated via drinking water for six weeks and induced hydronephrosis. Gross images of kidney tissues, disease rate, and kidney weight are shown. (B) Kinetics of C2-induced renal disease (C2RD) rate and kidney weight are shown. (C) Sectioned images of normal or C2RD kidney tissues. (D) Occurrence of unilateral or bilateral C2RD. Representative and pooled data are shown (n=6-15). *Significant differences from control or indicated groups ($P \leq 0.05$).

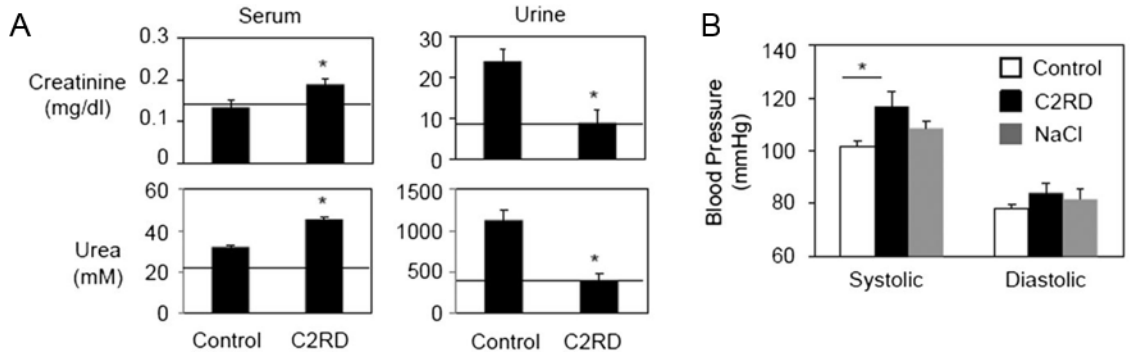

Figure 3.3 Renal function and blood pressure in C2RD mice.

(A) Creatinine and urea concentrations in serum or urine were measured. Normal and C2RD mice were compared. (B) Blood pressure was determined after C2- or NaCl-water feeding for six weeks. Pooled data from five to eight individual mice are shown. *Significant differences from control groups ($P \leq 0.05$).

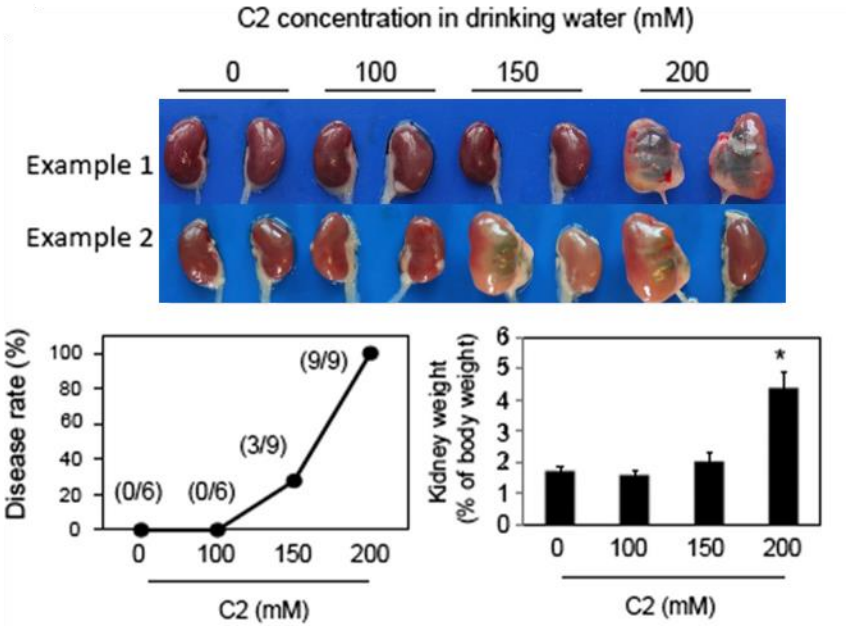

Figure 3.4 Occurrence of C2RD in a C2 dose-dependent manner.

Different C2 doses in drinking water. Mice were administered C2 water for six weeks. Disease rate and weight of kidneys are shown in indicated groups. Representative or pooled data from six to nine mice are shown. *Significant differences from non-treated group ($P \leq 0.05$).

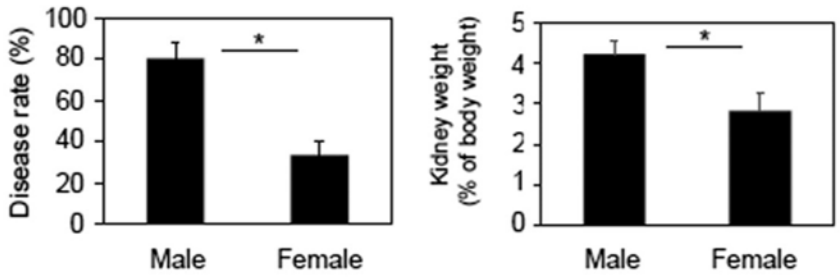

Figure 3.5 Sex biased C2RD development.

C2RD occurrence and kidney weights were compared between male and female mice. Pooled data from fourteen mice are shown. *Significant differences from male group ($P \leq 0.05$).

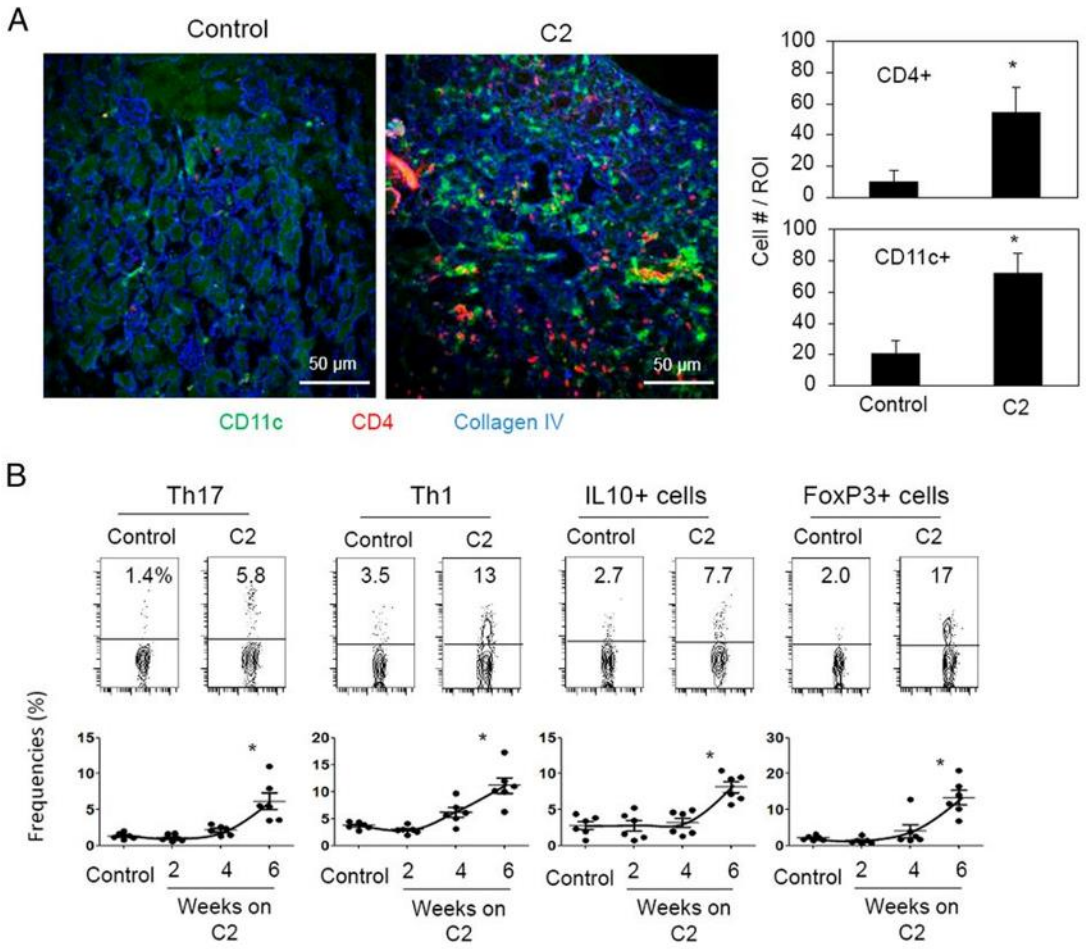

Figure 3.6 Kinetic changes of immune cells in C2RD kidney tissues.

(A) Infiltration of $CD4^+$ or $CD11c^+$ cells in kidney tissues identified with confocal analysis. (B) Frequencies of T cell subtypes determined by flow cytometry, which gated for $CD4^+$ T cells in kidney tissues. Dot plots shown from control or six weeks-fed mice. Representative or pooled data from six individual mice are shown. *Significant differences from control groups ($P \leq 0.05$).

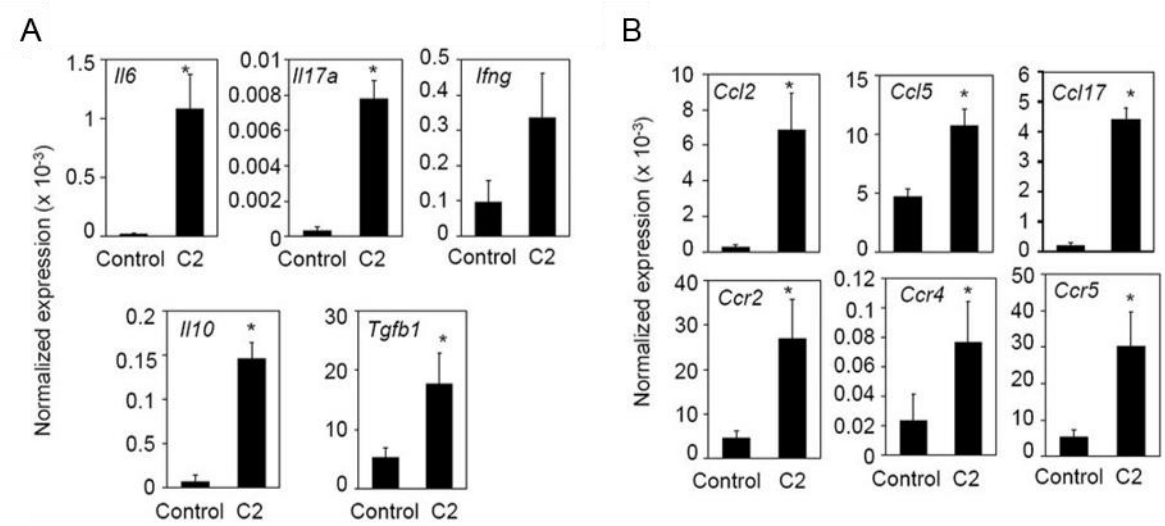

Figure 3.7 Expressions of cytokines, chemokines, and chemokine receptors in C2RD kidney tissues.

Kidney tissues were collected from normal and C2RD mice. Expression of cytokines (A), chemokines, or chemokine receptors (B) examined at mRNA level by qRT-PCR. Pooled data from three to six different tissues are shown. *Significant differences from control groups ($P \leq 0.05$).

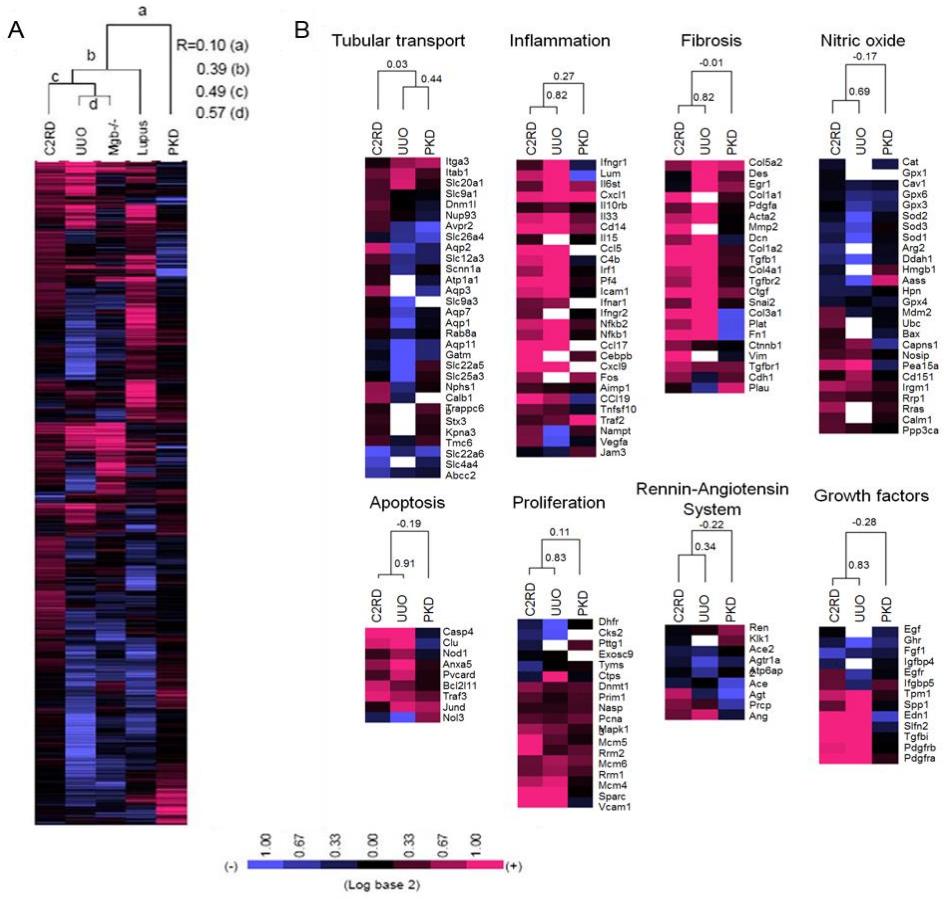

Figure 3.8 Comparative analysis of transtriptome among C2RD and other renal diseases.

(A) Gene expressions of C2RD kidney tissues compared with UUO, Mgb$^{-/-}$ congenital obstructive nephropathy, lupus nephritis, and polycystic kidney disease (PKD) (B) Genetic relationships between C2RD and UUO or PKD in functional groups. Microarray analysis of C2RD genes is shown based on published gene expression data in the Gene Expression Omnibus database for UUO, Mgb$^{-/-}$, Lupus, and PKD models. Pearson coefficient (r) values determine the closeness among different diseases.

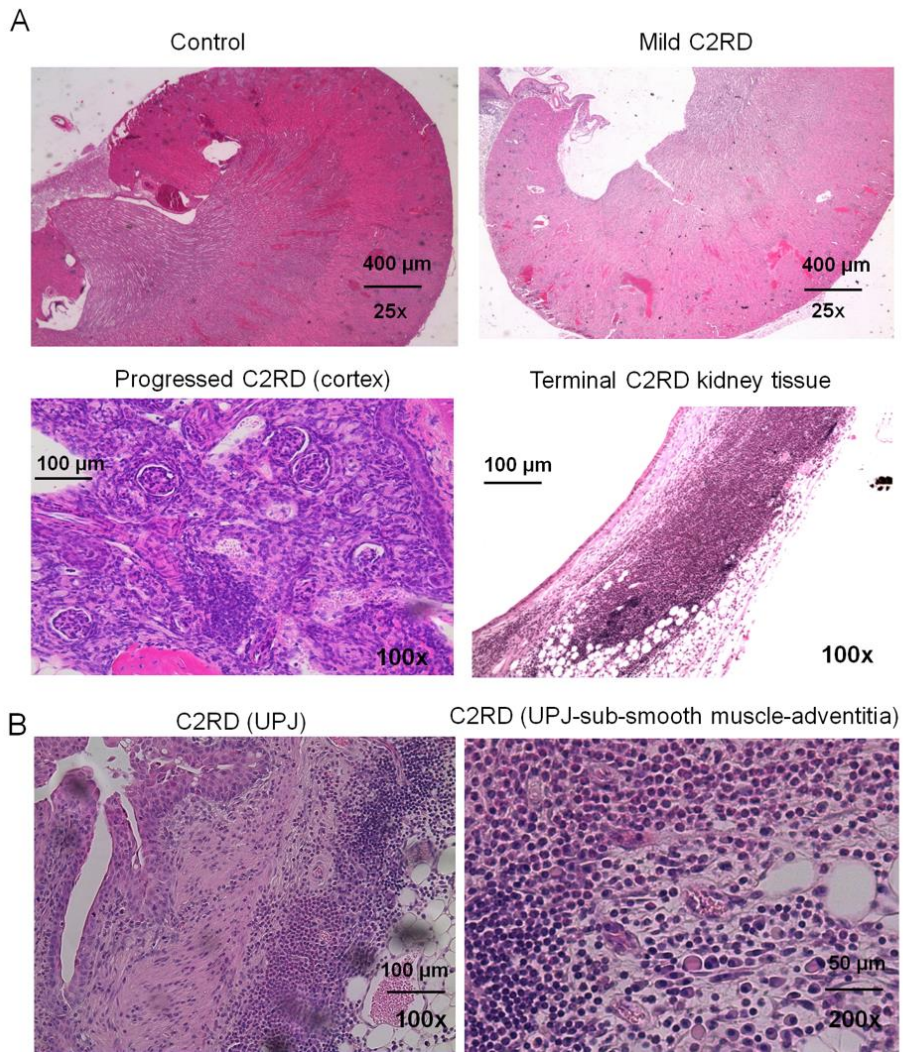

Figure 3.9 Histological analysis of C2RD kidney tissues.

(A) Kidney tissue sections were prepared at different developmental stages of C2RD and stained with hematoxylin and eosin (HnE). (B) Focused images of ureteropelvic junction (UPJ) in C2RD kidneys. Representative images from six individual mice are shown.

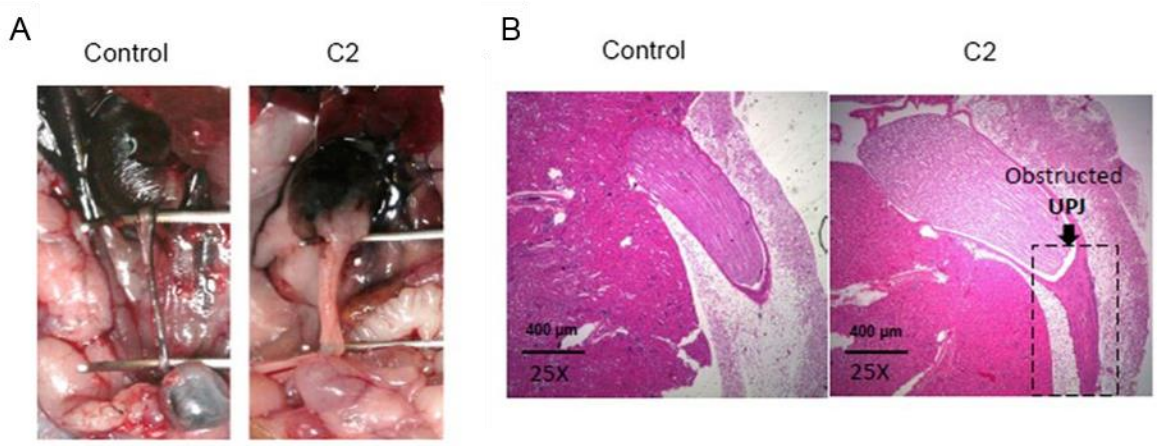

Figure 3.10 Ureteral obstruction in C2RD mice.

(A) Ureteral obstruction was evaluated. India ink was injected into the kidney pelvic area of normal and C2RD mice. (B) Histological analysis of ureteral obstruction in normal and C2RD mice. Original magnification ×25.

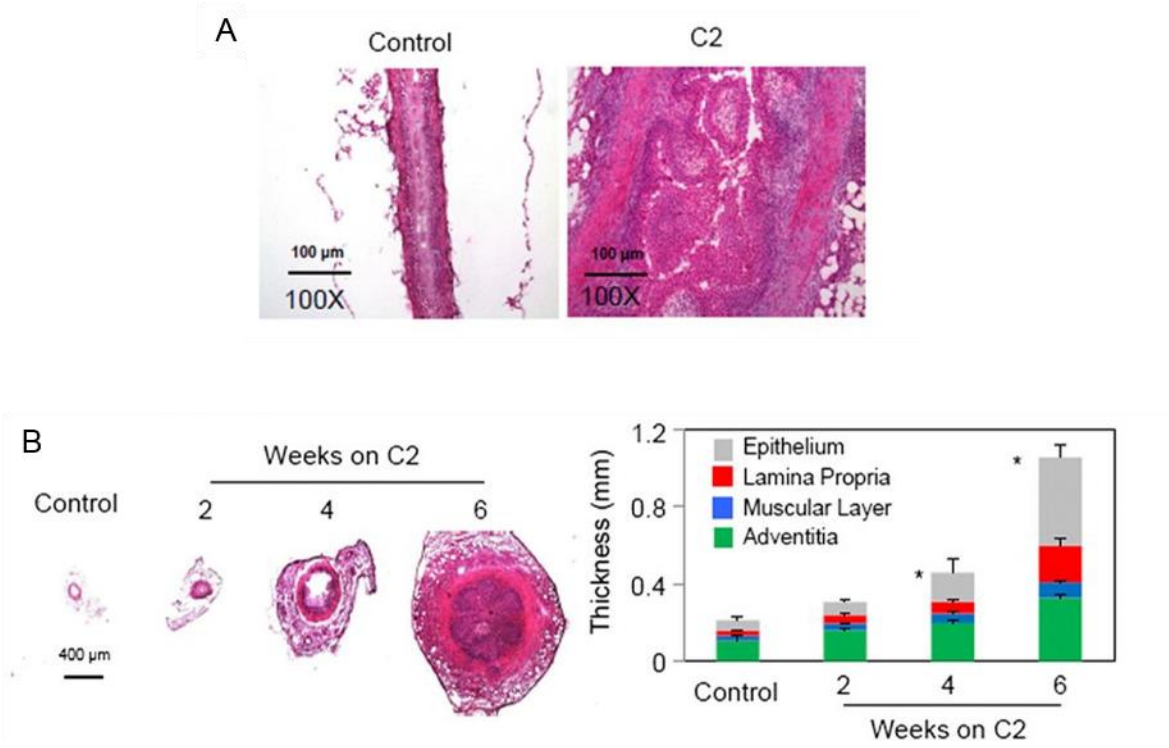

Figure 3.11 Ureteral hyperplasia in C2RD mice.

(A) Histological analysis of ureteral hyperplasia in C2RD mice. Longitudinal sections were obtained from proximal ureters and stained with HnE. (B) Changes in ureteral thickness were measured with cross sections. Each color of bar graph indicates the diameter of the ureteral structure. Original magnification ×100 (A) and ×25 (B). *Significant differences from control group ($P \leq 0.05$).

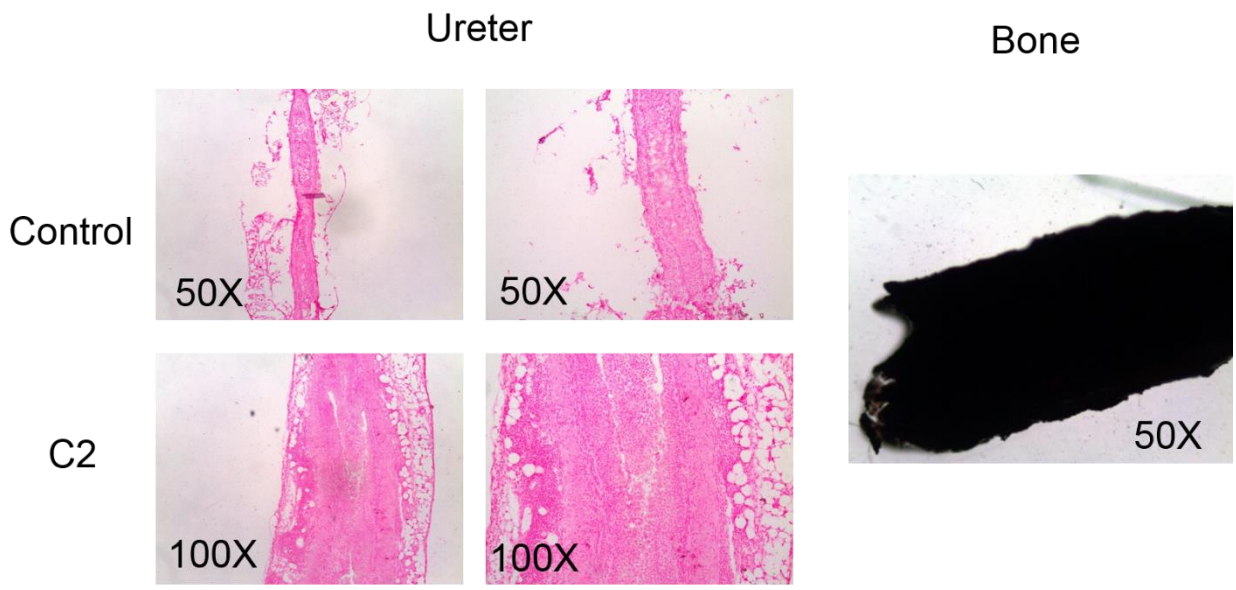

Figure 3.12 Von Kossa staining of ureter tissues

A mouse femur bone was used as a positive control. Representative data from at least four mice are shown.

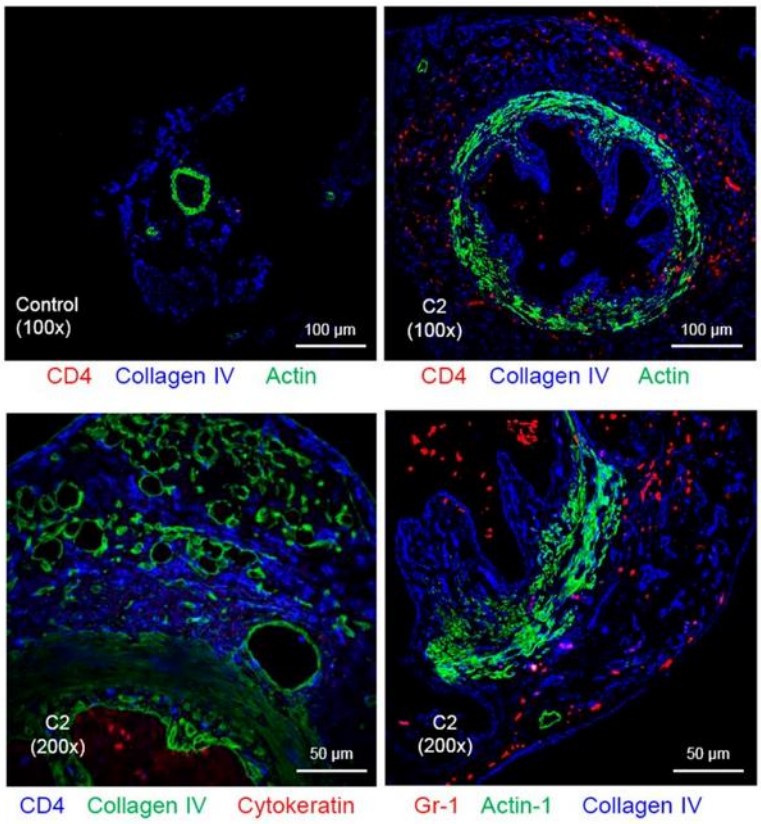

Figure 3.13 Changes in immune cells of C2RD ureter tissues.

Infiltrations of $CD4^+$, $Gr\text{-}1^+$, smooth muscle cells (actin), epithelial cells (cytokeratin), and collagen IV expression were represented with fluorescent conjugated antibodies using confocal analysis. Cross sections of proximal ureters in normal or C2RD mice were examined.

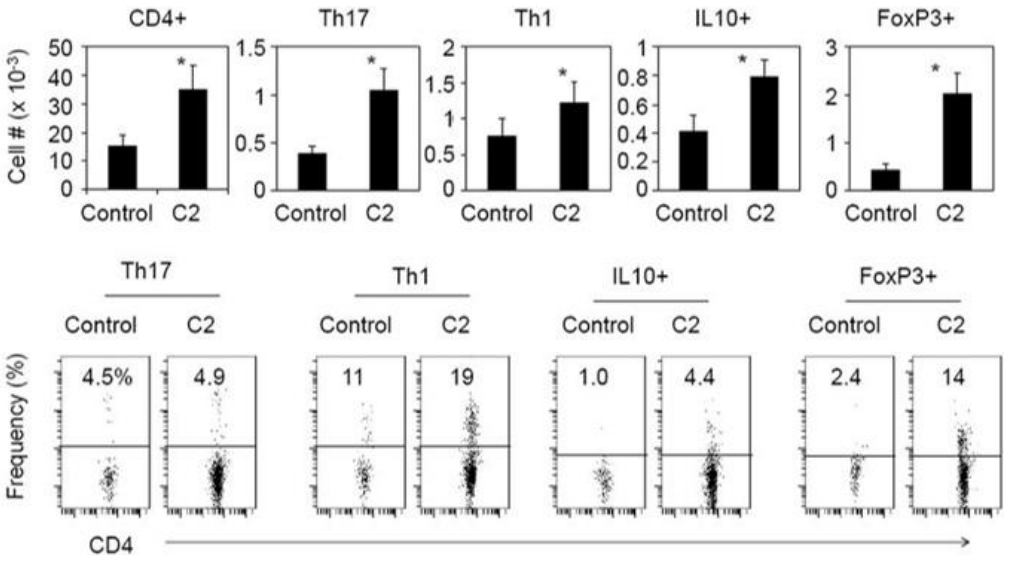

Figure 3.14 Effector or regulatory T cell changes in C2RD ureter tissues.

Numbers and frequencies of total $CD4^+$ T cells, effector T cells (Th17 and Th1) and regulatory T cells ($IL\text{-}10^+$ and $FoxP3^+$ T cells) are determined by flow cytometry, which gated for $CD4^+$ T cells in ureteral tissues. Pooled data or representative dot plots are from six control or C2RD mice. *Significant differences from control groups ($P \leq 0.05$).

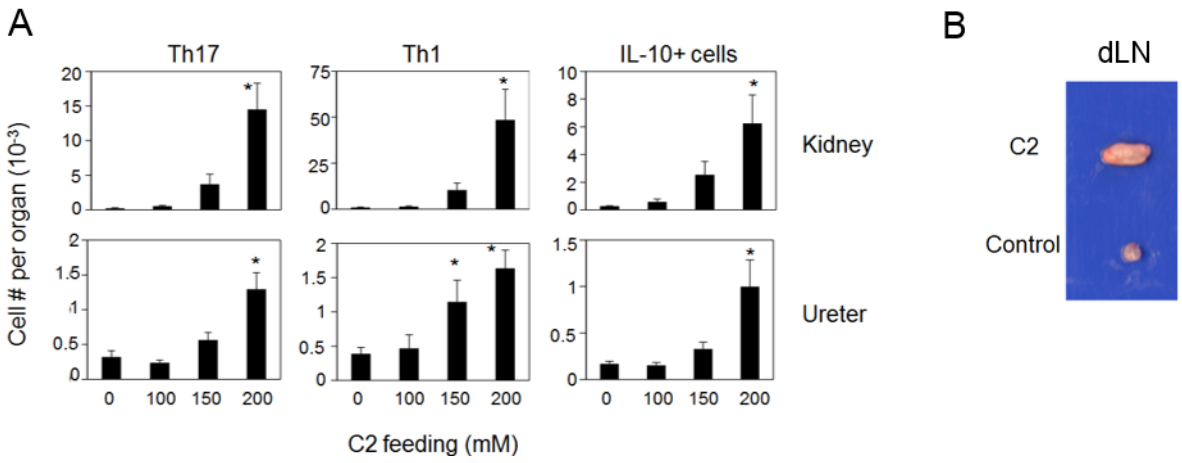

Figure 3.15 C2 dose-dependent changes of renal T cells in C2RD.

(A) Changes in the T cell numbers of kidneys at different doses of C2. (B) Aggrandized renal draining lymph nodes (dLN) with C2RD. Mice were fed with C2 water at indicated concentrations for six weeks and T cell numbers were determined by flow cytometry. Representative images or pooled data were obtained from six individual mice. *Significant differences from non-treated groups ($P \leq 0.05$).

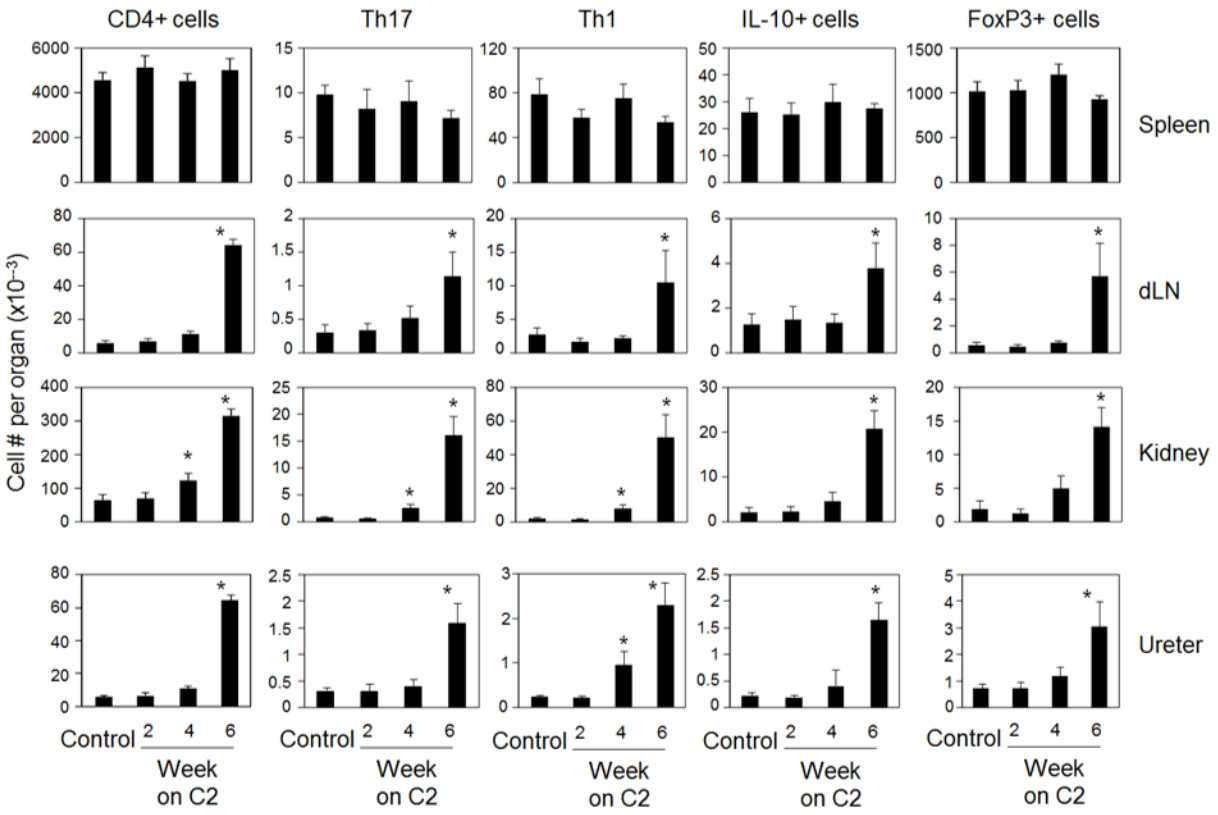

Figure 3.16 Kinetic changes in T cell numbers duringC2RD development.

Cells from spleen, dLN, kidneys or ureters were collected from C2-fed mice at indicated time points. To evaluate the T cell expansion, antibodies to CD4, IL-17, IFNγ, IL-10, or FoxP3 were applied and the numbers of $CD4^+$ cell, Th1, Th17, IL-10^+, and $FoxP3^+$ T cells were examined by flow cytometry. Pooled data were obtained from six individual mice. *Significant differences from Control groups ($P \leq 0.05$).

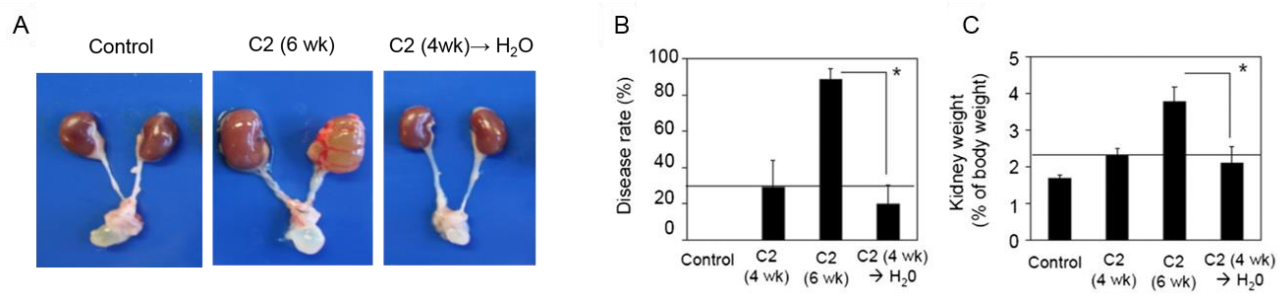

Figure 3.17 C2RD development by continuous exposure to C2.

C2 water was administered to mice for four weeks and switched to normal water for an additional two weeks, and C2RD development was compared to six weeks' feeding of C2. The effect of C2-withdrawal was investigated with gross images of renal tissues (A), disease rate (B), and kidney weight (C). Representative and pooled data are shown (n=6-18). *Significant differences from control or indicated groups ($P \leq 0.05$).

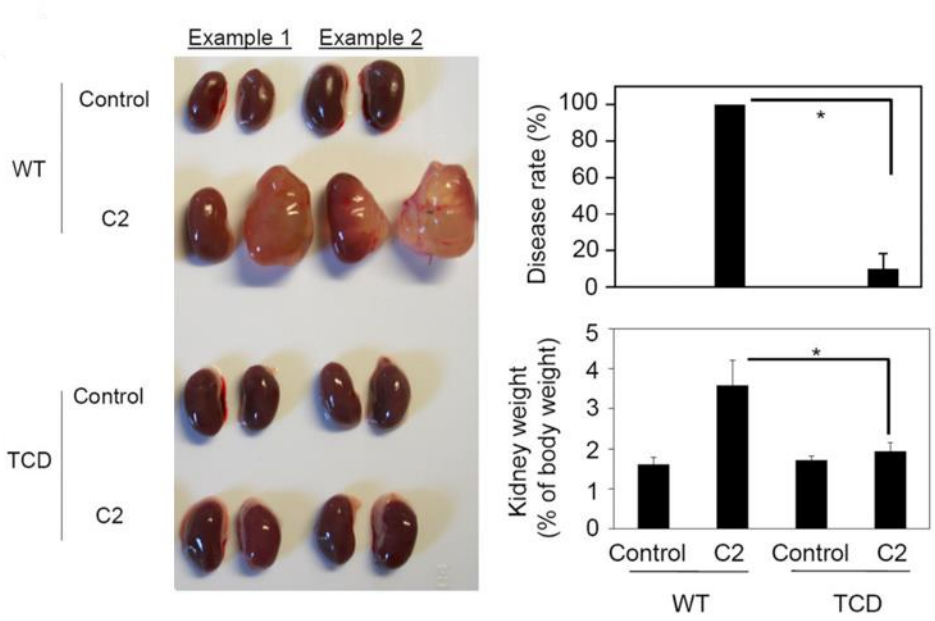

Figure 3.18 Role of T cells in C2RD development.

Gross images of renal tissues, disease rates, and relative kidney weights are shown. Wild-type (WT) or T cell (αβ-TCR)-deficient (TCD) mice were fed with regular or C2 (200 mM)-containing drinking water for six weeks. Representative or pooled data from eight individual mice are shown. *Significant differences from C2-fed WT group ($P \leq 0.05$).

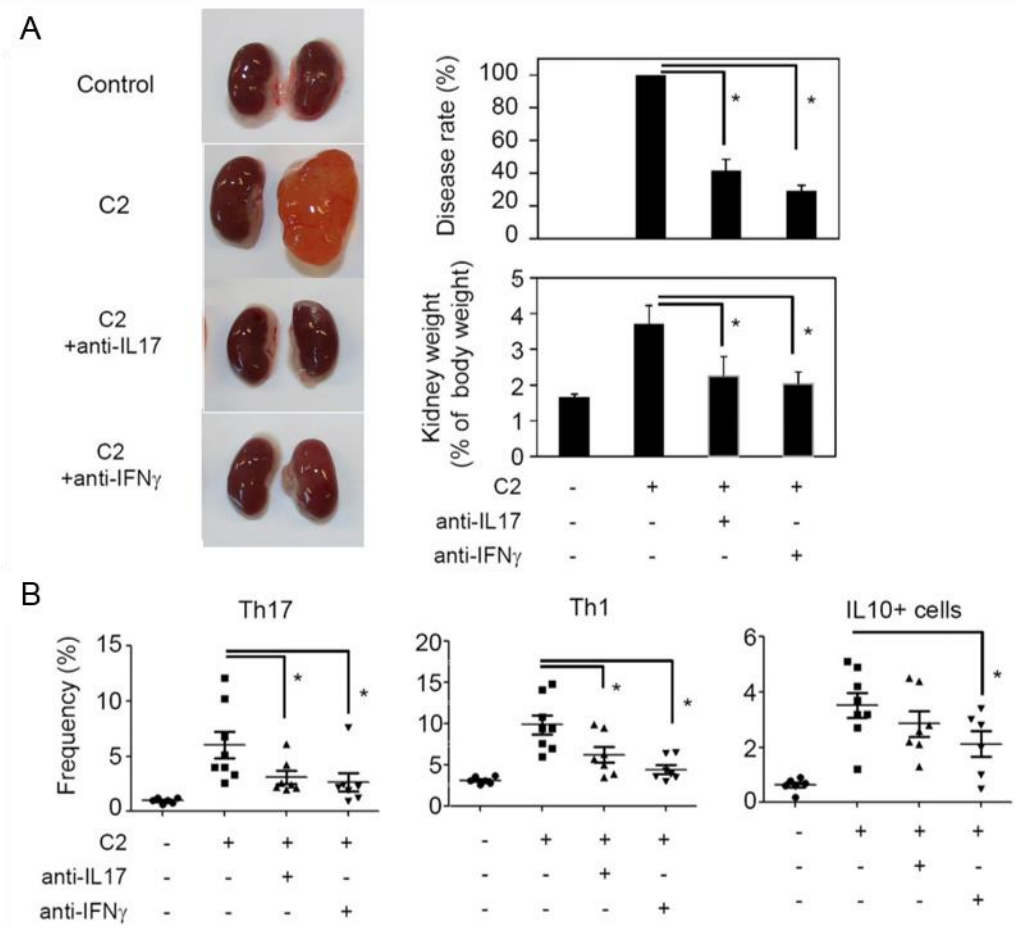

Figure 3.19 Roles of IL-17 and IFNγ in C2RD development.

(A) Gross images of renal tissues, disease rates, and relative kidney weights are shown. Mice were injected with neutralizing antibodies to IL-17 or IFNγ (100 μg/mouse, once a week) during the C2 feeding. (B) Frequencies of renal Th17, Th1, and IL-10^{+} T cells were determined by flow cytometry. Representative images and pooled data from six to eight individual mice are shown. *Significant differences from C2-alone groups ($P \leq 0.05$).

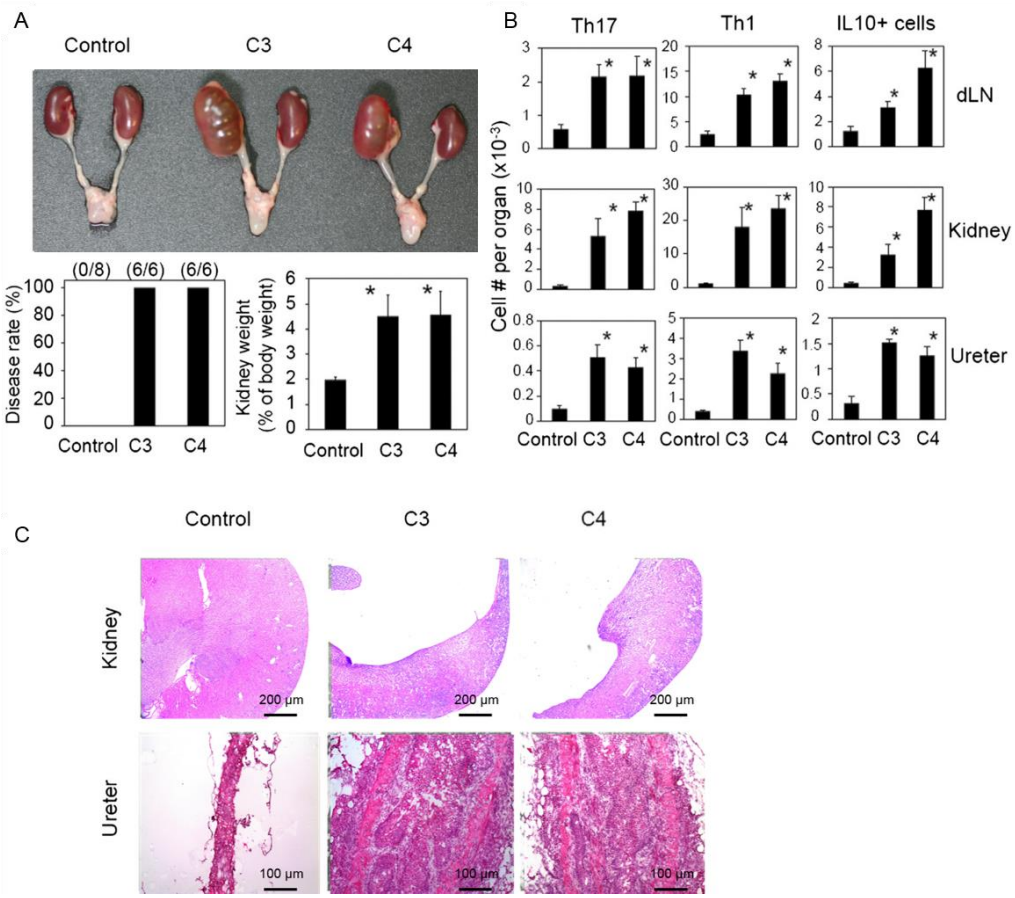

Figure 3.20 C2RD development by other SCFAs propionate (C3) and butyrate (C4).

(A) Gross images of renal tissues, disease rates, and relative kidney weights are shown. Mice were fed with C3 (200 mM) or C4 (200 mM)-infused drinking water for six weeks. (B) T cell number changes in the dLN, kidneys, or ureter tissues were examined by flow cytometry. (C) Histology of kidneys and proximal ureters were observed with HnE staining. Original magnification ×50 (kidneys) and ×100 (ureters). Representative and pooled data are shown (n=6-8). *Significant differences from control groups ($P \leq 0.05$).

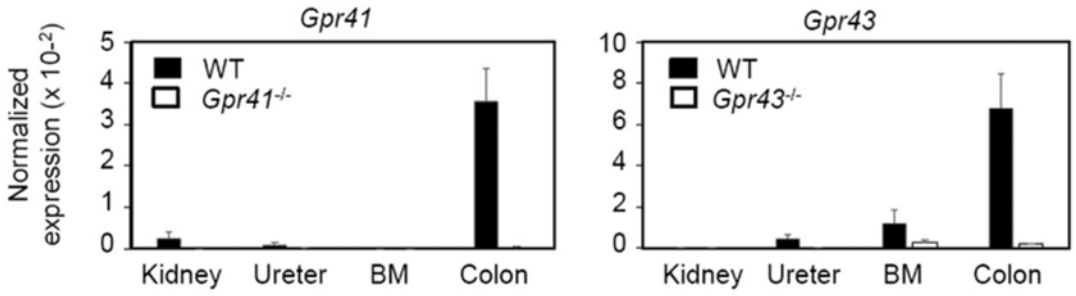

Figure 3.21 Expression of SCFA receptors GPR41 and GPR43.

Expression of *Gpr41* and *Gpr43* at mRNA level were determined by qRT-PCR. RNA was isolated from indicated tissues in WT and GPR-deficient mice. Pooled data from three individual mice are shown.

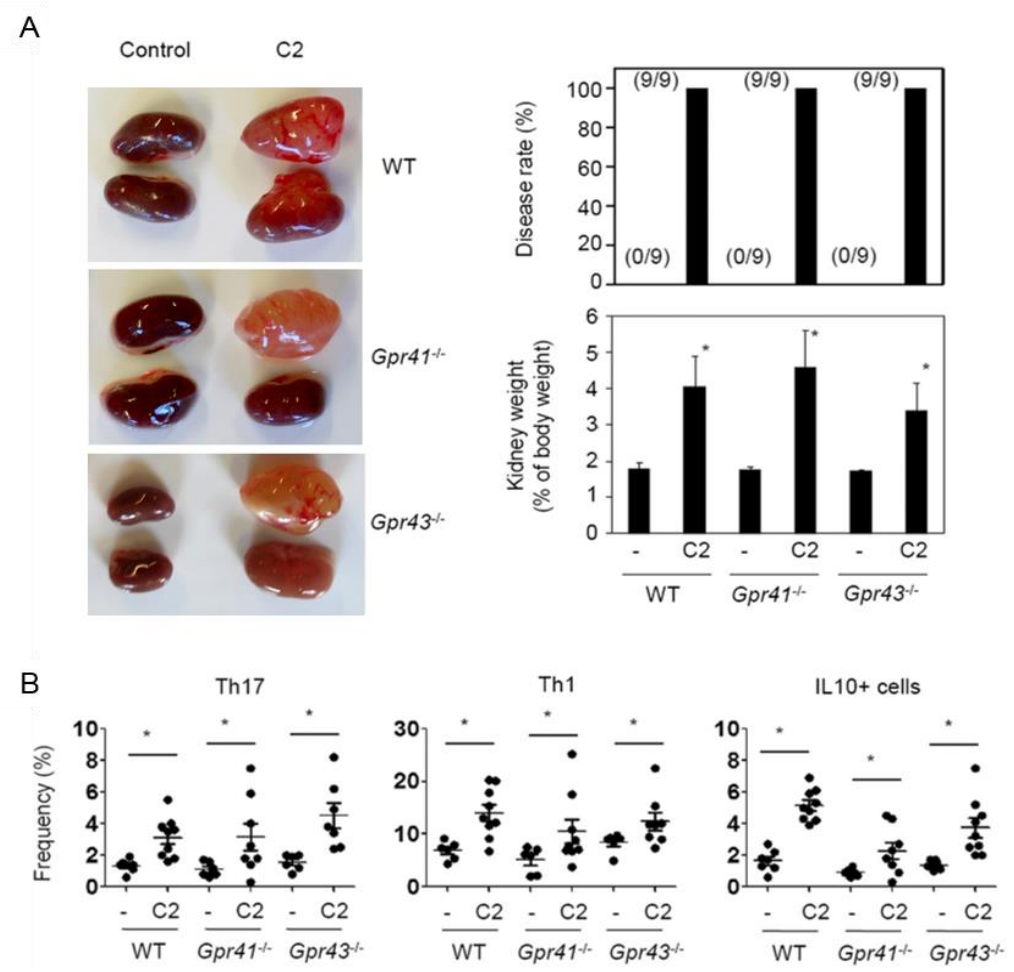

Figure 3.22 Role of GPR41 and GPR43 in C2RD development

(A) Gross images of renal tissues, disease rates, and relative kidney weights are shown. C2-water was administered to WT-, GPR41- or GPR43-deficient mice for 6 weeks. Frequencies of renal Th17, Th1, or IL-10^{+} T cells were examined by flow cytometry. Representative images and pooled data from six to eight individual mice are shown. *Significant differences from C2-only groups ($P \leq 0.05$).

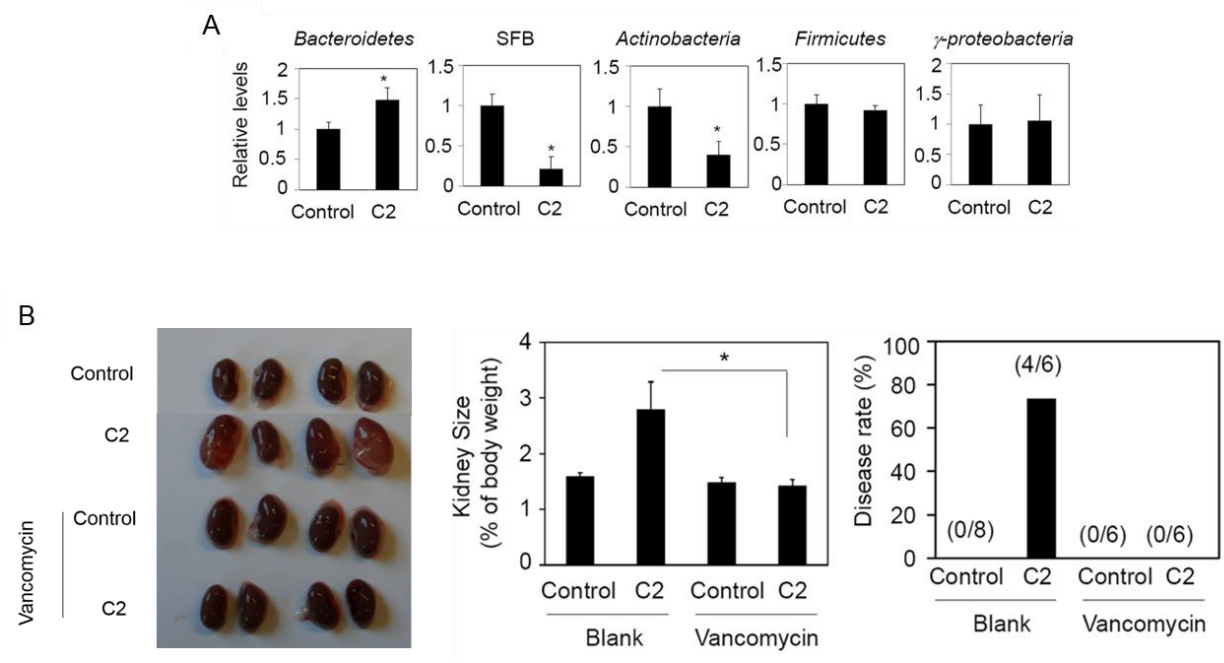

Figure 3.23 Role of gut microbiota in C2RD development

(A) The composition of selected gut microbiota is determined by qPCR using group-specific 16S rRNA sequences. Bacterial DNA from fecal material was isolated from normal or C2RD mice. (B) Mice were administered C2 water for six weeks in the presence or absence of vancomycin (0.5 g/L). Gross images of kidney tissues, C2RD rates, and relative kidney weight are shown. Representative image or pooled data six to eight individual mice are shown. *Significant differences from control or C2-alone groups ($P \leq 0.05$).

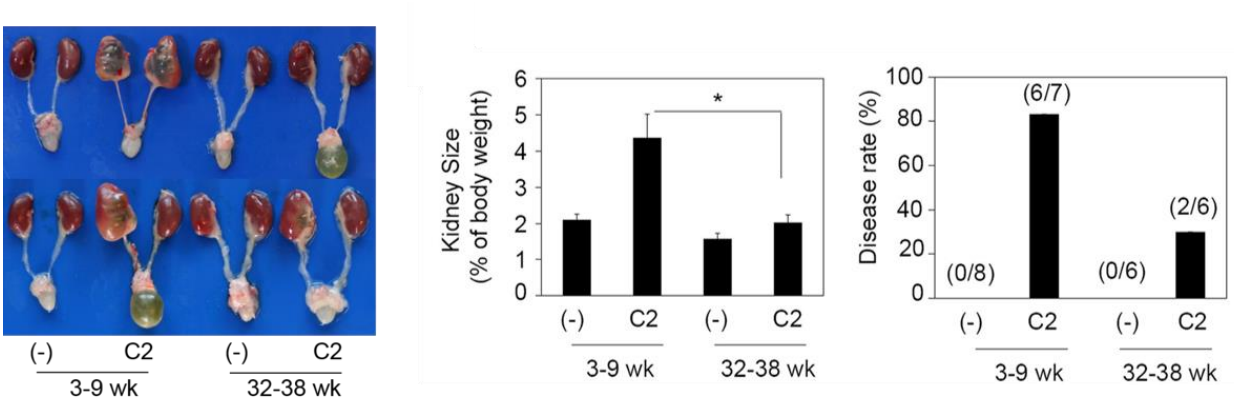

Figure 3.24 Effect of age on C2RD development.

Mice were fed C2-containing water for six weeks from the age of three week (younger) or thirty two weeks (older). Gross images of renal tissues, relative kidney weights, and disease rates are shown. Representative images and pooled data from six to eight individual mice are shown. *Significant differences from indicated group ($P \leq 0.05$).

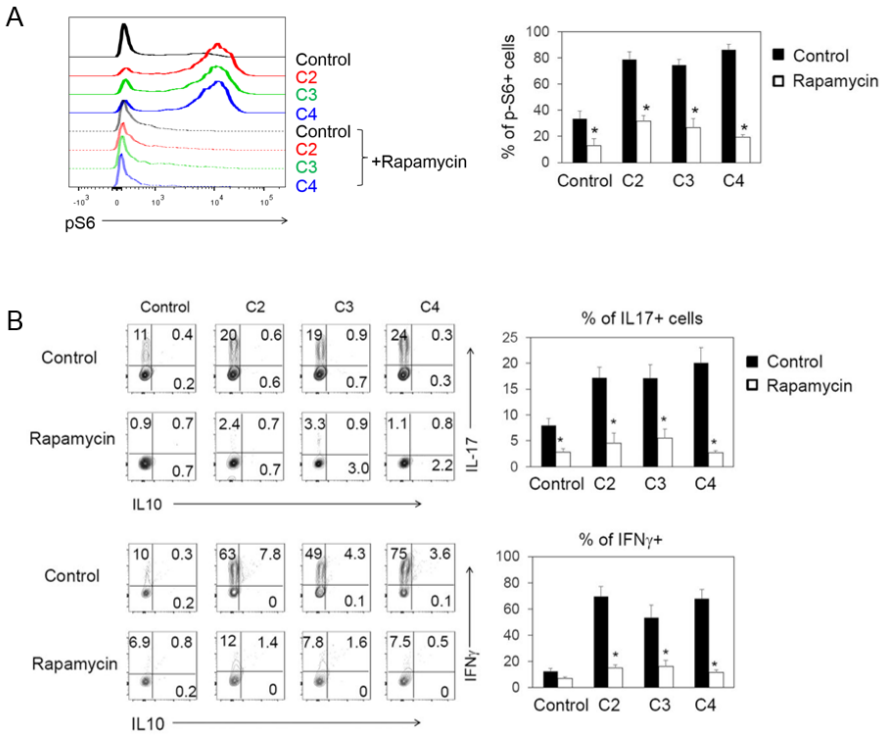

Figure 3.25 Effect of SCFAs and rapamycin on mTOR activity or effector T cell differentiation of renal dLN-T cells.

Total renal lymph node cells were activated with anti-CD3 in the presence of SCFAs and rapamycin (mTOR inhibitor). (A) mTOR activity among $CD4^+$ T cells was examined after three-day activation in Tnp polarizing condition. Levels of rS6 phosphorylation were evaluated by flow cytometry. (B) Differentiation into effector ($IL\text{-}17^+$ or $IFN\gamma^+$) T cells was examined after a five or six day culture in Th1 or Th17 polarizing conditions. Representative dot plots or pooled data from four experiments are shown. *Significant differences from control groups ($P \leq 0.05$).

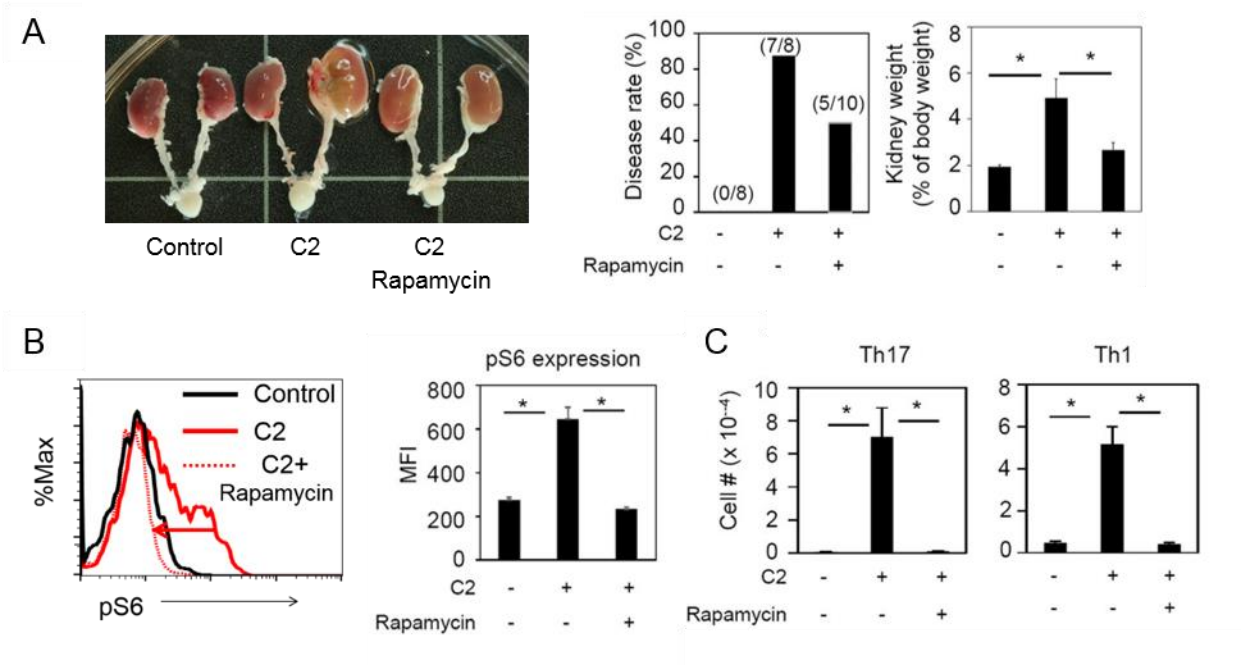

Figure 3.26 Role of rapamycin in C2RD development.

(A) Gross images of renal tissues, disease rates, and relative kidney weights are shown. Mice were fed normal or C2-water in the presence or absence of rapamycin (25 μg/ml) for six weeks. (B) mTOR activity (phosphorylation of rS6) in renal $CD4^+$ T cells in rapamycin-and/orC2-fed mice was examined by flow cytometry. (C) Effect of rapamycin and/or C2 administration on effector T cell numbers is shown. Representative images and pooled data from seven to ten individual mice are shown. *Significant differences from indicated groups ($P \leq 0.05$).

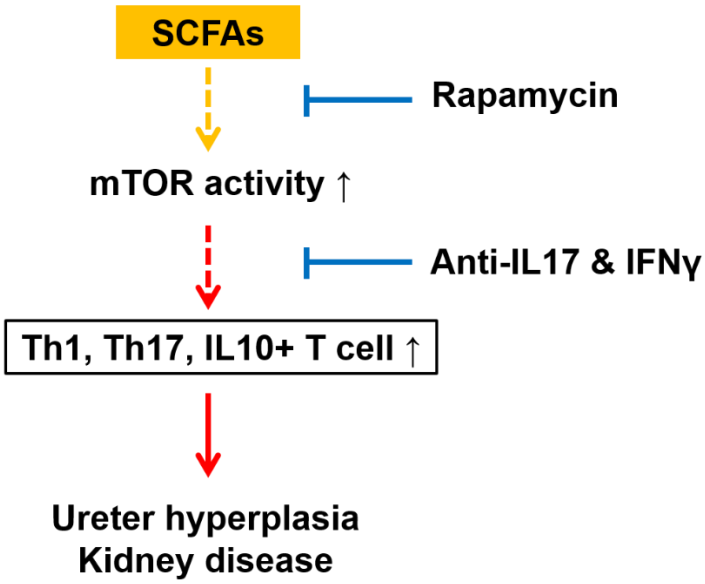

Figure 3.27 Impact of SCFAs on T cell in development of renal inflammation

Oral SCFAs feeding induced a chronic ureter hyperplasia and hydronephrosis. In affected tissues, inflammatory T cells were highly infiltrated, while T cell-deficient condition blocked disease development. Rapamycin a mTOR inhibitor, or neutralizing antibodies of IL-17 and IFNγ ameliorated the SCFA-mediated renal inflammation.

REFERENCES

REFERENCES

1. Flint HJ, Scott KP, Louis P, Duncan SH. The role of the gut microbiota in nutrition and health. Nature Reviews Gastroenterology and Hepatology. 2012;9(10):577-89.
2. Salyers AA. Energy sources of major intestinal fermentative anaerobes. The American Journal of Clinical Nutrition. 1979;32(1):158-63.
3. Macfarlane S, Macfarlane GT. Regulation of short-chain fatty acid production. Proceedings of the Nutrition Society. 2003;62(01):67-72.
4. Cummings J, Pomare E, Branch W, Naylor C, Macfarlane G. Short chain fatty acids in human large intestine, portal, hepatic and venous blood. Gut. 1987;28(10):1221-7.
5. Corrêa-Oliveira R, Fachi JL, Vieira A, Sato FT, Vinolo MAR. Regulation of immune cell function by short-chain fatty acids. Clinical & translational immunology. 2016;5(4):e73.
6. Tan J, McKenzie C, Potamitis M, Thorburn AN, Mackay CR, Macia L. The role of short-chain fatty acids in health and disease. Adv Immunol. 2014;121(9).
7. Fukuda S, Toh H, Hase K, Oshima K, Nakanishi Y, Yoshimura K, et al. Bifidobacteria can protect from enteropathogenic infection through production of acetate. Nature. 2011;469(7331):543-7.
8. Ragsdale SW, Pierce E. Acetogenesis and the Wood–Ljungdahl pathway of CO 2 fixation. Biochimica et Biophysica Acta (BBA)-Proteins and Proteomics. 2008;1784(12):1873-98.
9. Reichardt N, Duncan SH, Young P, Belenguer A, McWilliam Leitch C, Scott KP, et al. Phylogenetic distribution of three pathways for propionate production within the human gut microbiota. Isme j. 2014;8(6):1323-35.
10. Louis P, Flint HJ. Diversity, metabolism and microbial ecology of butyrate-producing bacteria from the human large intestine. FEMS microbiology letters. 2009;294(1):1-8.
11. Trompette A, Gollwitzer ES, Yadava K, Sichelstiel AK, Sprenger N, Ngom-Bru C, et al. Gut microbiota metabolism of dietary fiber influences allergic airway disease and hematopoiesis. Nature medicine. 2014;20(2):159-66.
12. Ziegler TR, Evans ME, Fernández-Estívariz C, Jones DP. Trophic and cytoprotective nutrition for intestinal adaptation, mucosal repair, and barrier function. Annual review of nutrition. 2003;23(1):229-61.
13. Kim CH, Park J, Kim M. Gut microbiota-derived short-chain fatty acids, T cells, and inflammation. Immune network. 2014;14(6):277-88.
14. Hadjiagapiou C, Schmidt L, Dudeja PK, Layden TJ, Ramaswamy K. Mechanism (s) of butyrate transport in Caco-2 cells: role of monocarboxylate transporter 1. American Journal of Physiology-Gastrointestinal and Liver Physiology. 2000;279(4):G775-G80.

15. Eberle JA-M, Widmayer P, Breer H. Receptors for short-chain fatty acids in brush cells at the “gastric groove”. Frontiers in physiology. 2014;5:152.
16. Brown AJ, Goldsworthy SM, Barnes AA, Eilert MM, Tcheang L, Daniels D, et al. The Orphan G protein-coupled receptors GPR41 and GPR43 are activated by propionate and other short chain carboxylic acids. Journal of Biological Chemistry. 2003;278(13):11312-9.
17. Milligan G, Stoddart LA, Smith NJ. Agonism and allosterism: the pharmacology of the free fatty acid receptors FFA2 and FFA3. British journal of pharmacology. 2009;158(1):146-53.
18. Thangaraju M, Cresci GA, Liu K, Ananth S, Gnanaprakasam JP, Browning DD, et al. GPR109A is a G-protein–coupled receptor for the bacterial fermentation product butyrate and functions as a tumor suppressor in colon. Cancer research. 2009;69(7):2826-32.
19. Singh N, Gurav A, Sivaprakasam S, Brady E, Padia R, Shi H, et al. Activation of Gpr109a, receptor for niacin and the commensal metabolite butyrate, suppresses colonic inflammation and carcinogenesis. Immunity. 2014;40(1):128-39.
20. Germain RN. T-cell development and the CD4–CD8 lineage decision. Nature Reviews Immunology. 2002;2(5):309-22.
21. Zúñiga-Pflücker JC. T-cell development made simple. Nature Reviews Immunology. 2004;4(1):67-72.
22. Dai Z, Lakkis FG. Cutting edge: secondary lymphoid organs are essential for maintaining the CD4, but not CD8, naive T cell pool. The Journal of Immunology. 2001;167(12):6711-5.
23. Kaech SM, Wherry EJ, Ahmed R. Effector and memory T-cell differentiation: implications for vaccine development. Nature Reviews Immunology. 2002;2(4):251-62.
24. Weaver CT, Hatton RD, Mangan PR, Harrington LE. IL-17 family cytokines and the expanding diversity of effector T cell lineages. Annu Rev Immunol. 2007;25:821-52.
25. Bettelli E, Carrier Y, Gao W, Korn T, Strom TB, Oukka M, et al. Reciprocal developmental pathways for the generation of pathogenic effector TH17 and regulatory T cells. Nature. 2006;441(7090):235-8.
26. Gavin MA, Rasmussen JP, Fontenot JD, Vasta V, Manganiello VC, Beavo JA, et al. Foxp3-dependent programme of regulatory T-cell differentiation. Nature. 2007;445(7129):771-5.
27. Luther SA, Cyster JG. Chemokines as regulators of T cell differentiation. Nature immunology. 2001;2(2):102-7.
28. Mucida D, Park Y, Kim G, Turovskaya O, Scott I, Kronenberg M, et al. Reciprocal TH17 and regulatory T cell differentiation mediated by retinoic acid. Science. 2007;317(5835):256-60.
29. Furusawa Y, Obata Y, Fukuda S, Endo TA, Nakato G, Takahashi D, et al. Commensal microbe-derived butyrate induces the differentiation of colonic regulatory T cells. Nature. 2013;504(7480):446-50.
30. Arpaia N, Campbell C, Fan X, Dikiy S, van der Veeken J, Liu H, et al. Metabolites produced by commensal bacteria promote peripheral regulatory T-cell generation. Nature. 2013;504(7480):451-5.

31. Smith PM, Howitt MR, Panikov N, Michaud M, Gallini CA, Bohlooly-Y M, et al. The microbial metabolites, short-chain fatty acids, regulate colonic Treg cell homeostasis. Science. 2013;341(6145):569-73.
32. Haghikia A, Jörg S, Duscha A, Berg J, Manzel A, Waschbisch A, et al. Dietary fatty acids directly impact central nervous system autoimmunity via the small intestine. Immunity. 2015;43(4):817-29.
33. Scott K, Duncan S, Flint H. Dietary fibre and the gut microbiota. Nutrition Bulletin. 2008;33(3):201-11.
34. Glenn G, Roberfroid M. Dietary modulation of the human colonic microbiota: introducing the concept of prebiotics. J nutr. 1995;125:1401-12.
35. Kimura I, Inoue D, Hirano K, Tsujimoto G. The SCFA receptor GPR43 and energy metabolism. Frontiers in endocrinology. 2014;5.
36. Maslowski KM, Vieira AT, Ng A, Kranich J, Sierro F, Yu D, et al. Regulation of inflammatory responses by gut microbiota and chemoattractant receptor GPR43. Nature. 2009;461(7268):1282-6.
37. Sina C, Gavrilova O, Förster M, Till A, Derer S, Hildebrand F, et al. G protein-coupled receptor 43 is essential for neutrophil recruitment during intestinal inflammation. The Journal of Immunology. 2009;183(11):7514-22.
38. Kim MH, Kang SG, Park JH, Yanagisawa M, Kim CH. Short-chain fatty acids activate GPR41 and GPR43 on intestinal epithelial cells to promote inflammatory responses in mice. Gastroenterology. 2013;145(2):396-406. e10.
39. Glauben R, Batra A, Stroh T, Erben U, Fedke I, Lehr HA, et al. Histone deacetylases: novel targets for prevention of colitis-associated cancer in mice. Gut. 2008;57(5):613-22.
40. Glauben R, Batra A, Fedke I, Zeitz M, Lehr HA, Leoni F, et al. Histone hyperacetylation is associated with amelioration of experimental colitis in mice. The Journal of Immunology. 2006;176(8):5015-22.
41. Turgeon N, Blais M, Gagné J-M, Tardif V, Boudreau F, Perreault N, et al. HDAC1 and HDAC2 restrain the intestinal inflammatory response by regulating intestinal epithelial cell differentiation. PLoS One. 2013;8(9):e73785.
42. Chang PV, Hao L, Offermanns S, Medzhitov R. The microbial metabolite butyrate regulates intestinal macrophage function via histone deacetylase inhibition. Proceedings of the National Academy of Sciences. 2014;111(6):2247-52.
43. Vinolo MA, Rodrigues HG, Hatanaka E, Sato FT, Sampaio SC, Curi R. Suppressive effect of short-chain fatty acids on production of proinflammatory mediators by neutrophils. The Journal of nutritional biochemistry. 2011;22(9):849-55.
44. Park J, Kim M, Kang SG, Jannasch AH, Cooper B, Patterson J, et al. Short-chain fatty acids induce both effector and regulatory T cells by suppression of histone deacetylases and regulation of the mTOR–S6K pathway. Mucosal immunology. 2015;8(1):80-93.
45. Tapmeier TT, Fearn A, Brown K, Chowdhury P, Sacks SH, Sheerin NS, et al. Pivotal role of CD4+ T cells in renal fibrosis following ureteric obstruction. Kidney international. 2010;78(4):351-62.

46. Park J, Goergen CJ, HogenEsch H, Kim CH. Chronically Elevated Levels of Short-Chain Fatty Acids Induce T Cell–Mediated Ureteritis and Hydronephrosis. The Journal of Immunology. 2016;196(5):2388-400.
47. Hopfer H, Holzer J, Hünemörder S, Paust H-J, Sachs M, Meyer-Schwesinger C, et al. Characterization of the renal CD4+ T-cell response in experimental autoimmune glomerulonephritis. Kidney international. 2012;82(1):60-71.
48. Summers SA, Steinmetz OM, Li M, Kausman JY, Semple T, Edgtton KL, et al. Th1 and Th17 cells induce proliferative glomerulonephritis. Journal of the American Society of Nephrology. 2009;20(12):2518-24.
49. Pisitkun P, Ha H-L, Wang H, Claudio E, Tivy CC, Zhou H, et al. Interleukin-17 cytokines are critical in development of fatal lupus glomerulonephritis. Immunity. 2012;37(6):1104-15.
50. Pindjakova J, Hanley SA, Duffy MM, Sutton CE, Weidhofer GA, Miller MN, et al. Interleukin-1 accounts for intrarenal Th17 cell activation during ureteral obstruction. Kidney international. 2012;81(4):379-90.
51. Dong X, Bachman LA, Miller MN, Nath KA, Griffin MD. Dendritic cells facilitate accumulation of IL-17 T cells in the kidney following acute renal obstruction. Kidney international. 2008;74(10):1294-309.
52. Kuroiwa T, Schlimgen R, Illei GG, McInnes IB, Boumpas DT. Distinct T cell/renal tubular epithelial cell interactions define differential chemokine production: implications for tubulointerstitial injury in chronic glomerulonephritides. The Journal of Immunology. 2000;164(6):3323-9.
53. Delgoffe GM, Kole TP, Zheng Y, Zarek PE, Matthews KL, Xiao B, et al. The mTOR kinase differentially regulates effector and regulatory T cell lineage commitment. Immunity. 2009;30(6):832-44.
54. Araki K, Turner AP, Shaffer VO, Gangappa S, Keller SA, Bachmann MF, et al. mTOR regulates memory CD8 T-cell differentiation. Nature. 2009;460(7251):108-12.
55. Zhang S, Readinger JA, DuBois W, Janka-Junttila M, Robinson R, Pruitt M, et al. Constitutive reductions in mTOR alter cell size, immune cell development, and antibody production. Blood. 2011;117(4):1228-38.
56. Cao W, Manicassamy S, Tang H, Kasturi SP, Pirani A, Murthy N, et al. Toll-like receptor–mediated induction of type I interferon in plasmacytoid dendritic cells requires the rapamycin-sensitive PI (3) K-mTOR-p70S6K pathway. Nature immunology. 2008;9(10):1157-64.
57. Turnquist HR, Cardinal J, Macedo C, Rosborough BR, Sumpter TL, Geller DA, et al. mTOR and GSK-3 shape the CD4+ T-cell stimulatory and differentiation capacity of myeloid DCs after exposure to LPS. Blood. 2010;115(23):4758-69.
58. Warner G, Hein KZ, Nin V, Edwards M, Chini CC, Hopp K, et al. Food Restriction Ameliorates the Development of Polycystic Kidney Disease. Journal of the American Society of Nephrology. 2015:ASN. 2015020132.
59. Li J, Ren J, Liu X, Jiang L, He W, Yuan W, et al. Rictor/mTORC2 signaling mediates TGFβ1-induced fibroblast activation and kidney fibrosis. Kidney international. 2015.

60. Chen G, Chen H, Wang C, Peng Y, Sun L, Liu H, et al. Rapamycin ameliorates kidney fibrosis by inhibiting the activation of mTOR signaling in interstitial macrophages and myofibroblasts. PloS one. 2012;7(3):e33626.
61. Wu M, Wen M, Chiu Y, Chiou Y, Shu K, Tang M-J. Rapamycin attenuates unilateral ureteral obstruction-induced renal fibrosis. Kidney international. 2006;69(11):2029-36.
62. Hochegger K, Jansky GL, Soleiman A, Wolf AM, Tagwerker A, Seger C, et al. Differential effects of rapamycin in anti-GBM glomerulonephritis. Journal of the American Society of Nephrology. 2008;19(8):1520-9.
63. Stratakis S, Stylianou K, Petrakis I, Mavroeidi V, Poulidaki R, Petra C, et al. Rapamycin ameliorates proteinuria and restores nephrin and podocin expression in experimental membranous nephropathy. Clinical and Developmental Immunology. 2013;2013.
64. Dong G, Liu Y, Zhang L, Huang S, Ding H-F, Dong Z. mTOR contributes to ER stress and associated apoptosis in renal tubular cells. American Journal of Physiology-Renal Physiology. 2015;308(3):F267-F74.
65. Appenzeller-Herzog C, Hall MN. Bidirectional crosstalk between endoplasmic reticulum stress and mTOR signaling. Trends in cell biology. 2012;22(5):274-82.
66. Ito N, Nishibori Y, Ito Y, Takagi H, Akimoto Y, Kudo A, et al. mTORC1 activation triggers the unfolded protein response in podocytes and leads to nephrotic syndrome. Laboratory Investigation. 2011;91(11):1584-95.
67. Pang M, Kothapally J, Mao H, Tolbert E, Ponnusamy M, Chin YE, et al. Inhibition of histone deacetylase activity attenuates renal fibroblast activation and interstitial fibrosis in obstructive nephropathy. American Journal of Physiology-Renal Physiology. 2009;297(4):F996-F1005.
68. Liu N, He S, Ma L, Ponnusamy M, Tang J, Tolbert E, et al. Blocking the class I histone deacetylase ameliorates renal fibrosis and inhibits renal fibroblast activation via modulating TGF-beta and EGFR signaling. PLoS One. 2013;8(1):e54001.
69. Andrade-Oliveira V, Amano MT, Correa-Costa M, Castoldi A, Felizardo RJ, de Almeida DC, et al. Gut bacteria products prevent AKI induced by ischemia-reperfusion. Journal of the American Society of Nephrology. 2015:ASN. 2014030288.
70. Costalonga EC, Silva FM, Noronha IL. Valproic Acid Prevents Renal Dysfunction and Inflammation in the Ischemia-Reperfusion Injury Model. BioMed Research International. 2016;2016.
71. Cosentino CC, Skrypnyk NI, Brilli LL, Chiba T, Novitskaya T, Woods C, et al. Histone deacetylase inhibitor enhances recovery after AKI. Journal of the American Society of Nephrology. 2013;24(6):943-53.
72. Vaziri ND, Wong J, Pahl M, Piceno YM, Yuan J, DeSantis TZ, et al. Chronic kidney disease alters intestinal microbial flora. Kidney international. 2013;83(2):308-15.
73. Vaziri ND, Yuan J, Nazertehrani S, Ni Z, Liu S. Chronic kidney disease causes disruption of gastric and small intestinal epithelial tight junction. American journal of nephrology. 2013;38(2):99-103.

74. Wong J, Piceno YM, DeSantis TZ, Pahl M, Andersen GL, Vaziri ND. Expansion of urease-and uricase-containing, indole-and p-cresol-forming and contraction of short-chain fatty acid-producing intestinal microbiota in ESRD. American journal of nephrology. 2014;39(3):230-7.
75. KUNIN CM. A guide to use of antibiotics in patients with renal disease: A table of recommended doses and factors governing serum levels. Annals of Internal Medicine. 1967;67(1):151-8.
76. Ramezani A, Raj DS. The gut microbiome, kidney disease, and targeted interventions. Journal of the American Society of Nephrology. 2014;25(4):657-70.
77. Bird ST, Etminan M, Brophy JM, Hartzema AG, Delaney JA. Risk of acute kidney injury associated with the use of fluoroquinolones. Canadian Medical Association Journal. 2013;185(10):E475-E82.
78. Lomaestro BM. Fluoroquinolone-induced renal failure. Drug safety. 2000;22(6):479-85.
79. Jensen J-US, Hein L, Lundgren B, Bestle MH, Mohr T, Andersen MH, et al. Kidney failure related to broad-spectrum antibiotics in critically ill patients: secondary end point results from a 1200 patient randomised trial. BMJ open. 2012;2(2):e000635.
80. Machado RA, de Souza Constantino L, Tomasi CD, Rojas HA, Vuolo FS, Vitto MF, et al. Sodium butyrate decreases the activation of NF-κB reducing inflammation and oxidative damage in the kidney of rats subjected to contrast-induced nephropathy. Nephrology Dialysis Transplantation. 2012:gfr807.
81. Matsumoto N, Riley S, Fraser D, Al-Assaf S, Ishimura E, Wolever T, et al. Butyrate modulates TGF-β1 generation and function: Potential renal benefit for Acacia (sen) SUPERGUM™(gum arabic)? Kidney international. 2006;69(2):257-65.
82. Kishimoto K, Kinoshita K, Hino S, Yano T, Nagare Y, Shimazu H, et al. Therapeutic effect of retinoic acid on unilateral ureteral obstruction model. Nephron Experimental nephrology. 2011;118(3):e69-e78.
83. Kang SG, Park J, Cho JY, Ulrich B, Kim CH. Complementary roles of retinoic acid and TGF-beta1 in coordinated expression of mucosal integrins by T cells. Mucosal immunology. 2011;4(1):66-82.
84. Kamanaka M, Kim ST, Wan YY, Sutterwala FS, Lara-Tejero M, Galan JE, et al. Expression of interleukin-10 in intestinal lymphocytes detected by an interleukin-10 reporter knockin tiger mouse. Immunity. 2006;25(6):941-52.
85. Merger M, Viney JL, Borojevic R, Steele-Norwood D, Zhou P, Clark DA, et al. Defining the roles of perforin, Fas/FasL, and tumour necrosis factor alpha in T cell induced mucosal damage in the mouse intestine. Gut. 2002;51(2):155-63.
86. Kiefer J, Beyer-Sehlmeyer G, Pool-Zobel BL. Mixtures of SCFA, composed according to physiologically available concentrations in the gut lumen, modulate histone acetylation in human HT29 colon cancer cells. Br J Nutr. 2006;96(5):803-10.
87. Hinnebusch BF, Meng S, Wu JT, Archer SY, Hodin RA. The effects of short-chain fatty acids on human colon cancer cell phenotype are associated with histone hyperacetylation. J Nutr. 2002;132(5):1012-7.
88. Smith PM, Howitt MR, Panikov N, Michaud M, Gallini CA, Bohlooly YM, et al. The Microbial Metabolites, Short-Chain Fatty Acids, Regulate Colonic Treg Cell Homeostasis. Science. 2013.

89. Delgoffe GM, Kole TP, Zheng Y, Zarek PE, Matthews KL, Xiao B, et al. The mTOR kinase differentially regulates effector and regulatory T cell lineage commitment. Immunity. 2009;30(6):832-44.
90. Lee K, Gudapati P, Dragovic S, Spencer C, Joyce S, Killeen N, et al. Mammalian target of rapamycin protein complex 2 regulates differentiation of Th1 and Th2 cell subsets via distinct signaling pathways. Immunity. 2010;32(6):743-53.
91. Ochanuna Z, Geiger-Maor A, Dembinsky-Vaknin A, Karussis D, Tykocinski ML, Rachmilewitz J. Inhibition of effector function but not T cell activation and increase in FoxP3 expression in T cells differentiated in the presence of PP14. PLoS One. 2010;5(9):e12868.
92. Chi Y, Gao K, Li K, Nakajima S, Kira S, Takeda M, et al. Purinergic control of AMPK activation by ATP released through connexin 43 hemichannels–pivotal roles in hemichannel-mediated cell injury. J Cell Sci. 2014;127(7):1487-99.
93. Inoki K, Kim J, Guan K-L. AMPK and mTOR in cellular energy homeostasis and drug targets. Annual review of pharmacology and toxicology. 2012;52:381-400.
94. Chi H. Regulation and function of mTOR signalling in T cell fate decisions. Nature Reviews Immunology. 2012;12(5):325-38.
95. Fenton T, Gwalter J, Ericsson J, Gout I. Histone acetyltransferases interact with and acetylate p70 ribosomal S6 kinases in vitro and in vivo. The international journal of biochemistry & cell biology. 2010;42(2):359-66.
96. Weichhart T, Costantino G, Poglitsch M, Rosner M, Zeyda M, Stuhlmeier KM, et al. The TSC-mTOR signaling pathway regulates the innate inflammatory response. Immunity. 2008;29(4):565-77.
97. Saraiva M, Christensen JR, Veldhoen M, Murphy TL, Murphy KM, O'Garra A. Interleukin-10 production by Th1 cells requires interleukin-12-induced STAT4 transcription factor and ERK MAP kinase activation by high antigen dose. Immunity. 2009;31(2):209-19.
98. Stumhofer JS, Silver JS, Laurence A, Porrett PM, Harris TH, Turka LA, et al. Interleukins 27 and 6 induce STAT3-mediated T cell production of interleukin 10. Nature immunology. 2007;8(12):1363-71.
99. Ma J, Meng Y, Kwiatkowski DJ, Chen X, Peng H, Sun Q, et al. Mammalian target of rapamycin regulates murine and human cell differentiation through STAT3/p63/Jagged/Notch cascade. The Journal of clinical investigation. 2010;120(1):103-14.
100. Tao R, de Zoeten EF, Özkaynak E, Chen C, Wang L, Porrett PM, et al. Deacetylase inhibition promotes the generation and function of regulatory T cells. Nature medicine. 2007;13(11):1299-307.
101. Hardie DG, Alessi DR. LKB1 and AMPK and the cancer-metabolism link-ten years after. BMC biology. 2013;11(1):1.
102. Wildenberg ME, Vos ACW, Wolfkamp SC, Duijvestein M, Verhaar AP, Te Velde AA, et al. Autophagy attenuates the adaptive immune response by destabilizing the immunologic synapse. Gastroenterology. 2012;142(7):1493-503. e6.
103. Wang Z, Zang C, Cui K, Schones DE, Barski A, Peng W, et al. Genome-wide mapping of HATs and HDACs reveals distinct functions in active and inactive genes. Cell. 2009;138(5):1019-31.

104. Corraliza I, Campo M, Soler G, Modolell M. Determination of arginase activity in macrophages: a micromethod. Journal of immunological methods. 1994;174(1):231-5.
105. Goergen CJ, Li HH, Francke U, Taylor CA. Induced chromosome deletion in a Williams-Beuren syndrome mouse model causes cardiovascular abnormalities. Journal of vascular research. 2011;48(2):119-29.
106. Park J, Kim M, Kang SG, Jannasch AH, Cooper B, Patterson J, et al. Short-chain fatty acids induce both effector and regulatory T cells by suppression of histone deacetylases and regulation of the mTOR-S6K pathway. Mucosal immunology. 2015;8(1):80-93.
107. Barman M, Unold D, Shifley K, Amir E, Hung K, Bos N, et al. Enteric salmonellosis disrupts the microbial ecology of the murine gastrointestinal tract. Infection and immunity. 2008;76(3):907-15.
108. Trompette A, Gollwitzer ES, Yadava K, Sichelstiel AK, Sprenger N, Ngom-Bru C, et al. Gut microbiota metabolism of dietary fiber influences allergic airway disease and hematopoiesis. Nature medicine. 2014;20(2):159-66.
109. Iseki K, Iseki C, Ikemiya Y, Fukiyama K. Risk of developing end-stage renal disease in a cohort of mass screening. Kidney international. 1996;49(3):800-5.
110. Burne MJ, Daniels F, El Ghandour A, Mauiyyedi S, Colvin RB, O'Donnell MP, et al. Identification of the CD4+ T cell as a major pathogenic factor in ischemic acute renal failure. The Journal of clinical investigation. 2001;108(9):1283-90.
111. Woltman AM, De Haij S, Boonstra JG, Gobin SJ, Daha MR, Van Kooten C. Interleukin-17 and CD40-ligand synergistically enhance cytokine and chemokine production by renal epithelial cells. Journal of the American Society of Nephrology. 2000;11(11):2044-55.
112. Wu B, Brooks JD. Gene expression changes induced by unilateral ureteral obstruction in mice. The Journal of urology. 2012;188(3):1033-41.
113. Becknell B, Carpenter AR, Allen JL, Wilhide ME, Ingraham SE, Hains DS, et al. Molecular basis of renal adaptation in a murine model of congenital obstructive nephropathy. PloS one. 2013;8(9):e72762.
114. Pandey P, Qin S, Ho J, Zhou J, Kreidberg JA. Systems biology approach to identify transcriptome reprogramming and candidate microRNA targets during the progression of polycystic kidney disease. BMC systems biology. 2011;5(1):56.
115. Reddy PS, Legault HM, Sypek JP, Collins MJ, Goad E, Goldman SJ, et al. Mapping similarities in mTOR pathway perturbations in mouse lupus nephritis models and human lupus nephritis. Arthritis research & therapy. 2008;10(6):R127.
116. Klein J, Gonzalez J, Miravete M, Caubet C, Chaaya R, Decramer S, et al. Congenital ureteropelvic junction obstruction: human disease and animal models. International journal of experimental pathology. 2011;92(3):168-92.
117. Ubeda C, Taur Y, Jenq RR, Equinda MJ, Son T, Samstein M, et al. Vancomycin-resistant Enterococcus domination of intestinal microbiota is enabled by antibiotic treatment in mice and precedes bloodstream invasion in humans. The Journal of clinical investigation. 2010;120(12):4332-41.
118. Hwang I, Park YJ, Kim Y-R, Kim YN, Ka S, Lee HY, et al. Alteration of gut microbiota by vancomycin and bacitracin improves insulin resistance via glucagon-like peptide 1 in diet-induced obesity. The FASEB Journal. 2015;29(6):2397-411.

119. Lam JS, Breda A, Schulam PG. Ureteropelvic junction obstruction. The Journal of urology. 2007;177(5):1652-8.
120. Braun WE, Schold JD, Stephany BR, Spirko RA, Herts BR. Low-dose rapamycin (sirolimus) effects in autosomal dominant polycystic kidney disease: an open-label randomized controlled pilot study. Clinical Journal of the American Society of Nephrology. 2014:CJN. 02650313.
121. Shillingford JM, Leamon CP, Vlahov IR, Weimbs T. Folate-conjugated rapamycin slows progression of polycystic kidney disease. Journal of the American Society of Nephrology. 2012;23(10):1674-81.
122. Kupferman JC, Druschel CM, Kupchik GS. Increased prevalence of renal and urinary tract anomalies in children with Down syndrome. Pediatrics. 2009;124(4):e615-e21.
123. Kumar J, Gordillo R, Kaskel FJ, Druschel CM, Woroniecki RP. Increased prevalence of renal and urinary tract anomalies in children with congenital hypothyroidism. The Journal of pediatrics. 2009;154(2):263-6.
124. Holmén N, Lundgren A, Lundin S, Bergin AM, Rudin A, Sjövall H, et al. Functional CD4+ CD25high regulatory T cells are enriched in the colonic mucosa of patients with active ulcerative colitis and increase with disease activity. Inflammatory bowel diseases. 2006;12(6):447-56.
125. Zhang L, Yang X-Q, Cheng J, Hui R-S, Gao T-W. Increased Th17 cells are accompanied by FoxP3+ Treg cell accumulation and correlated with psoriasis disease severity. Clinical immunology. 2010;135(1):108-17.
126. Littman DR, Rudensky AY. Th17 and regulatory T cells in mediating and restraining inflammation. Cell. 2010;140(6):845-58.
127. Jiang L, Xu L, Mao J, Li J, Fang L, Zhou Y, et al. Rheb/mTORC1 signaling promotes kidney fibroblast activation and fibrosis. Journal of the American Society of Nephrology. 2013:ASN. 2012050476.
128. Chang C-H, Li J-R, Shu K-H, Fu Y-C, Wu M-J. Hydronephrotic Urine in the Obstructed Kidney Promotes Urothelial Carcinoma Cell Proliferation, Migration, Invasion through the Activation of mTORC2-AKT and ERK Signaling Pathways. PloS one. 2013;8(9):e74300.
129. Lee YK, Menezes JS, Umesaki Y, Mazmanian SK. Proinflammatory T-cell responses to gut microbiota promote experimental autoimmune encephalomyelitis. Proceedings of the National Academy of Sciences. 2011;108(Supplement 1):4615-22.
130. Qin J, Li Y, Cai Z, Li S, Zhu J, Zhang F, et al. A metagenome-wide association study of gut microbiota in type 2 diabetes. Nature. 2012;490(7418):55-60.
131. Zhang X, Zhang D, Jia H, Feng Q, Wang D, Liang D, et al. The oral and gut microbiomes are perturbed in rheumatoid arthritis and partly normalized after treatment. Nature medicine. 2015.
132. Weisheit CK, Engel DR, Kurts C. Dendritic cells and macrophages: Sentinels in the kidney. Clinical Journal of the American Society of Nephrology. 2015:CJN. 07100714.
133. Berndt BE, Zhang M, Owyang SY, Cole TS, Wang TW, Luther J, et al. Butyrate increases IL-23 production by stimulated dendritic cells. American Journal of Physiology-Gastrointestinal and Liver Physiology. 2012;303(12):G1384-G92.

134. Machida Y, Kitamoto K, Izumi Y, Shiota M, Uchida J, Kira Y, et al. Renal fibrosis in murine obstructive nephropathy is attenuated by depletion of monocyte lineage, not dendritic cells. Journal of pharmacological sciences. 2010;114(4):464-73.
135. Gottschalk C, Kurts C. The debate about dendritic cells and macrophages in the kidney. Frontiers in immunology. 2015;6.

VITA

VITA

Jeongho Park

Education

2009-2016 **Ph.D.** in Immunology (Advisor: Chang H. Kim)
Purdue University, West Lafayette, USA

2007-2009 **M.S.** in Preventive Veterinary Medicine (Advisor: Hyukmoo Kwon)
Kangwon National University, Chuncheon, Korea

2000-2007 **D.V.M.**
Kangwon National University, Chuncheon, Korea

Publications

[1] Myunghoo Kim, Yaqing Qie, **Jeongho Park**, and Chang H. Kim. Gut Microbial Metabolites Fuel Host Antibody Responses. 2016. 20.2:202-214. Cell Host & Microbe.

[2] **Jeongho Park**, Craig J. Goergen, Harm HogenEsch, and Chang H. Kim. Chronically elevated levels of short-chain fatty acids induce T cell-mediated tissue inflammation in the renal system. 2016.196.5:2388-2400. The Journal of Immunology.

[3] **Jeongho Park**, Myunghoo Kim, Seung G. Kang, Amber Hopf Jannasch, Bruce Cooper, John Patterson, and Chang H. Kim. Short chain fatty acids induce both effector and regulatory T cells through suppression of histone deacetylases and activation of p70 S6 kinase. 2015. 8.1:80-93. Mucosal Immunology.

[4] Chang H. Kim, **Jeongho Park,** and Myunghoo Kim. Gut Microbiota-Derived Short-Chain Fatty Acids, T Cells, and Inflammation. 2014 *Immune network* 14.6: 277-288. Immune Network

[5] Myunghoo Kim, Seung G. Kang, **Jeongho Park**, Masashi Yanagisawa, and Chang H. Kim. Short chain fatty acids regulate anti-bacterial inflammatory responses and clearance

of pathogenic bacteria through epithelial GPR41 and GPR43. 2013. 145:396-406 Gastroenterology.

[6] Jeeho Lee, Ben Ulrich, Jungyoon Cho, **Jeongho Park**, Chang H Kim. Progesterone promotes differentiation of human cord blood fetal T cells into T regulatory cells but suppresses their differentiation into Th17 cells. 2011. 187:1778-1787. The Journal of Immunology.

[7] Seung G.Kang, **Jeongho Park**, Jungyoon Cho, Ben Ulrich, Chang H Kim. Complementary roles of retinoic acid and TGF-beta1 in coordinated expression of mucosal integrins by T cells. 2011. 4:66-82.Mucosal Immunology.

[8] Park MJ, **Park JH**, Kwon HM. Mice as potential carriers of infectious bursal disease virus (IBDV). 2010 183:352-354 The Veterinary Journal.

[9] **Park Jeong-Ho,** Sung Haan-Woo, Yoon Byung-Il, Pak Son-Il, Kwon Hyuk-Moo. Efficacy of Genetic Adjuvant (Plasmid-Expressed Chicken Interleukin-6) and Chemical Adjuvant (Levamisole) on the Protective Immunity of Genetic Vaccine against Infectious Bursal Disease Virus. 2009 45.2:91-98. The Korean Journal of Microbiology.

[10] **Park JH**, Sung HW, Kwon HM. Evaluation of protective immunity against vvIBDV provided by a heterologous prime-boost strategy: in ovo priming with DNA vaccine, boosting with killed vaccine, and the adjuvant effects of plasmid-encoded chicken interleukin-2 and chicken interferon-γ. 200910:131–139. Journal of Veterinary Science.

[11] **Park JH**, Han JH, Kwon HM. Sequence analysis of the ORF 7 region of TGEV isolated in Korea. 2008. 36:71-78. Virus Genes.

Awards

[1] **Jeongho Park,** Myunghoo Kim, Seung G. Kang, John Patterson, and Chang H. Kim.
Gut T cells are regulated by commensal microbial metabolites.
(2016 Phi Zeta manuscript awards, Purdue University)

[2] **Jeongho Park,** Craig J. Goergen, Harm HogenEsch**,** and Chang H. Kim.
Impact of gut microbial metabolites on Kidney function
(2015 Phi Zeta competition poster awards, Purdue University)

[3] **Jeongho Park,** Myunghoo Kim, Seung G. Kang, John Patterson, and Chang H. Kim.
Impact of gut microbial metabolites on T cell immunity
(2014 Phi Zeta competition poster awards, Purdue University)
[4] Myunghoo Kim, Seung G. Kang, **Jeongho Park**, Masashi Yanagisawa, and Chang H. Kim.
The commensal bacteria metabolites short chain fatty acids positively regulateepithelial innate immune responses in the gut
(2014 AAI Trainee Poster Award)

Oral Presentation

[1] 145th AVMA annual convention, 2008, New Orleans,USA.
Park JH, Sung HW, Kwon HM. Evaluation of priming with *in ovo* DNA vaccine and boosting with killed vaccine strategies for protective immunity against IBDV and effects of plasmid-encoded chicken interleukin-2 and chicken interferon-γ.
[2] Autumn Immunology Conference, 2010, Chicago, USA
Seung G. Kang, **Jeongho Park**, Jungyoon Cho, Ben Ulrich, Chang H Kim. Complementary roles of retinoic acid and TGF-beta1 in coordinated expression of mucosal integrins by T cells.